AD-A184 368 SIMULATED NUCLEAR MULTIBURSTS CONDUCTED IN A WATER AANK 1/1
(U) TRW ELECTRONICS AND DEFENSE SECTOR REDONDO BEACH CA
R G COLBERT ET AL 30 JAN 85 DNA TR-84-411
UNCLASSIFIED DNA001-83-C-0262 F/G 19/11 NL

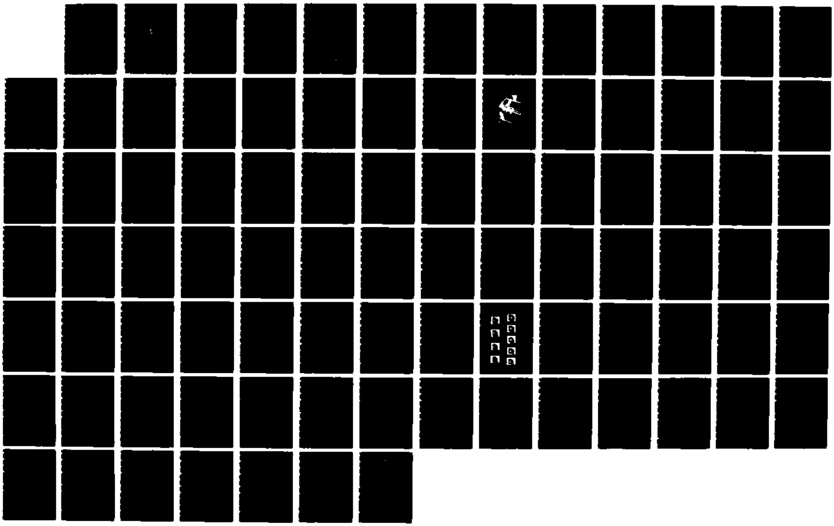

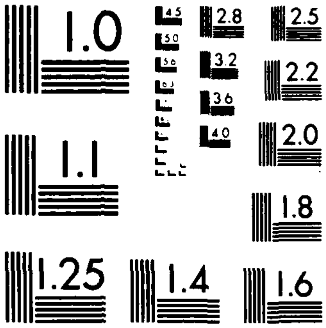

MICROCOPY RESOLUTION TEST CHART
NATIONAL BUREAU OF STANDARDS-1963-A

DTIC FILE COPY

(12)

DNA-TR-84-411

AD-A184 368

SIMULATED NUCLEAR MULTIBURSTS CONDUCTED IN A WATER TANK

R. G. Colbert
A. W. Zimmerman
TRW Electronics and Defense Sector
One Space Park
Redondo Beach, CA 90278

30 January 1985

Technical Report

CONTRACT No. DNA 001-83-C-0262

Approved for public release;
distribution is unlimited.

THIS WORK WAS SPONSORED BY THE DEFENSE NUCLEAR AGENCY
UNDER RDT&E RMSS CODE B344084466 Y99QMXSG00007 H2590D.

Prepared for
Director
DEFENSE NUCLEAR AGENCY
Washington, DC 20305-1000

87 9 9 285

CUT HERE AND RETURN

DISTRIBUTION LIST UPDATE

This mailer is provided to enable DNA to maintain current distribution lists for reports. We would appreciate your providing the requested information.

- ☐ Add the individual listed to your distribution list.
- ☐ Delete the cited organization/individual.
- ☐ Change of address.

NAME: ______________________________

ORGANIZATION: ______________________________

OLD ADDRESS	**CURRENT ADDRESS**
____________________	____________________
____________________	____________________
____________________	____________________

TELEPHONE NUMBER: (   ) ______________________________

SUBJECT AREA(s) OF INTEREST:

____________________	____________________
____________________	____________________
____________________	____________________

DNA OR OTHER GOVERNMENT CONTRACT NUMBER: ______________________________

CERTIFICATION OF NEED-TO-KNOW BY GOVERNMENT SPONSOR (if other than DNA):

SPONSORING ORGANIZATION: ______________________________

CONTRACTING OFFICER OR REPRESENTATIVE: ______________________________

SIGNATURE: ______________________________

Director
Defense Nuclear Agency
ATTN: [redacted] TITL
Washington, DC 20305-1000

Director
Defense Nuclear Agency
ATTN: [redacted] TITL
Washington, DC 20305-1000

UNCLASSIFIED

SECURITY CLASSIFICATION OF THIS PAGE

REPORT DOCUMENTATION PAGE

1a. REPORT SECURITY CLASSIFICATION UNCLASSIFIED	1b. RESTRICTIVE MARKINGS
2a. SECURITY CLASSIFICATION AUTHORITY N/A since Unclassified 2b. DECLASSIFICATION / DOWNGRADING SCHEDULE N/A since Unclassified	3. DISTRIBUTION / AVAILABILITY OF REPORT Approved for public release; distribution is unlimited.
4. PERFORMING ORGANIZATION REPORT NUMBER(S)	5. MONITORING ORGANIZATION REPORT NUMBER(S) DNA-TR-84-411
6a. NAME OF PERFORMING ORGANIZATION TRW Electronics and Defense Sector 6b. OFFICE SYMBOL (If applicable)	7a. NAME OF MONITORING ORGANIZATION Director Defense Nuclear Agency
6c. ADDRESS (City, State, and ZIP Code) One Space Park Redondo Beach, CA 90278	7b. ADDRESS (City, State, and ZIP Code) Washington, DC 20305-1000
8a. NAME OF FUNDING / SPONSORING ORGANIZATION 8b. OFFICE SYMBOL (If applicable)	9. PROCUREMENT INSTRUMENT IDENTIFICATION NUMBER DNA 001-83-C-0262
8c. ADDRESS (City, State, and ZIP Code)	10. SOURCE OF FUNDING NUMBERS PROGRAM ELEMENT NO: 62715H PROJECT NO: Y99QMXS TASK NO: G WORK UNIT ACCESSION NO: DH008037

11. TITLE (Include Security Classification)
SIMULATED NUCLEAR MULTIBURSTS CONDUCTED IN A WATER TANK

12. PERSONAL AUTHOR(S)
Colbert, R. G. and Zimmerman, A. W.

13a. TYPE OF REPORT	13b. TIME COVERED	14. DATE OF REPORT (Year, Month, Day)	15. PAGE COUNT
Technical	FROM 831007 TO 850130	850130	86

16. SUPPLEMENTARY NOTATION
This work was sponsored by the Defense Nuclear Agency under RDT&E RMSS Code B344084466 Y99QMXSG00007 H2590D.

17. COSATI CODES			18. SUBJECT TERMS (Continue on reverse if necessary and identify by block number)
FIELD	GROUP	SUB-GROUP	
18	3		Multiple Bursts; Saltwater
8	3		Nuclear Clouds; Nuclear Explosion Simulation

19. ABSTRACT (Continue on reverse if necessary and identify by block number)

Simultaneous multiple cloud experiments were carried out in a water tank. Salt was used to achieve a linear density gradient in the tank to simulate the atmosphere. A nuclear fireball was simulated with a high density "bubble" of saltwater dropped into the top of the tank. The bubble grew by turbulent entrainment as it fell into saltwater with an increasing density. The fall stops when the density inside the cloud reaches the density of its environment.

Cloud dimensions were obtained for 5, 6 and 7 burst events. These cloud dimensions were compared with a model which is good fit to data from other multiburst experiments. The model and the data from this program are in good agreement.

These tests utilized existing hardware. Recommendations are made for a new facility which would be capable of simulating up to 70 bursts with an arbitrary time sequence. Instrumentation techniques to provide data other than cloud dimensions, e.g., velocity and

20. DISTRIBUTION / AVAILABILITY OF ABSTRACT ☐ UNCLASSIFIED/UNLIMITED ☒ SAME AS RPT ☐ DTIC USERS	21. ABSTRACT SECURITY CLASSIFICATION UNCLASSIFIED
22a. NAME OF RESPONSIBLE INDIVIDUAL Sandra E. Young	22b. TELEPHONE (Include Area Code): (202) 325-7042 22c. OFFICE SYMBOL: DNA/CSTI

DD FORM 1473, 84 MAR — 83 APR edition may be used until exhausted. All other editions are obsolete.

SECURITY CLASSIFICATION OF THIS PAGE
UNCLASSIFIED

19. ABSTRACT (Continued)

density, are also recommended.

PREFACE

The work described in this report was supported by the Defense Nuclear Agency under Contract DNA001-83-C-0262. The Contract Technical Monitor was Mr. George Ullrich.

The experimental work was done under the direction of R. G. Colbert. Mr. Colbert was also responsible for the test facility and instrumentation recommendations for an extended test capability. The tests were done at the TRW Technology Test Center by H. Rungaldier and K. L. Beach. The analysis of the test results was carried out by A. W. Zimmerman.

CONVERSION TABLE

Table of Conversion Factors
for Units Used in This Report

Physical Quantity	From	To Metric (SI) Units	Multiply By
Length	Inch	Meter	.0254

TABLE OF CONTENTS

Section		Page
	PREFACE	iv
	CONVERSION TABLE	v
	LIST OF ILLUSTRATIONS	vii
	LIST OF TABLES	ix
	NOMENCLATURE	x
1.	INTRODUCTION	1
2.	OBJECTIVES	2
3.	EXPERIMENTS	3
	3.1 APPARATUS	3
	3.2 TEST	3
	3.2.1 Test Procedures	7
	3.3 DATA REDUCTION	11
	3.4 TEST RESULTS	14
4.	ANALYSIS OF TEST RESULTS	48
	4.1 SCALING	48
	4.1.1 General	48
	4.1.2 Scaling Tests	48
	4.2 SINGLE CLOUD TESTS	49
	4.2.1 Single Cloud Theory	49
	4.2.2 Comparison of Test Results with Theory and with Earlier Tests	51
	4.3 MULTIBURST TESTS	54
	4.3.1 Test Data Summary	54
	4.3.2 Comparison with Results with Multiburst Model	54
	4.4 APPLICATION TO NUCLEAR CLOUDS	56
5.	RECOMMENDED TEST FACILITY AND INSTRUMENTATION FOR EXTENDED CAPABILITY	59
	5.1 INTRODUCTION	59
	5.2 EXPERIMENTAL APPARATUS	59
	5.2.1 Tank and Fill Apparatus	59
	5.2.2 Cloud Release Mechanism	62

(TABLES OF CONTENTS CONT'D)

Section		Page
	5.3 INSTRUMENTATION	62
	5.3.1 General	65
	5.3.2 Laser Induced Fluorescence (LIF)	65
	5.3.3 Video Data Acquisition	66
	5.3.4 Velocity Measurements	66
6.	CONCLUSIONS AND RECOMMENDATIONS	69
7.	REFERENCES	70

LIST OF ILLUSTRATIONS

Figure		Page
3-1.	Experimental Setup for Multiburst Tests.	4
3-2.	Cloud Release Mechanisms.	5
3-3.	Multiburst Cluster Arrangement.	8
3-4.	Measured Density Versus Depth for Three Tests.	9
3-5.	Measured Density Versus Depth for Test 1.4, 1.5 and 1.6.	10
3-6.	Cloud Parameters for Multiburst Tests.	12
3-7.	Data Correction Method.	13
3-8.	Dimension Time Histories: Test No. 1.1.	15
3-9.	Dimension Time Histories: Test No. 1.2.	16
3-10.	Dimension Time Histories: Test No. 1.4.	17
3-11.	Dimension Time Histories: Test No. 1.5.	18
3-12.	Dimension Time Histories: Test No. 1.6.	19
3-13.	Dimension Time Histories: Test No. 5.1.	20
3-14.	Dimension Time Histories: Test No. 5.3.	21
3-15.	Dimension Time Histories: Test No. 6.1.	22
3-16.	Dimension Time Histories: Test No. 6.2.	23
3-17.	Dimension Time Histories: Test No. 6.3.	24
3-18.	Dimension Time Histories: Test No. 6.4.	25
3-19.	Dimension Time Histories: Test No. 6.5.	26
3-20.	Dimension Time Histories: Test No. 6.6.	27
3-21.	Dimension Time Histories: Test No. 6.7.	28
3-22.	Dimension Time Histories: Test No. 7.1.	29
3-23.	Dimension Time Histories: Test No. 7.2.	30
3-24.	Cloud Outline: Test No. 1.1, 10 Seconds.	31
3-25.	Cloud Outline: Test No. 1.2, 10 Seconds.	32

(LIST OF ILLUSTRATIONS CONT'D)

Figure		Page
3-26.	Cloud Outline: Test No. 1.4, 9 Seconds.	33
3-27.	Cloud Outline: Test No. 1.5, 8 Seconds.	34
3-28.	Cloud Outline: Test No. 1.6, 8.25 Seconds.	35
3-29.	Cloud Outline: Test No. 5.1, 9.75 Seconds.	36
3-30.	Cloud Outline: Test No. 5.3, 12.25 Seconds.	37
3-31.	Cloud Outline: Test No. 6.1, 9.75 Seconds.	38
3-32.	Cloud Outline: Test No. 6.2, 10 Seconds.	39
3-33.	Cloud Outline: Test No. 6.3, 11.25 Seconds.	40
3-34.	Cloud Outline: Test No. 6.4, 11 Seconds.	41
3-35.	Cloud Outline: Test No. 6.5, 10.8 Seconds.	42
3-36.	Cloud Outline: Test No. 6.6, 11 Seconds.	43
3-37.	Cloud OUtline: Test No. 6.7, 11 Seconds.	44
3-38.	Cloud Outline: Test No. 7.1, 11 Seconds.	45
3-39.	Cloud Outline: Test No. 7.2, 9.75 Seconds.	46
3-40.	Sample Test Photographs, Test 6.1.	47
4-1.	Comparison of Theoretical and Experimental Cloud Dimensions for Scaling Tests (1.4, 1.5 and 1.6).	50
4-2.	Comparison of Theoretical and Experimental Cloud Dimensions for Reference Single Burst Tests (1.1 & 1.2).	52
4-3.	Comparison of Theoretical and Experimental Cloud Dimensions for Reference Single Bursts for Earlier Program (Reference 1).	53
5-1.	Gravity Feed Fill Method.	60
5-2.	Metering Pump Fill Method.	61
5-3.	Release Mechanism Design #1.	63
5-4.	Release Mechanism Design #2.	64
5-5.	Laser Induced Fluorescence Calibration Setup.	67

LIST OF TABLES

Table		Page
3-1.	Multiple Burst Cloud Interaction Study Phase 1 - Test Matrix.	6
4-1.	Cloud Top Height and Horizontal Radius at 10 Seconds (Stabilization or Time of First Peak).	55
4-2.	Model Prediction Compared with Water Tank Experiments.	57

NOMENCLATURE

D = Cloud Diameter

D_{FB} = Fireball Diameter at Pressure Equilibrium

F_o = $(4/3)\pi r^3 g\left[(\rho_1-\rho_o)/\rho_1\right] = (1/\rho_1)x$ Total Buoyancy Released from the Source at $t = 0$.

G = $-(g/\rho_1)(d\rho_e/dx)$

g = Acceleration Due to Gravity

H = Cloud Height

N = Number of Bursts

R = Height Above Lens Axis of Symmetry (See Figure 3-7)

R = Nondimensional Cloud Radius (Section 4)

Re = Reynolds Number

r = Cloud Radius (Section 4)

t = Time

t_1 = Nondimensional Time

u = Vertical Velocity

x = Cloud Altitude (to Cloud Center)

X = Nondimensional Altitude (to Cloud Center)

Δx = Horizontal Spacing Between Bursts

$\widetilde{\Delta x}$ = $\Delta x/D_{FB}$

α = Entrainment Constant

κ = Diffusivity

ν = Kinematic Viscosity

ρ = Average Density Inside Cloud

ρ_o = Average Initial Density Inside Cloud

ρ_1 = Ambient Density at Source Level

ρ_e = Ambient Density at Cloud Level

Subscripts

B	=	Bottom
C	=	Center
MB	=	Multiburst
S	=	Single Burst
T,TOP	=	Top
1	=	Center (Side 1)
2	=	Center (Side 2)

1. INTRODUCTION

Detonation of many nuclear weapons in a limited domain of time and space may occur in an attack on existing or planned missile basing areas. The mushroom clouds from such an attack may overlap and information about the interaction between clouds is required. This requirement arises from the fact that the dust and debris environment in these clouds may cause severe or fatal damage to a vehicle (launch vehicle or reentry vehicle) flying through such a cloud too soon after burst. Calculations and experiment have been performed to quantify interaction effects but the uncertainties remain very large.

The program reported here is part of a continuing experimental effort to quantify multiburst cloud interactions. The program consists of a series of experiments conducted in a tank filled with a linearly stratified saltwater solution. The stratification (density gradient) simulates the density gradient in the atmosphere up to the tropopause. A slightly heavier solution of dyed saltwater in a cup is released at the top of the tank to simulate a weapon burst. The cloud falls, spreads and comes to rest just as the mushroom cloud from a nuclear weapon burst rises, spreads and reaches a stabilization altitude. Turbulent entrainment and the density gradient governs the motion in both cases and similiar clouds occur.

Up to seven similtaneous bursts were simulated. This program is a continuation of an earlier effort reported in Reference 1 and most of the same hardware was utilized.

The specific objectives are given in the next section. Section 3 describes the experiments and the data reduction. The analysis of the data is presented in Section 4. Section 5 discusses extensions to the test facility and the instrumentation that are recommended to further exploit this technique for doing multiburst tests. Finally, the conclusions and recommendations are presented in Section 6.

2. OBJECTIVES

The specific objectives of this program are:

1) to extend prior multiple cloud experiments in a water tank to the largest number of simultaneous bursts using existing hardware,

2) to apply the data to nuclear clouds and

3) to design the apparatus to extend the experiments to larger numbers of bursts or more general attacks.

3. EXPERIMENTS

3.1 APPARATUS

The cloud experiments were performed at the TRW Technology Test Center and all of the apparatus with the exception of the cloud release mechanism was provided by the test center.

The experimental apparatus consisted of a water tank, cloud release mechanism, two 35 mm cameras, and one video camera. The tank measuring 1x1x1 meter has two glass walls for photography purposes and two steel walls. Figure 3-1 shows the details of the test tank.

The cloud release mechanism used was identical to the device used in the previous multiple cloud experiments (Reference 1) only slightly modifed for use on the new test tank and using a new stiffer spring in the release mechanism. Replacing the spring may have some effect on cloud development, this is discussed in more detail in Section 4. Figure 3-2 shows a photograph of the release mechanism. The mechanism consisted of hemispherical cups with a radius of 2.5 centimeters. The cups are mounted on a shaft that is spring loaded and causes the cups to rotate 180 degrees, simultaneously releasing the heavy dyed salt water solution contained in all the cups into the test tank and forming clouds with negative buoyancy. The cloud release mechanism can be setup for a maximum of 7 clouds.

Two 35 mm cameras were used to obtain cloud data, one camera was stationed for a side view and the other for a top view of the developing clouds. A video camera was used for the side view.

3.2 TEST

Single cloud and multiple cloud tests were conducted. The matrix of the tests performed is shown in Table 3-1. The primary objective of the tests was to obtain multiple cloud results up to the maximum possible (7) using the existing apparatus. Single cloud tests were done to provide reference values of cloud dimensions to compare with multiple cloud results. Tests with two and three clouds were not conducted since they have been simulated in the previous experiments (Reference 1).

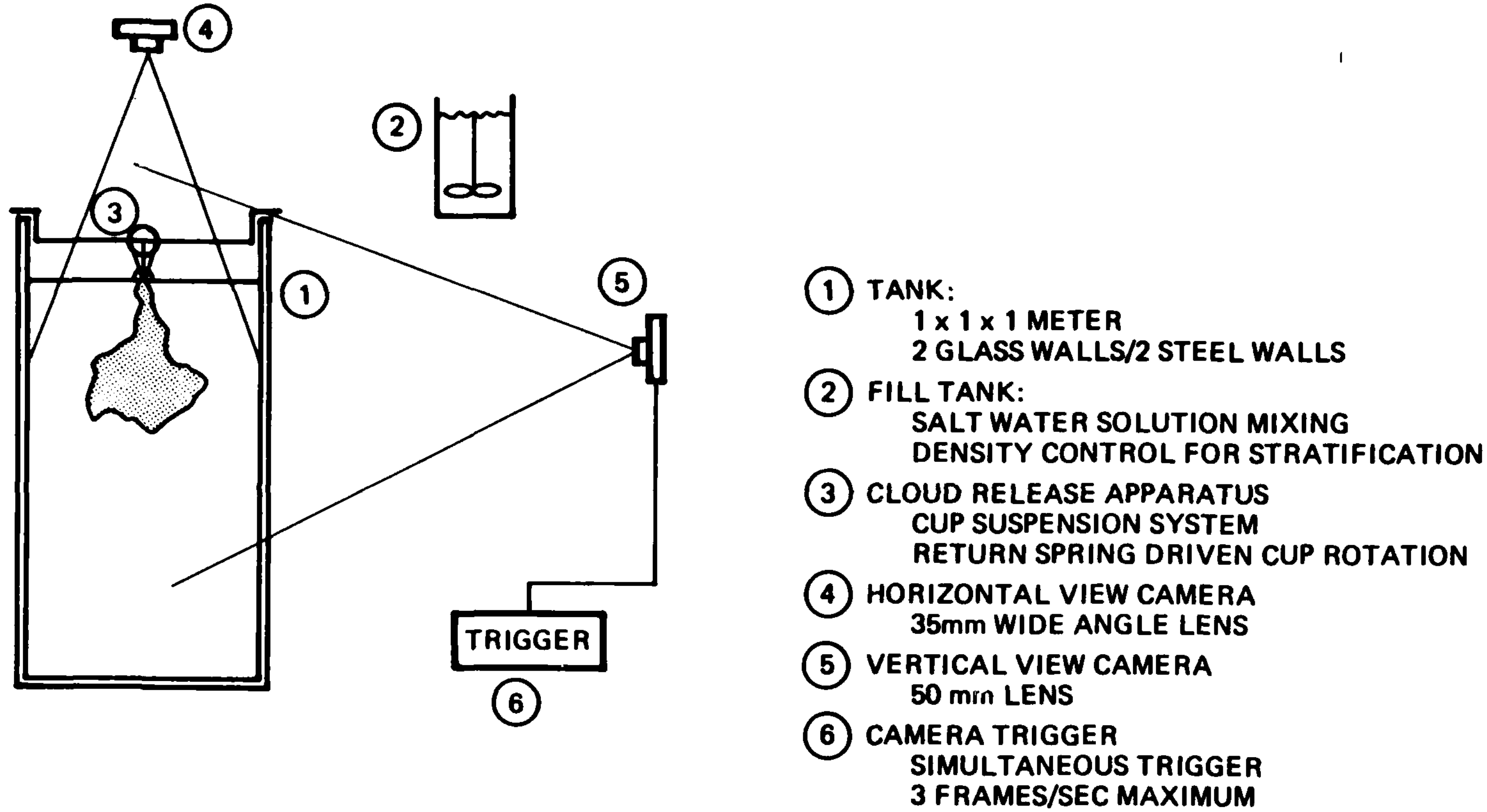

Figure 3-1. Experimental Setup for Multiburst Tests.

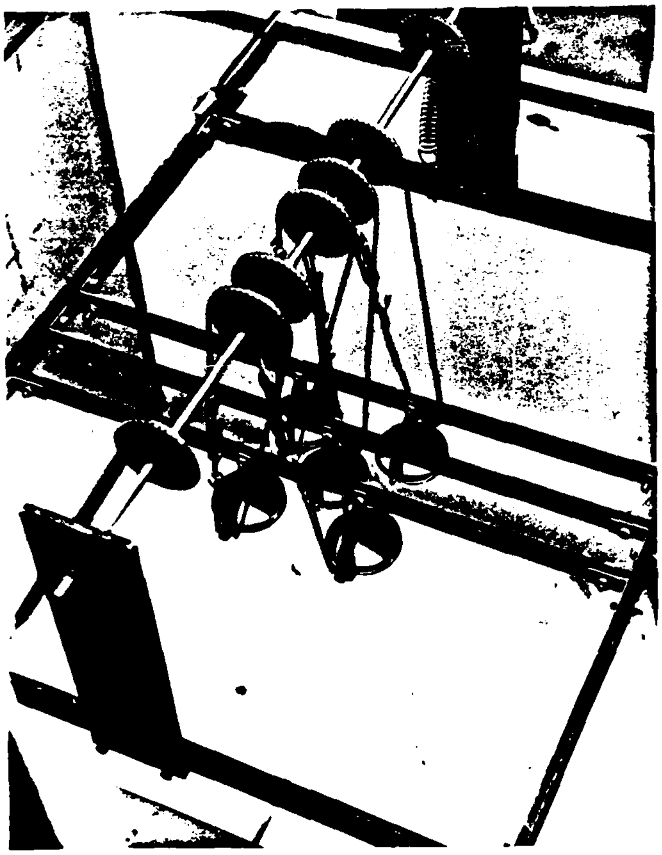

Figure 3-2. Cloud Release Mechanisms.

TABLE 3-1.

MULTIPLE BURST CLOUD INTERACTION
STUDY PHASE I - TEST MATRIX

TEST CATEGORY	NO. OF CLOUDS	SPACING (INCHES)	NO. OF TESTS
SINGLE	1	———	3
SINGLE*	1	———	3
MULTIPLE**	5	2.4	2
MULTIPLE**	6	4.0, 6.0	2, 2
MULTIPLE**	6	2.4	3
MULTIPLE**	7	2.4	2

* 3 SINGLE CLOUD TEST WERE PERFORMED WITH DOUBLED DENSITY GRADIENT AS A SCALING TEST

** ALL SIMULTANEOUSLY RELEASED

The multiple cloud tests consisted of 5, 6 and 7 clouds. The 6 and 7 cloud tests were arranged in a hexagonal pattern, one cloud at each corner and in the case of the 7 cloud test the additional cloud was located in the center of the cluster. The 5 cloud test was in the form of a square with one cloud at each corner and one in the center. The spacing parameter S referred to in the test matrix is depicted in Figure 3-3.

3.2.1 Test Procedures

The test tank was filled with a salt water solution in such a manner as to obtain the required linear density gradient. The linear density gradient simulates a stratified atmosphere. Slight variations in the gradients occured from test to test.

When the dyed cup fluid is released it forms a cloud that is initially overdense driven by buoyancy it falls and mixes with the environment finally coming to a rest when the cloud density is the same as the average density in the test tank.

The volume of the test tank was 1 cubic meter, and it took about two hours to fill. The fill was done very slowly to minimize mixing. After the filling, density measurements were taken in three inch increments along the depth. Density measurements were taken using a hydrometer and these values used to verify that a proper density gradient had been obtained.

Fifteen of the cloud tests used a specific gravity of 1.1 for the dyed cup fluid, and a density gradient shown in Figure 3-4 for the stratified atmosphere. The other three tests (all single cloud) had a cup specific gravity of 1.2 and a density gradient shown in Figure 3-5. These three tests were done in order to check scaling laws. Section 4 will discuss these tests in more detail.

When the dyed cup fluid was released by the cloud release mechanism the 35 mm cameras and video camera were activated. The 35 mm cameras were triggered every 1/3 of a second for the first ten seconds of the test and then every second for the next twelve seconds. This photographic data was then analyzed as described in the next section. The video data was not analyzed in depth but was intended to be a qualitative record of the tests.

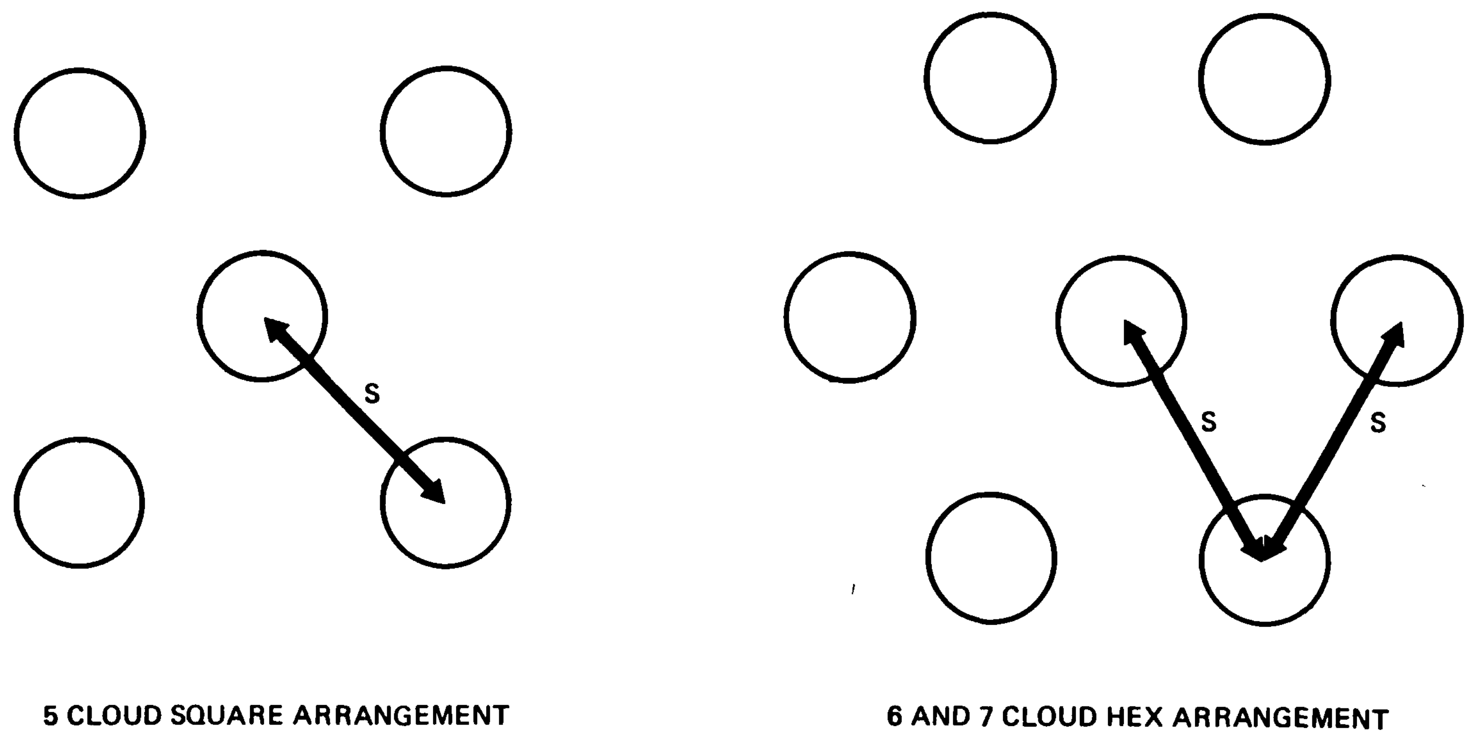

Figure 3-3. Multiburst Cluster Arrangement.

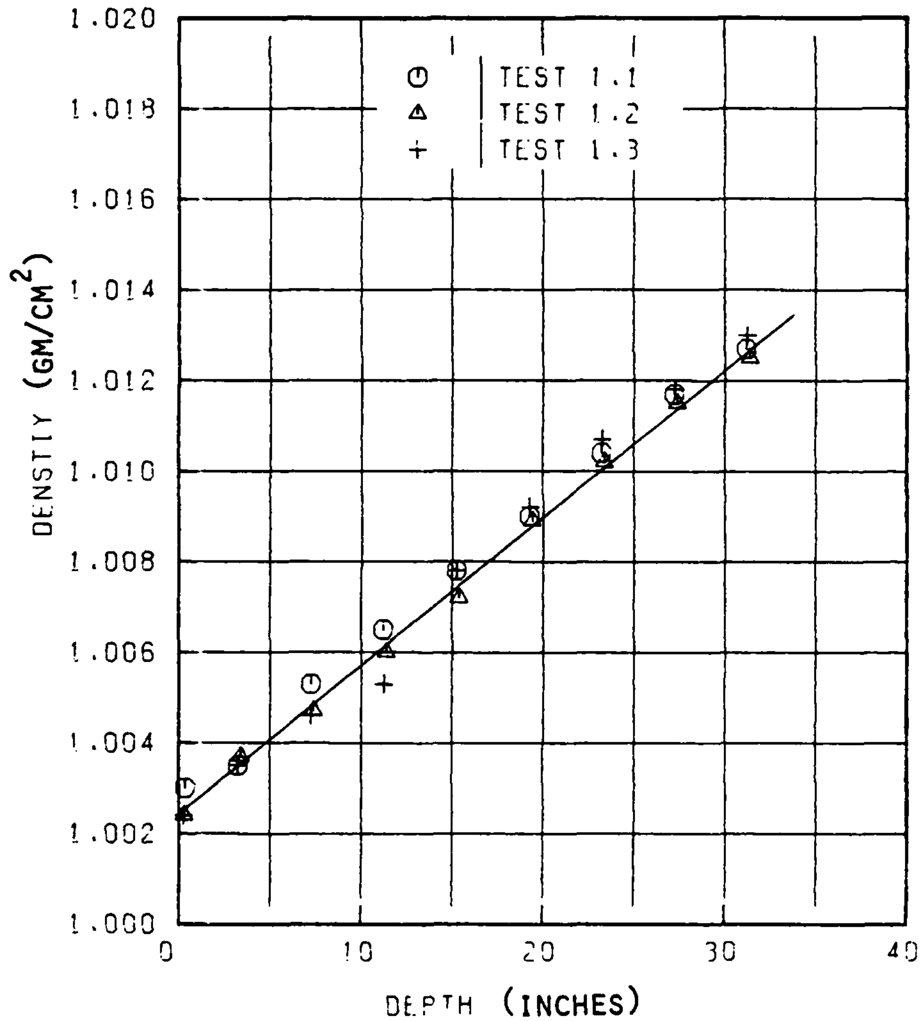

Figure 3-4. Measured Density Versus Depth for Three Tests.

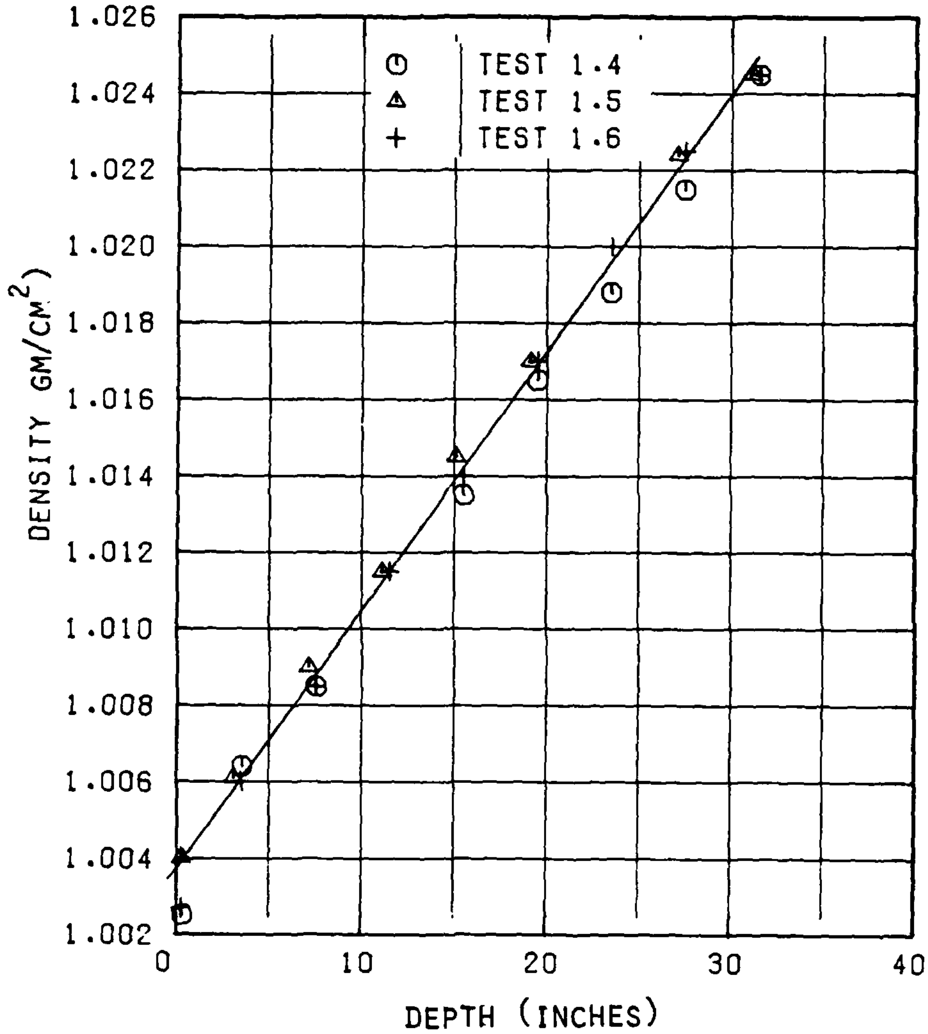

Figure 3-5. Measured Density Versus Depth for Test 1.4, 1.5 and 1.6.

3.3 DATA REDUCTION

The 35 mm photographic data from the 17 cloud tests were reduced by the following method. Each picture was placed in a dark room enlarger and the image projected upon a digitizing pad. The projected image or cloud outline was digitized as was the cloud height, center height, and radius. Figure 3-6 shows the details of how the height, center height and radius were picked. Caution must be taken when analyzing the data on clouds heights and radius. There were many cases when the cloud outlines take on odd shapes and exact definitions of the cloud dimensions were uncertain. In such cases it is wise to examine the cloud outlines as well as the cloud time histories in order to identify cases when the cloud exhibits this feature. Cloud time histories showing the cloud height, cloud middle height and radius for each test are presented in the next section. In addition, samples of the cloud outlines for each test are given.

The digitized data is not usable until corrections and scale factors are applied so that the actual physical dimensions of the cloud are obtained. Light from the object cloud passes through water, glass and air interfaces before striking the camera lens. Because the light passes these interfaces, refraction* of the light takes place causing the image on the film to be larger then the real cloud. Figure 3-7 shows a typical example. In this case a point at the top of the cloud is distorted by refraction and is "seen" by the camera to be R height above the camera lens plane. Using Snell's Law the correct dimension R can be obtained.

A simple computer program was used to facilitate Snell's Law calculations to all digitized points, and produce data files used to make cloud outline plots and time histories. The dimension D in the figure is uncertain for any one point but is assumed to be 18 inches (mid point of test tank) for all calculations. This procedure produces an error of less then 1/2 inch in R.

For the top view a similar procedure was used, and the dimension D was assumed to be the cloud center height** determined from the front view data.

---

* The phenomenon of refraction is described by Snell's Law.

** The cloud center height is the average of the vertical coordinates of H_1 and H_2 shown in Figure 3-6.

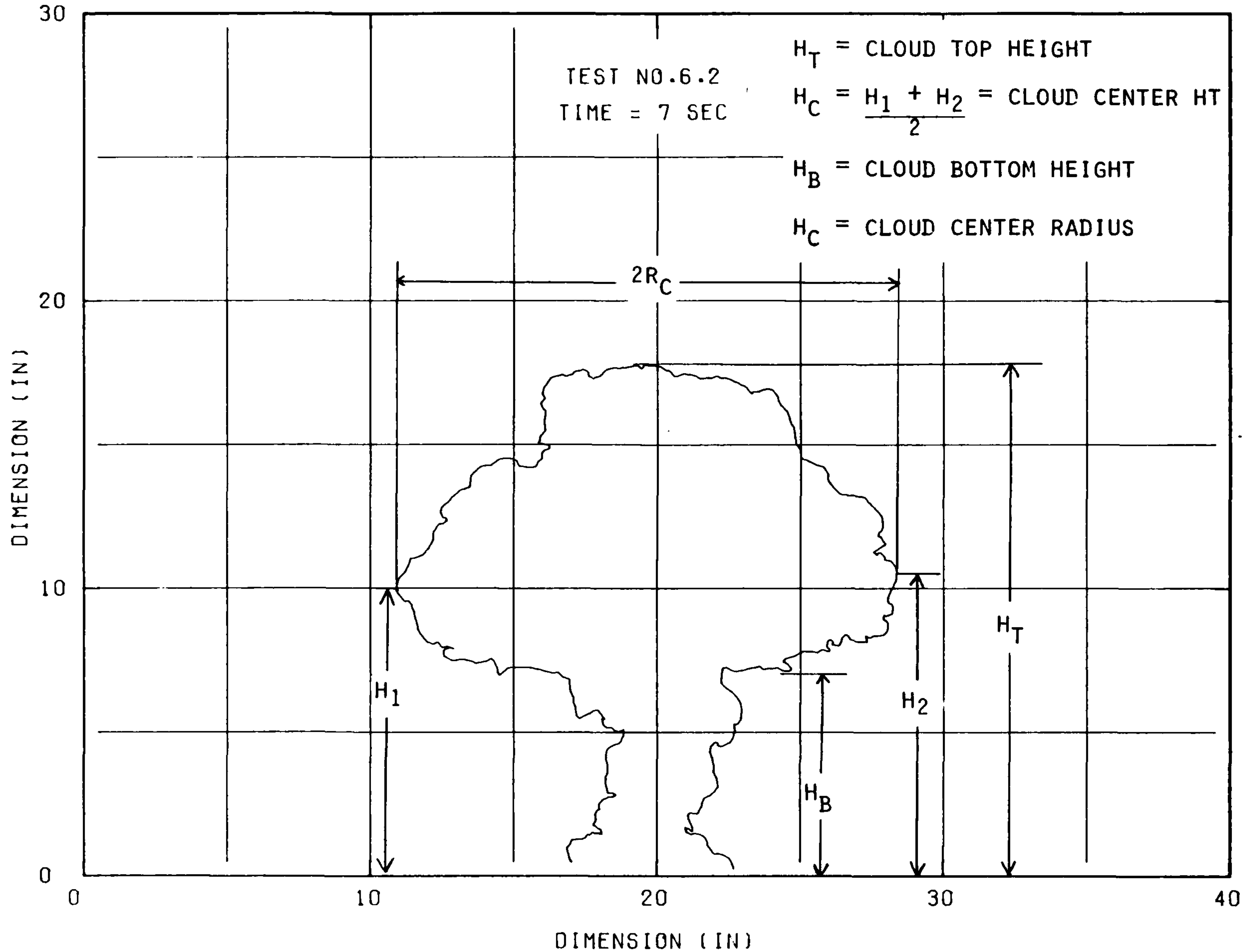

Figure 3-6. Cloud Parameters for Multiburst Tests.

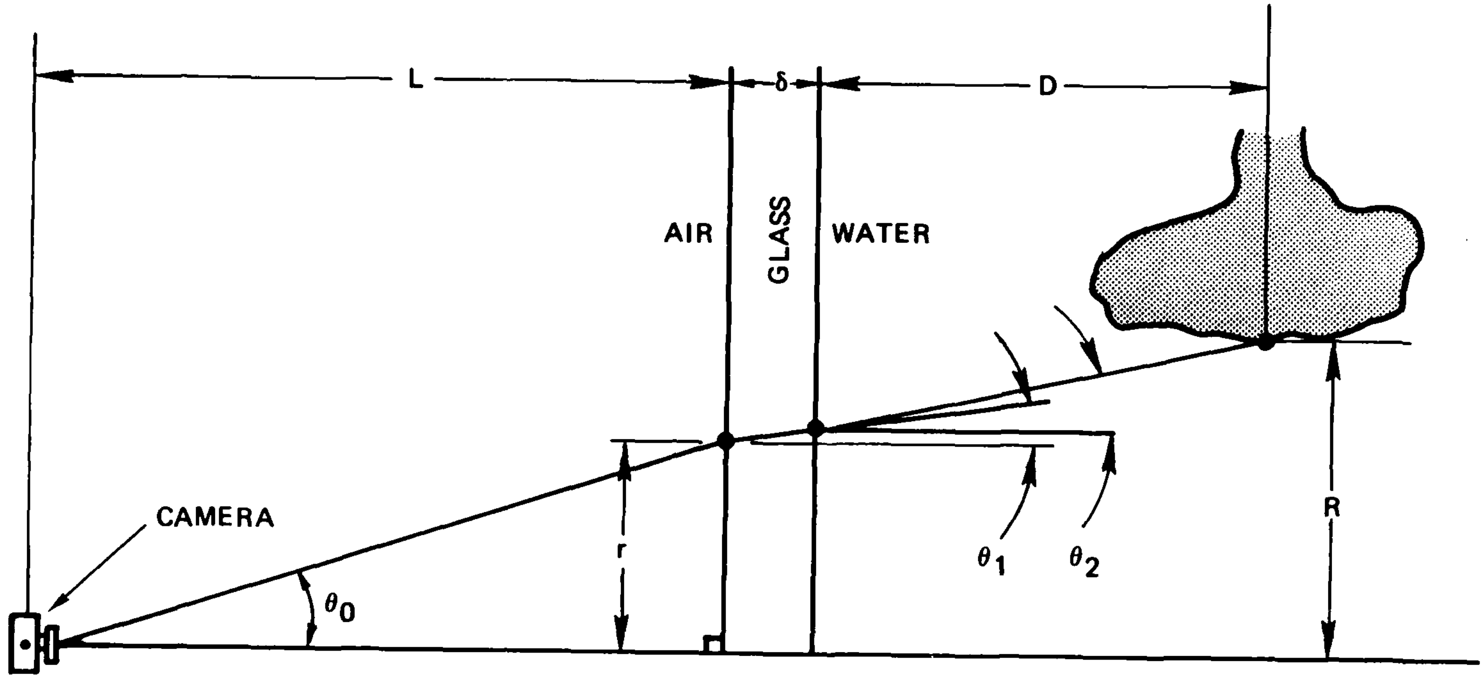

$$R = r + \delta \tan \theta_1 + D \tan \theta_2$$

WHERE $\theta_0 = \tan^{-1} (r/L)$

$$\theta_1 = \sin^{-1} (\sin \theta_0 / n_{PA})$$

$$\theta_2 = \sin^{-1} (\sin \theta_1 / n_{WP})$$

LENGTHS

$L = 84.25$ IN.

$\delta = 0.5$ IN.

$D = 18$ IN.

INDEX OF REFRACTION

$n_{PA} = 1.52$

$n_{WP} = 0.8736$

Figure 3-7. Data Correction Method.

3.4 TEST RESULTS

Cloud time histories showing the cloud height, cloud middle height and radius are shown in Figures 3-8 through 3-23.* Figures 3-24 through 3-39 show cloud outlines at the time of peak cloud height.

Data for single cloud test 1.3 and multiple cloud test 5.2 were omitted because anomalies that occurred during these test invalidated the results.

Sample photographs of test 6.1 are shown in Figure 3-40.

---

* Symbols used to indicate dimensions are not consistant from figure to figure.

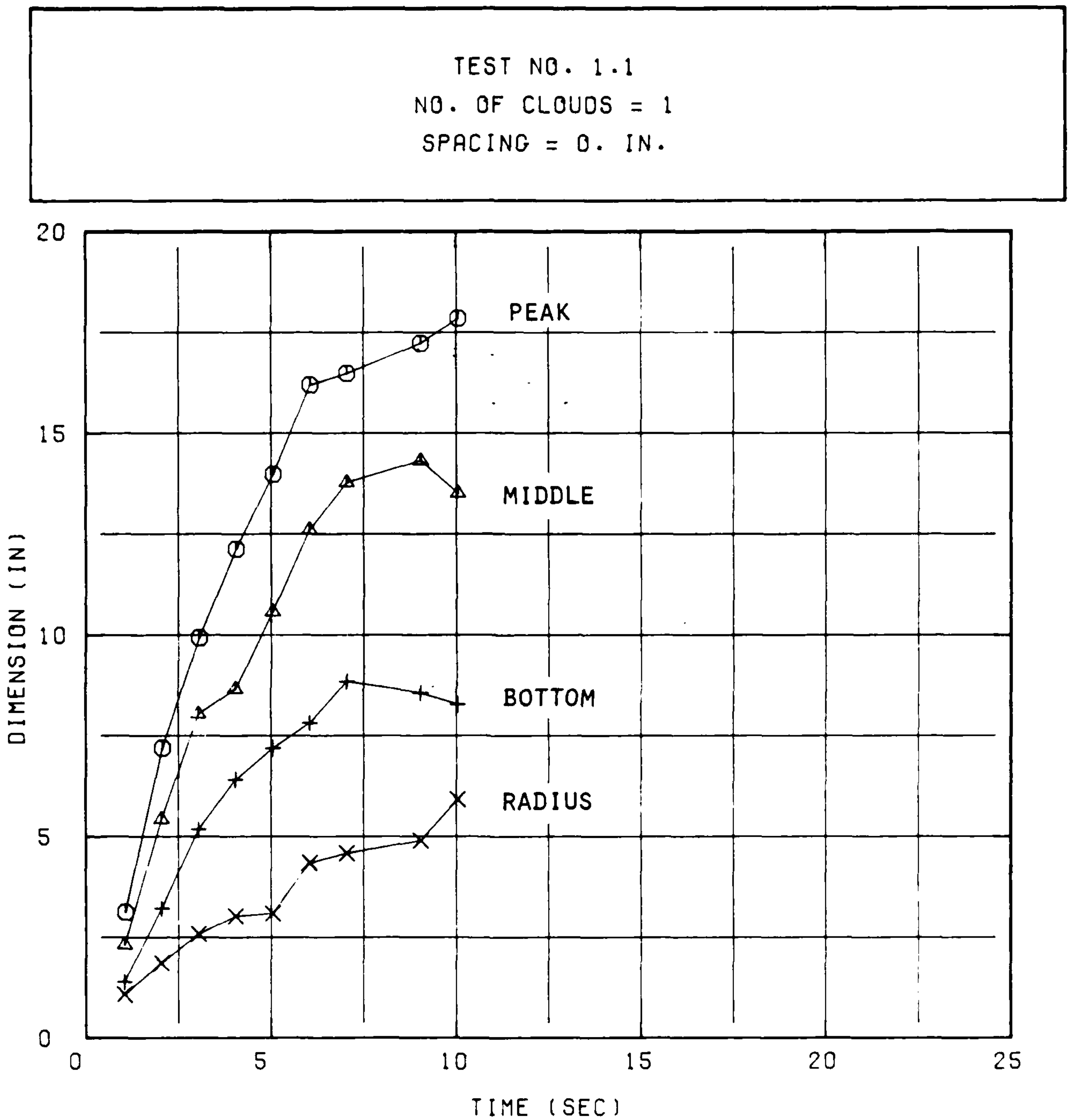

Figure 3-8. Dimension Time Histories: Test No. 1.1.

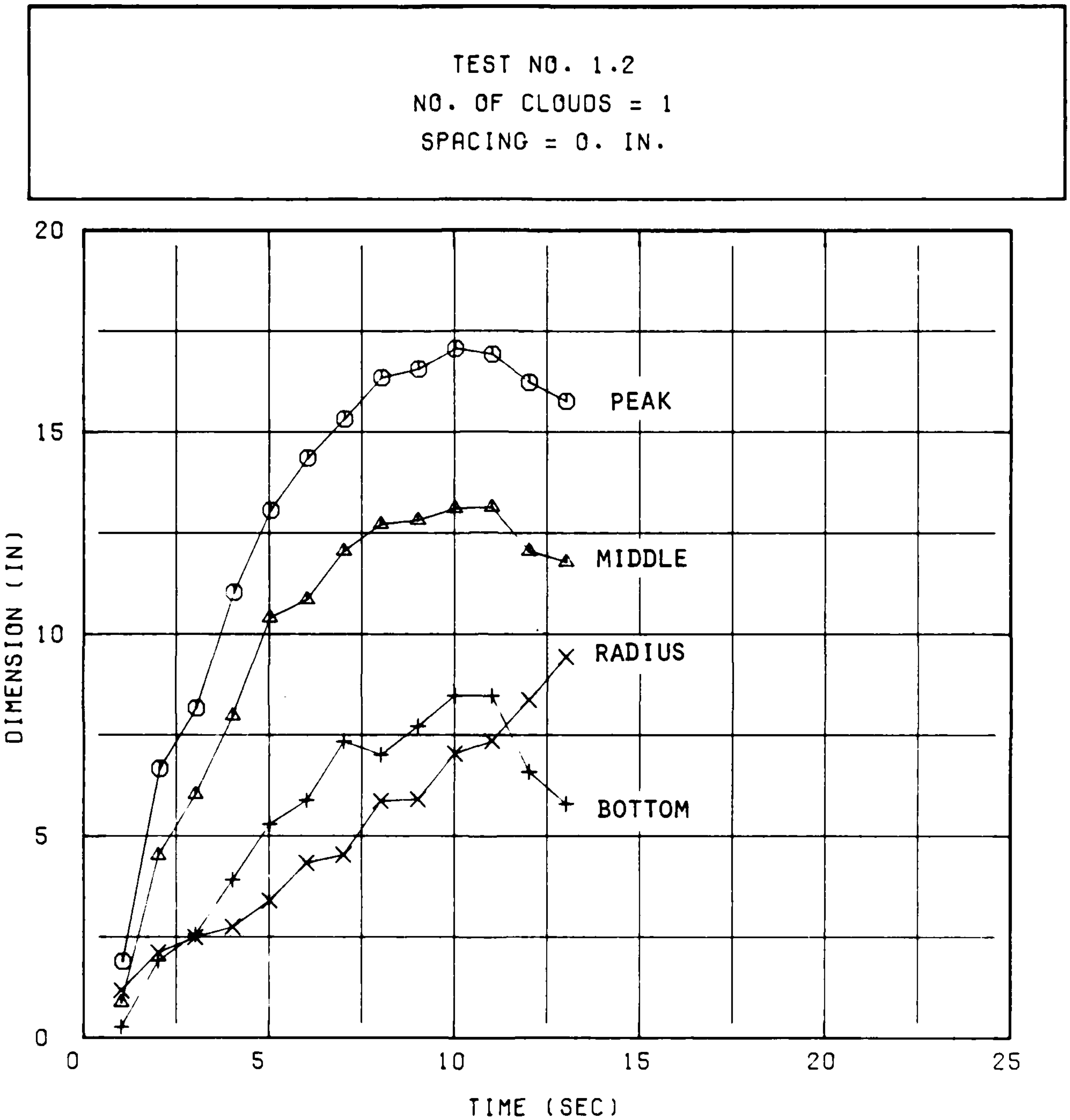

Figure 3-9. Dimension Time Histories: Test No. 1.2.

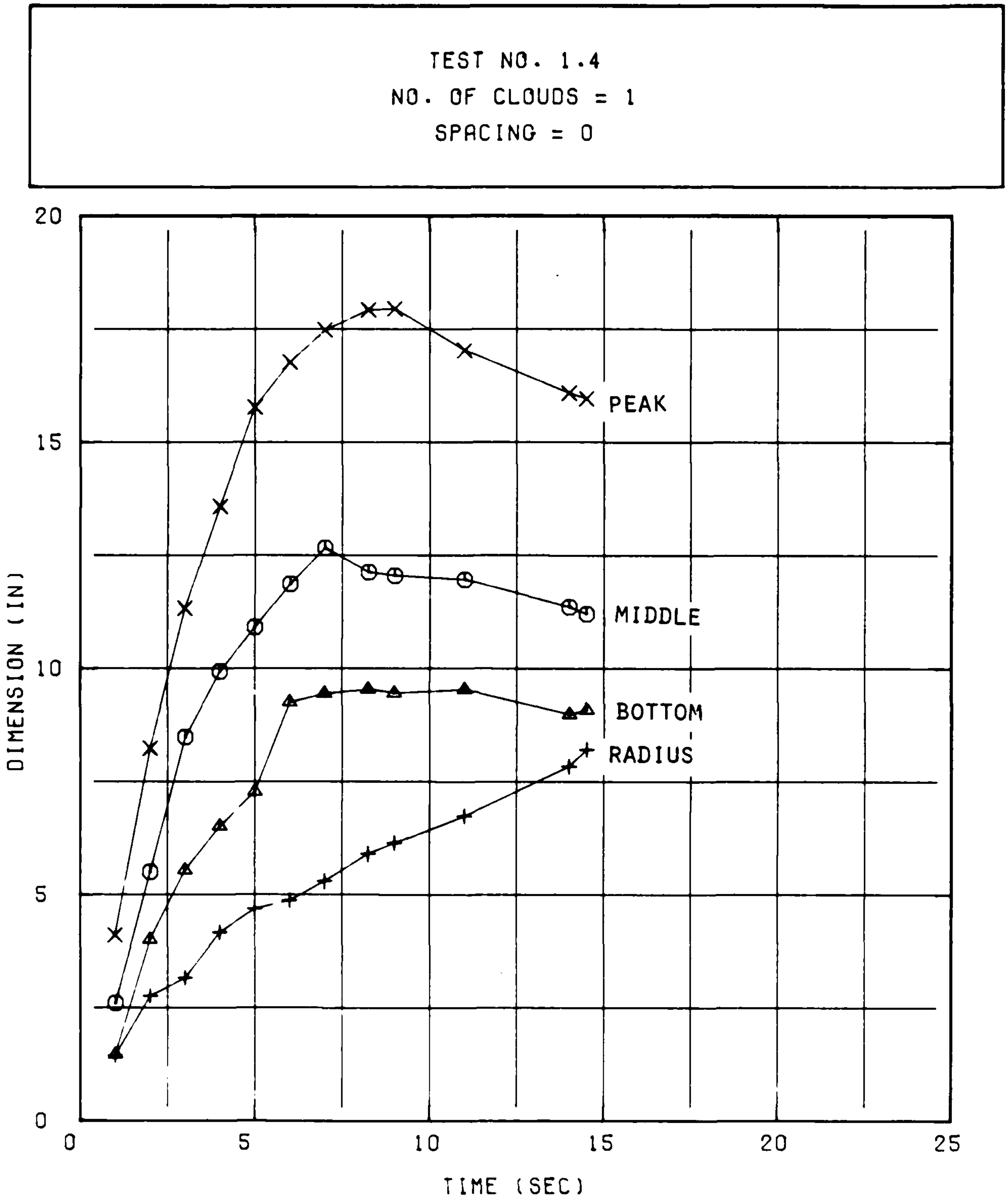

Figure 3-10. Dimension Time Histories: Test No. 1.4.

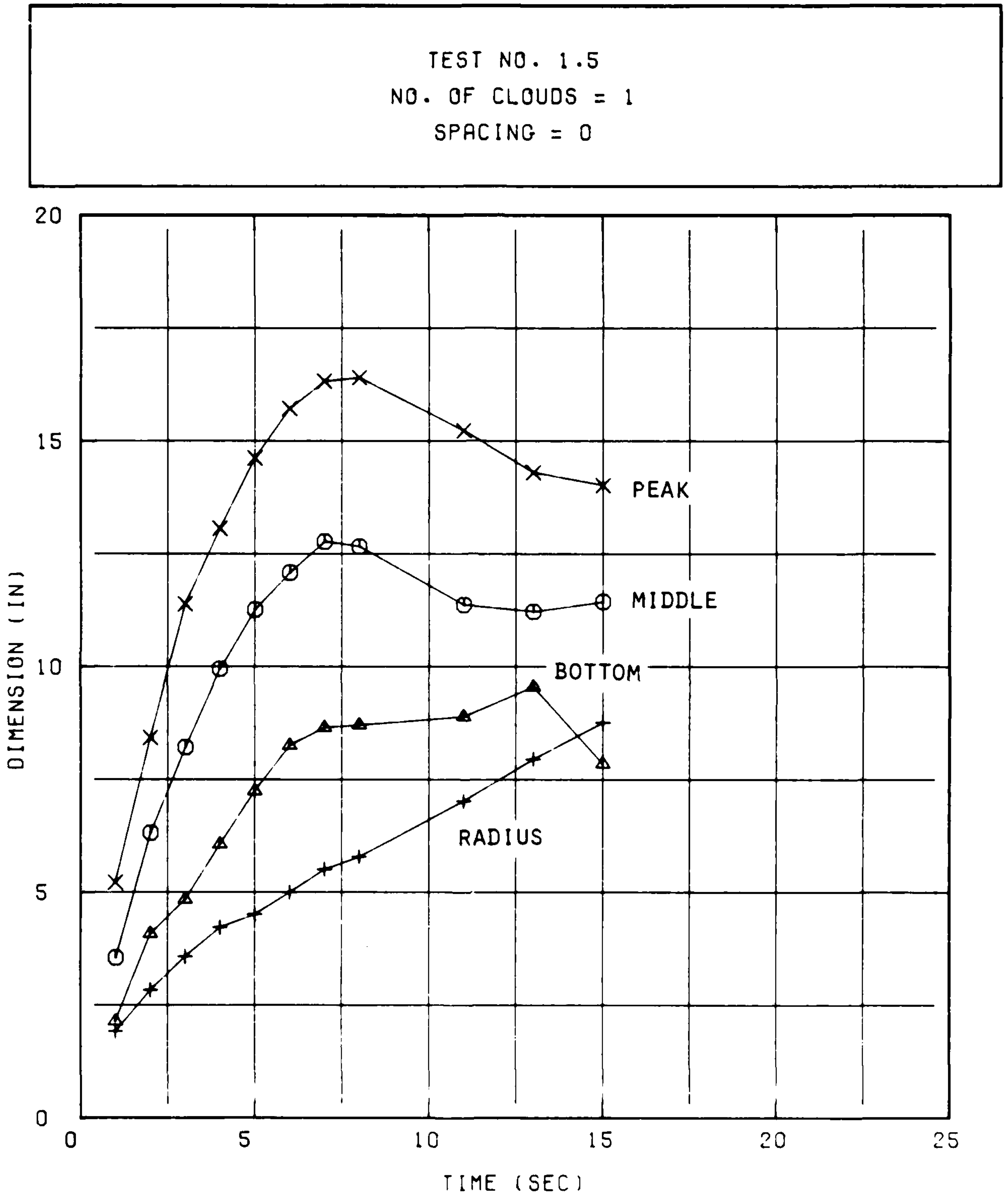

Figure 3-11. Dimension Time Histories: Test No. 1.5.

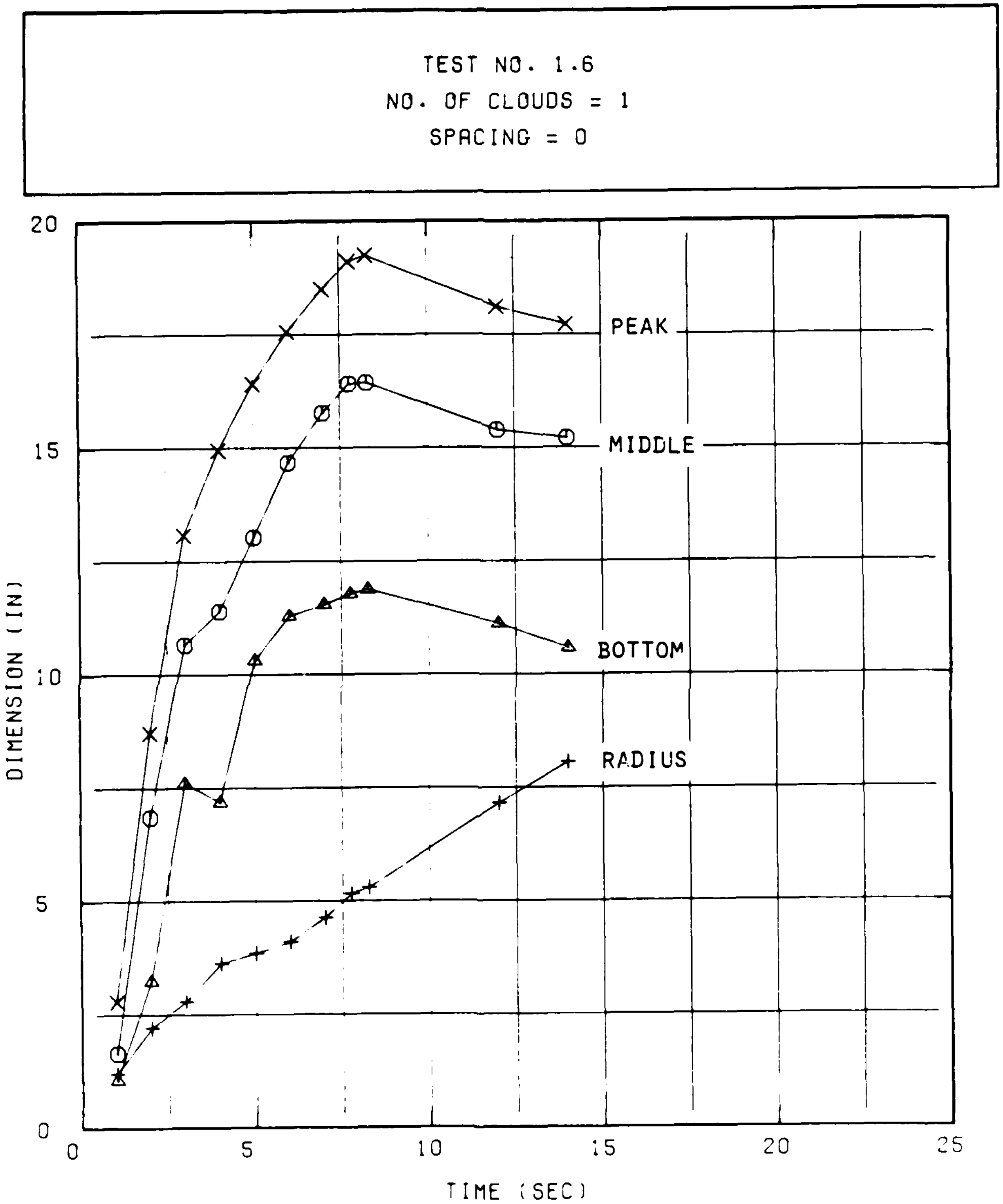

Figure 3-12. Dimension Time Histories: Test No. 1.6.

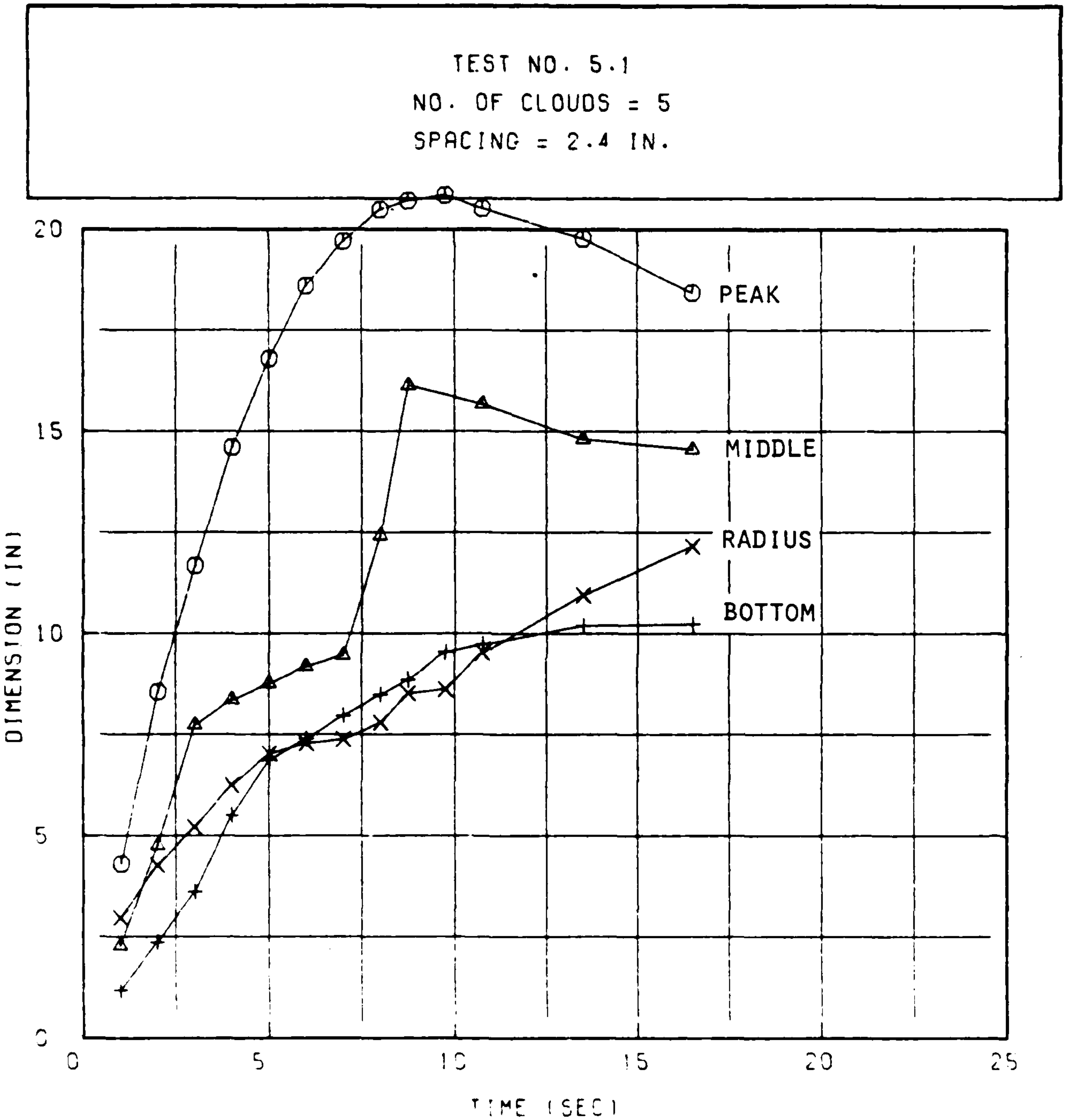

Figure 3-13. Dimension Time Histories: Test No. 5.1.

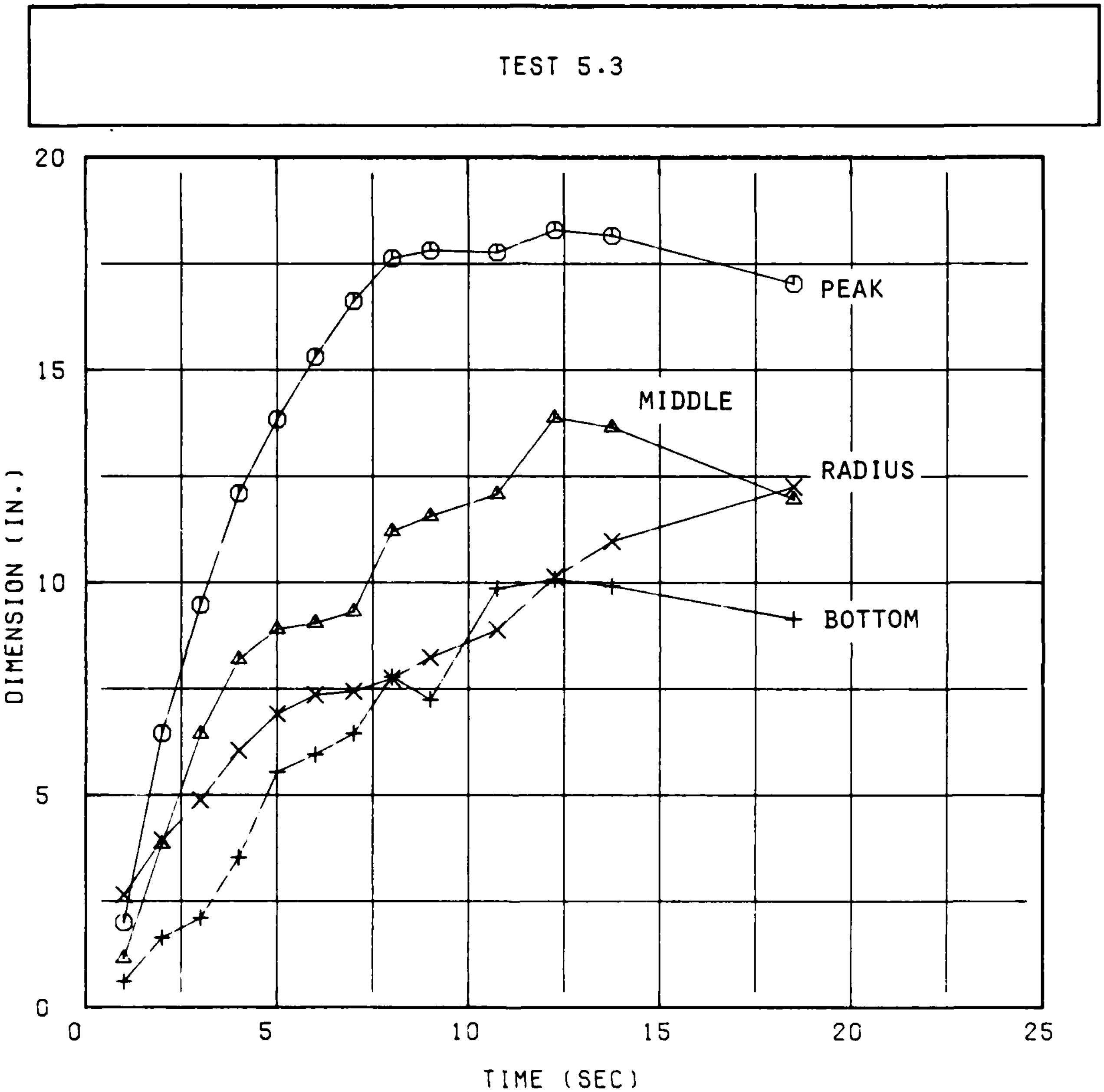

Figure 3-14. Dimension Time Histories: Test No. 5.3.

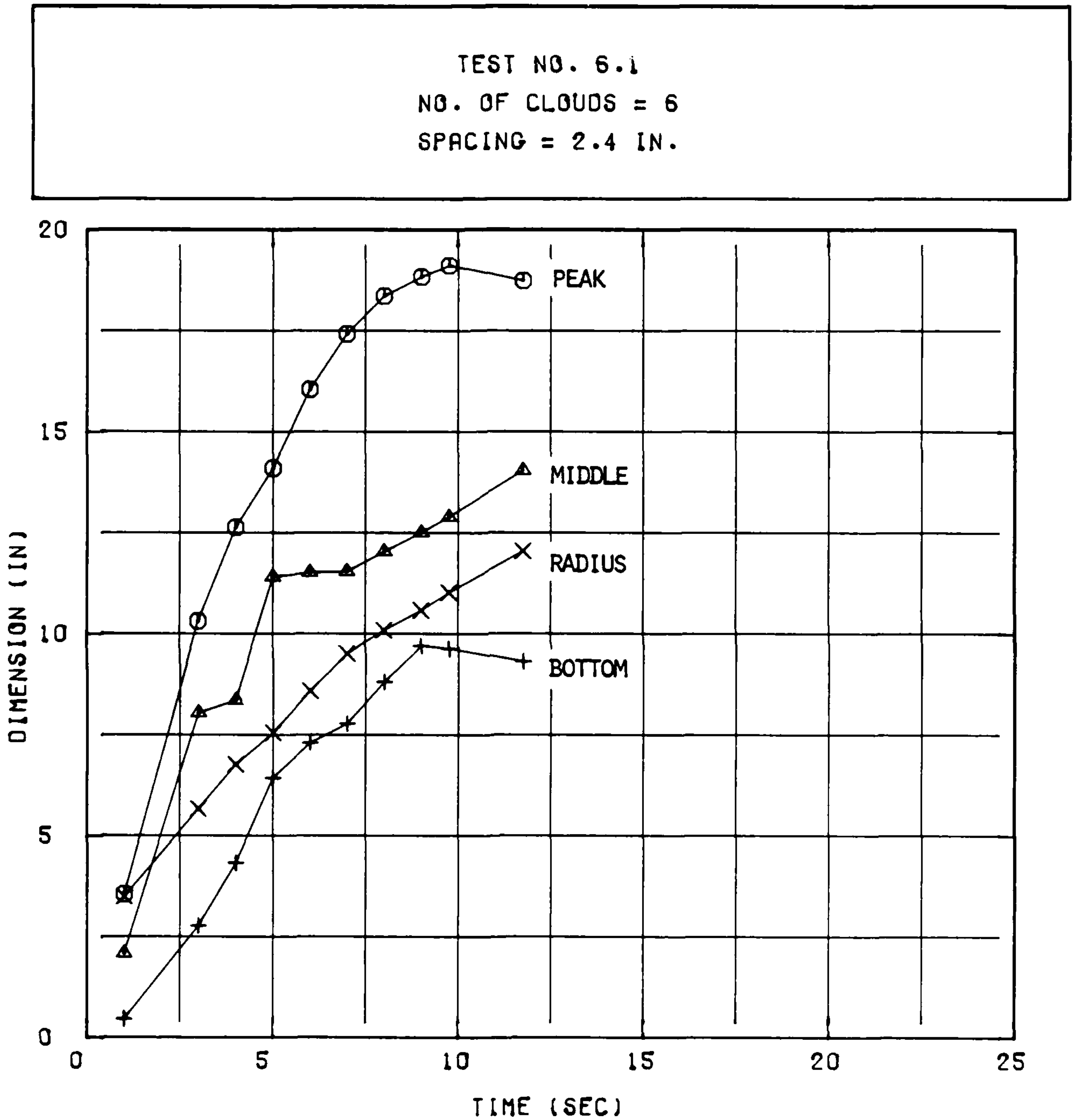

Figure 3-15. Dimension Time Histories: Test No. 6.1.

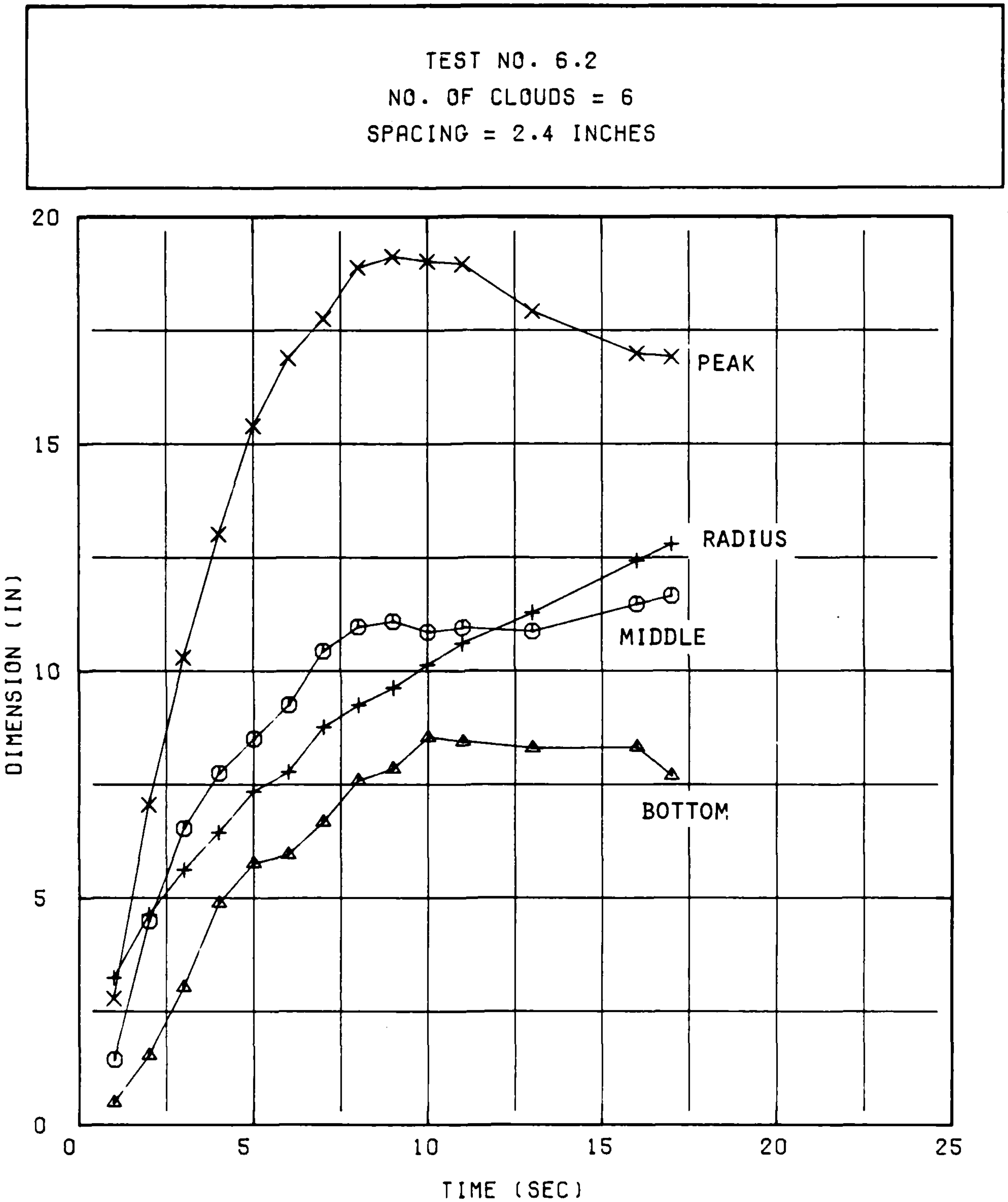

Figure 3-16. Dimension Time Histories: Test No. 6.2.

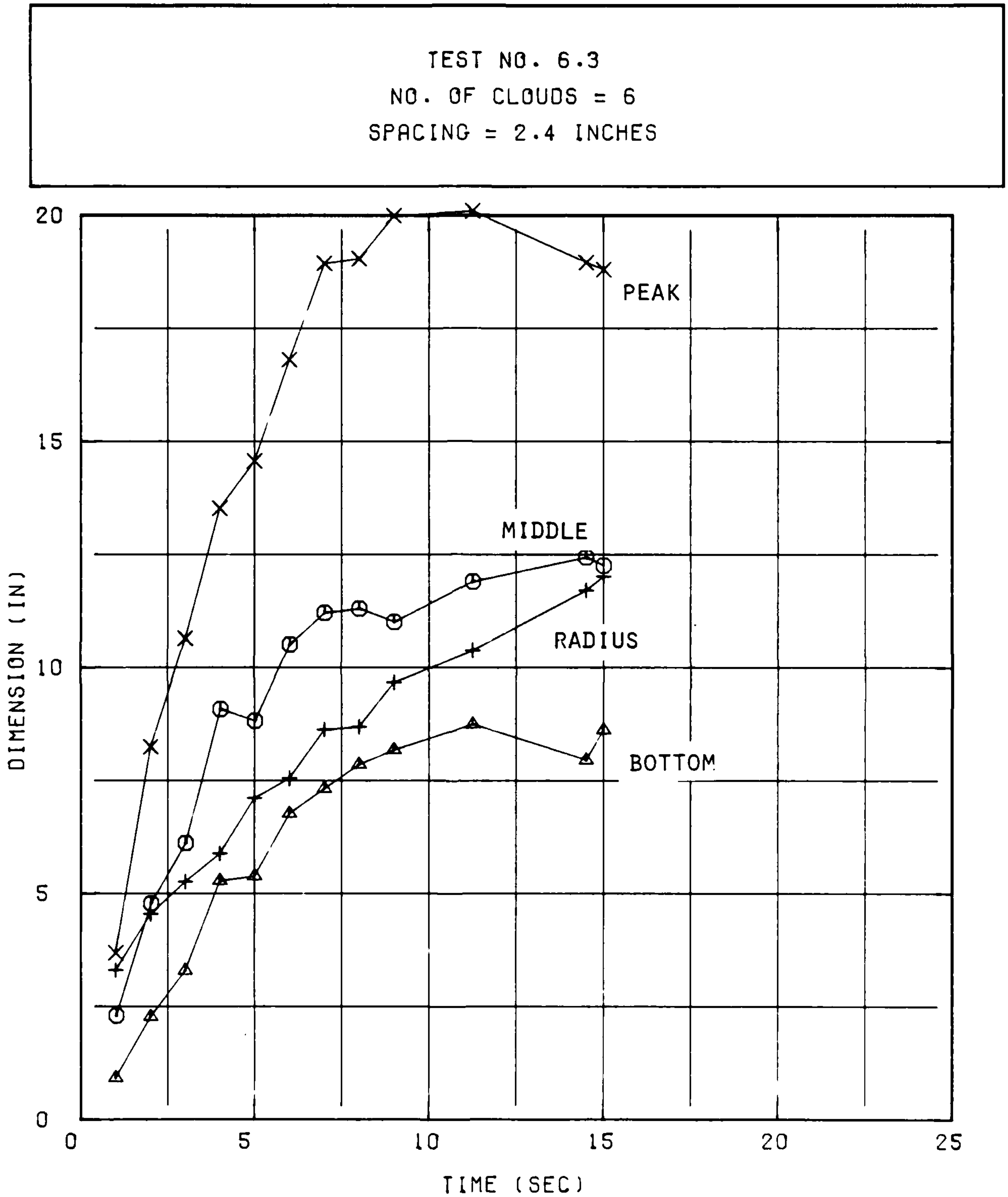

Figure 3-17. Dimension Time Histories: Test No. 6.3.

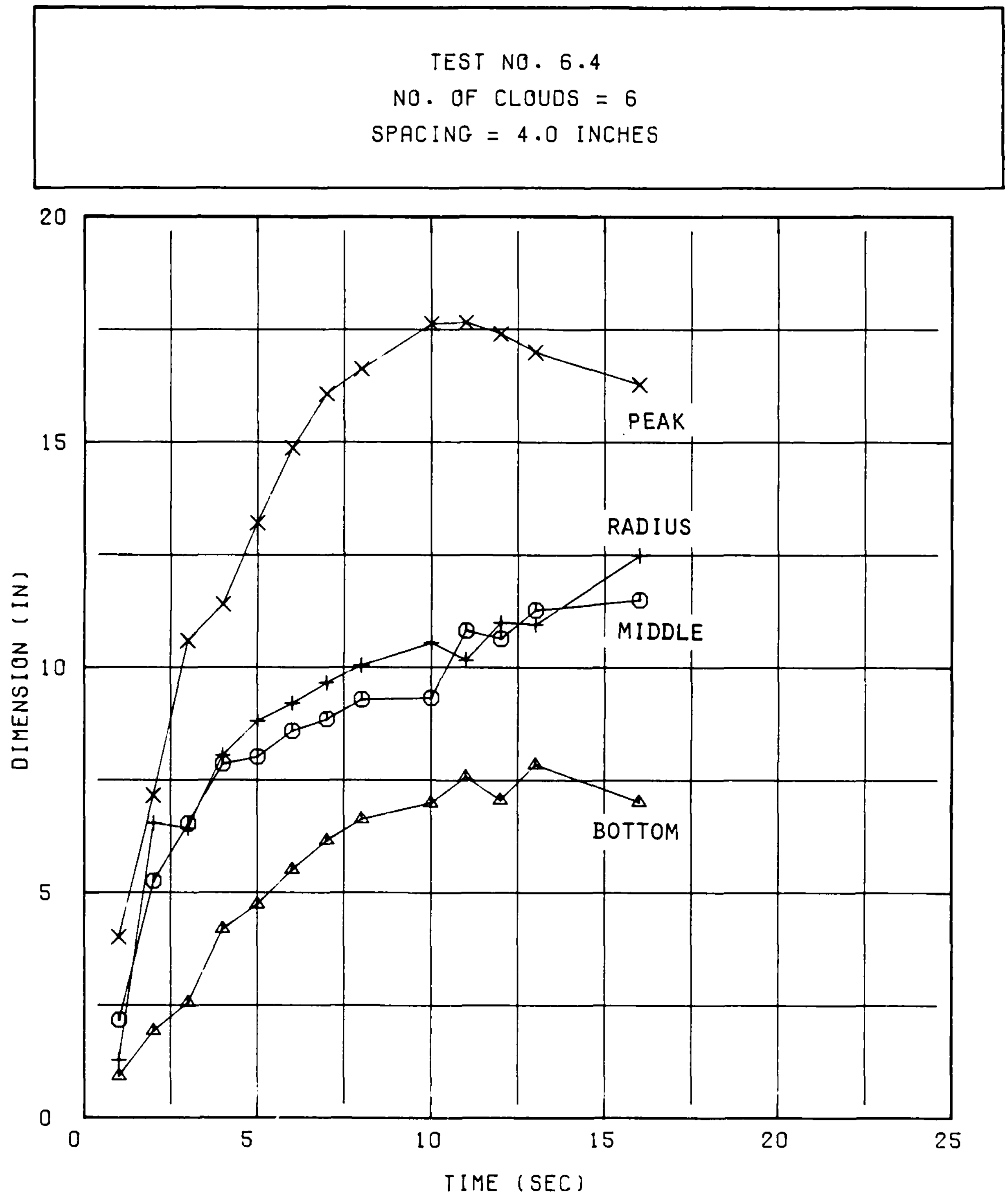

Figure 3-18. Dimension Time Histories: Test No. 6.4.

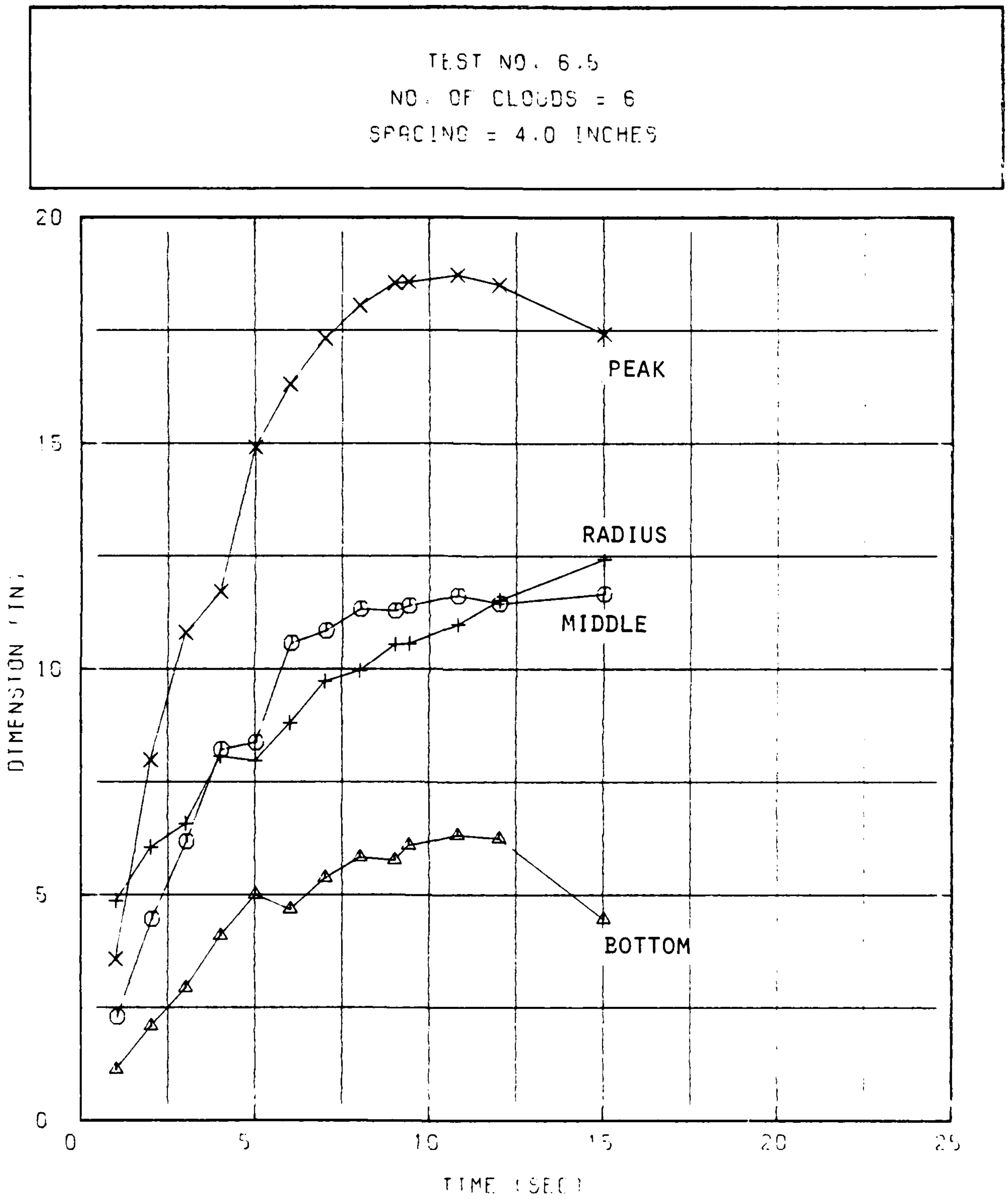

Figure 3-19. Dimension Time Histories: Test No. 6.5.

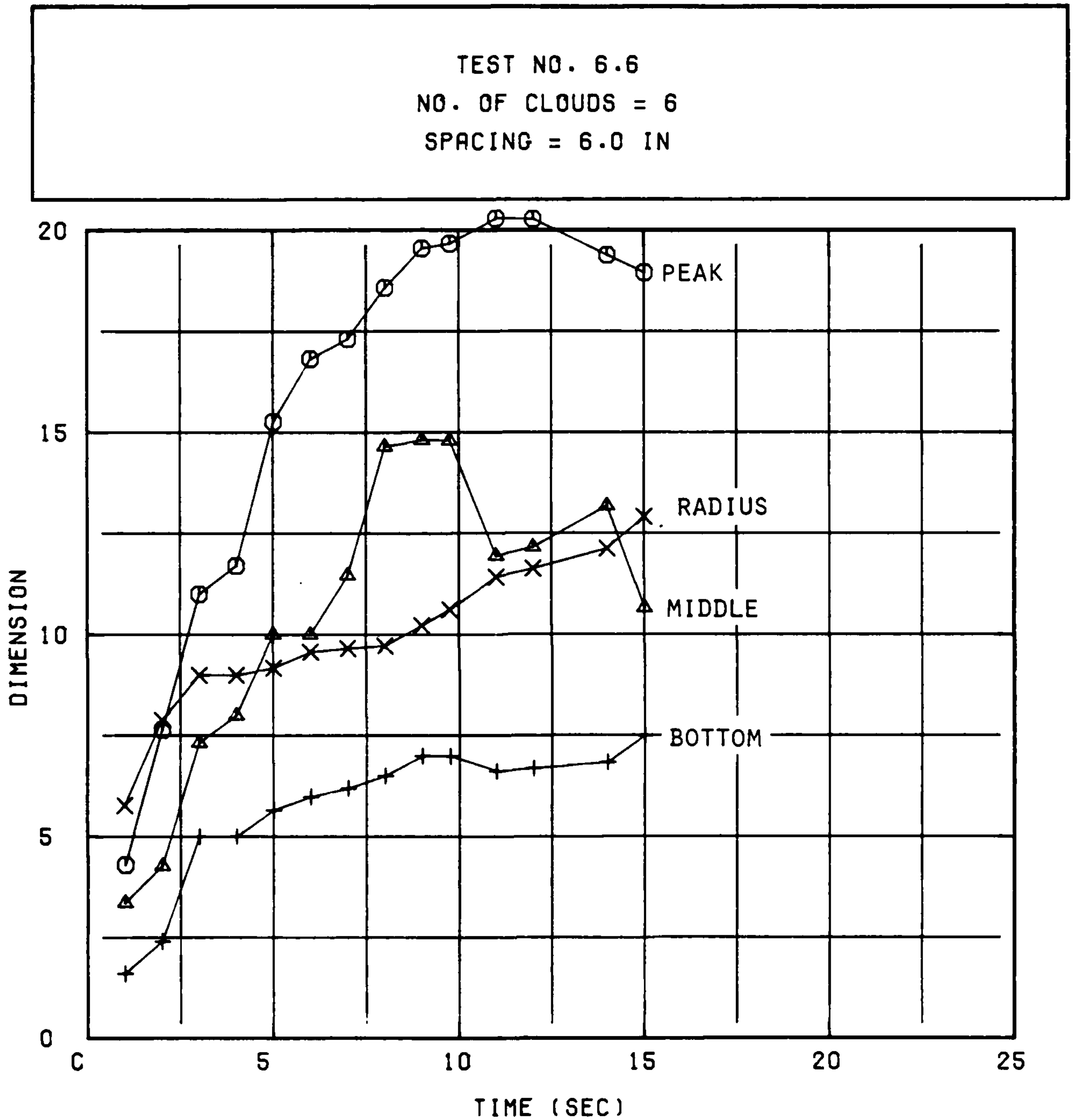

Figure 3-20. Dimension Time Histories: Test No. 6.6.

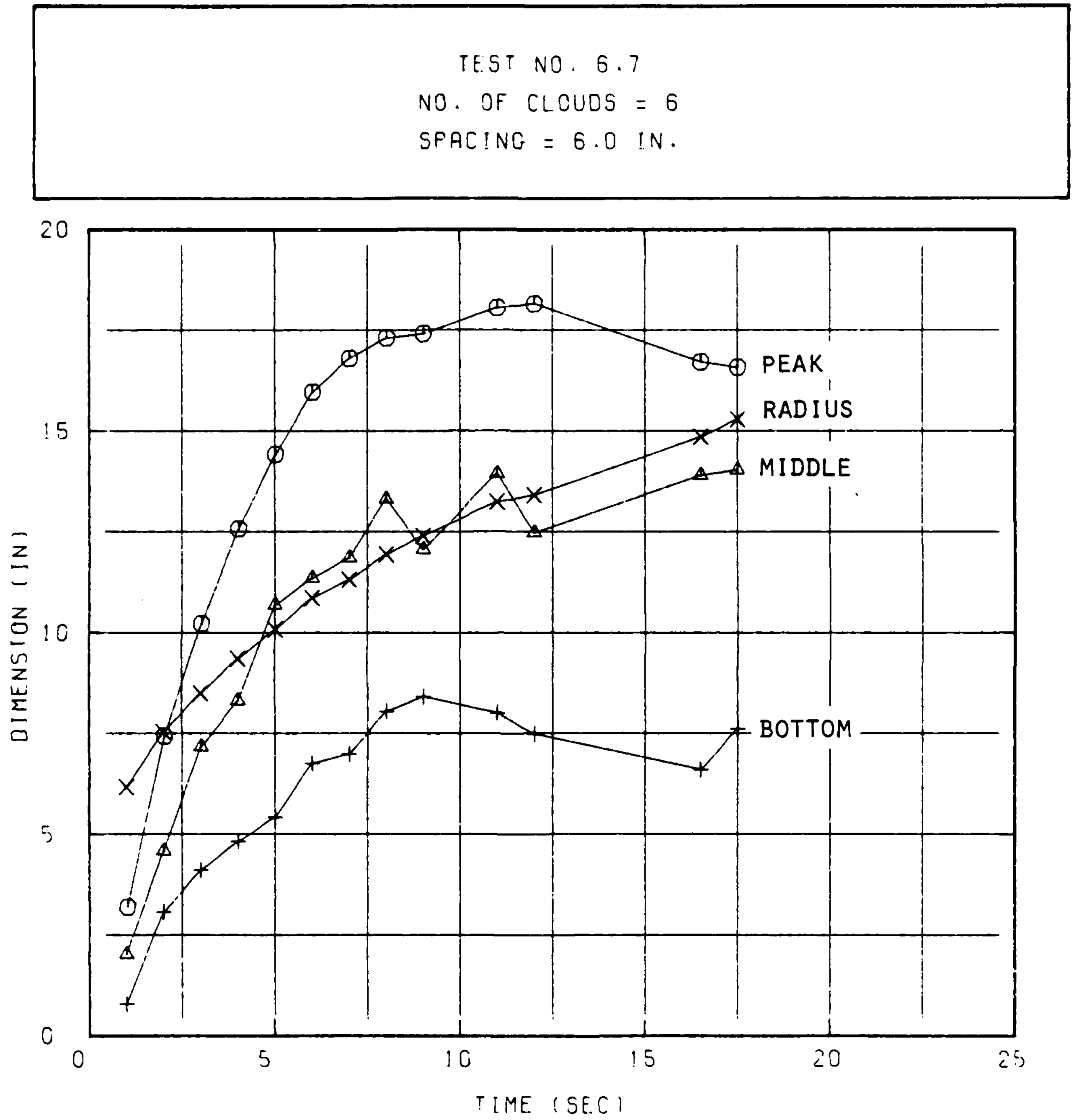

Figure 3-21. Dimension Time Histories: Test No. 6.7.

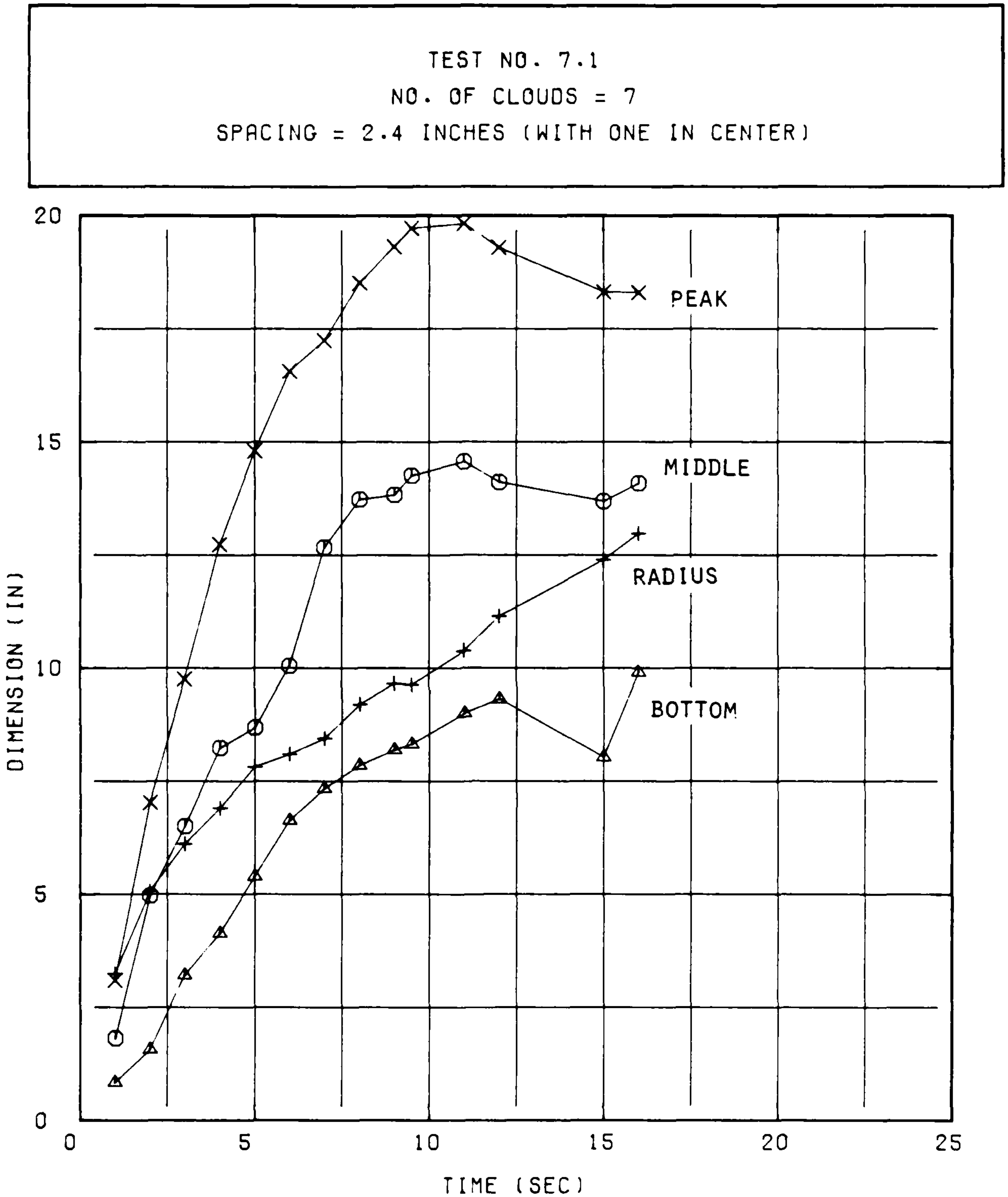

Figure 3-22. Dimension Time Histories: Test No. 7.1.

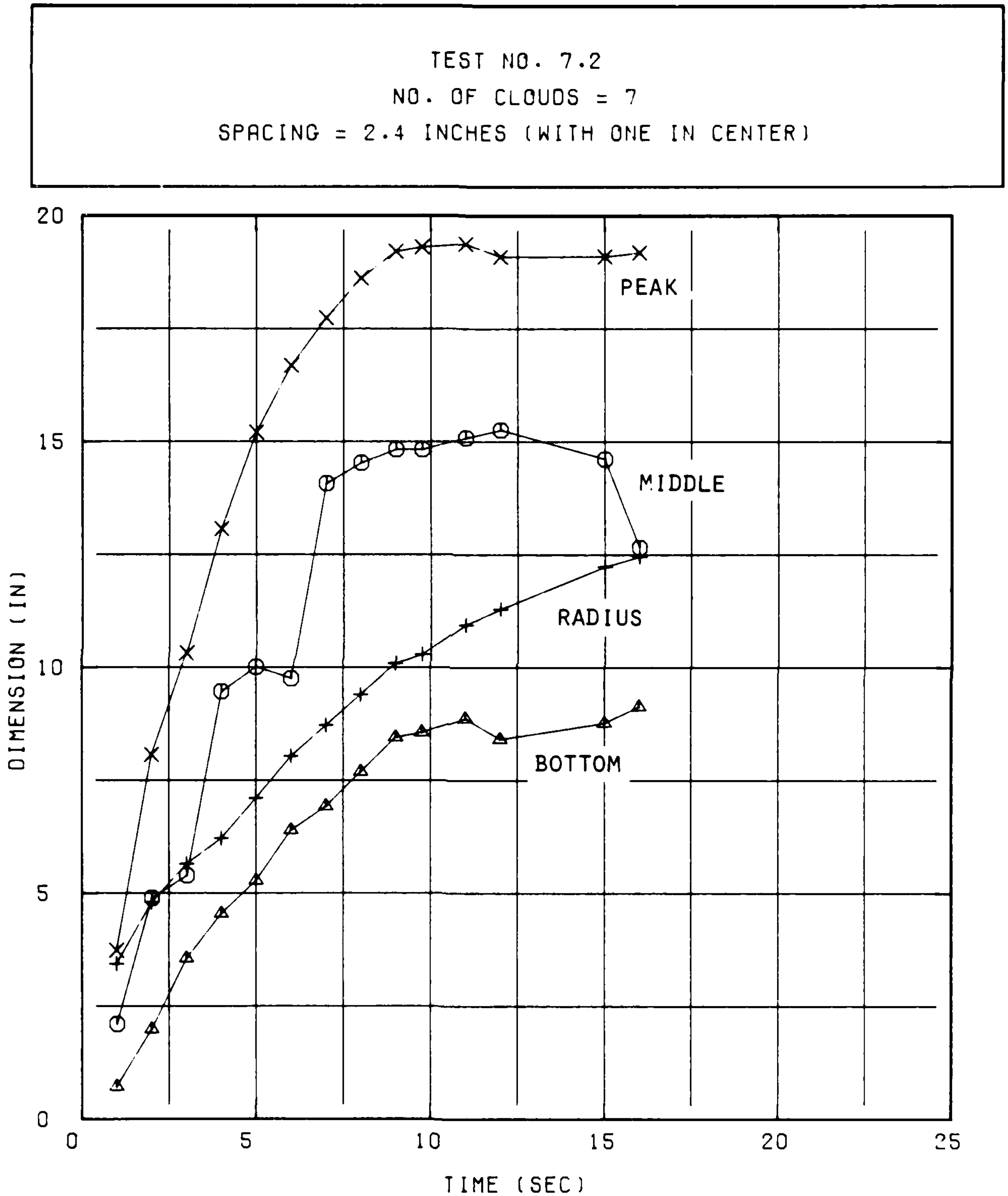

Figure 3-23. Dimension Time Histories: Test No. 7.2.

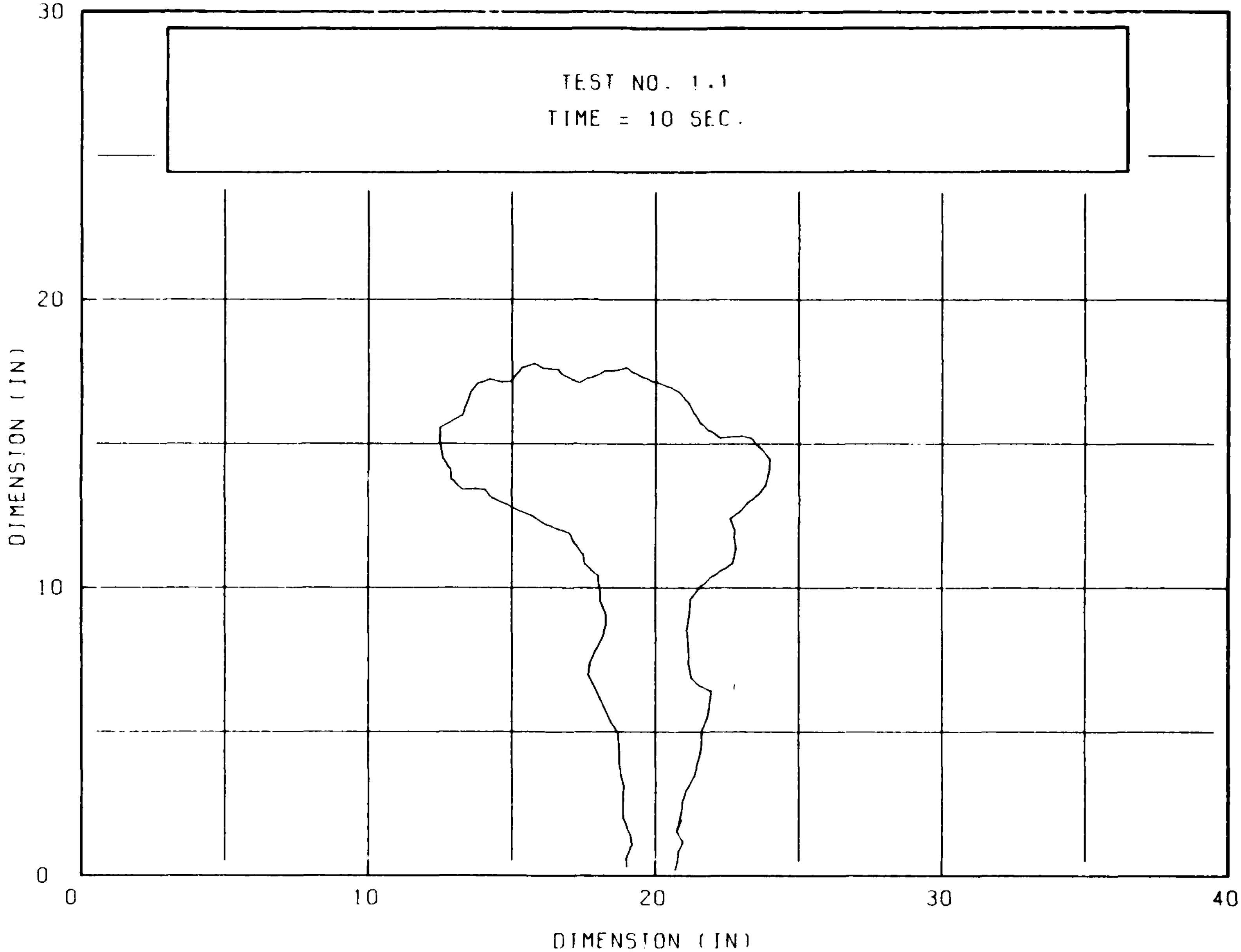

Figure 3-24. Cloud Outline: Test No. 1.1, 10 Seconds.

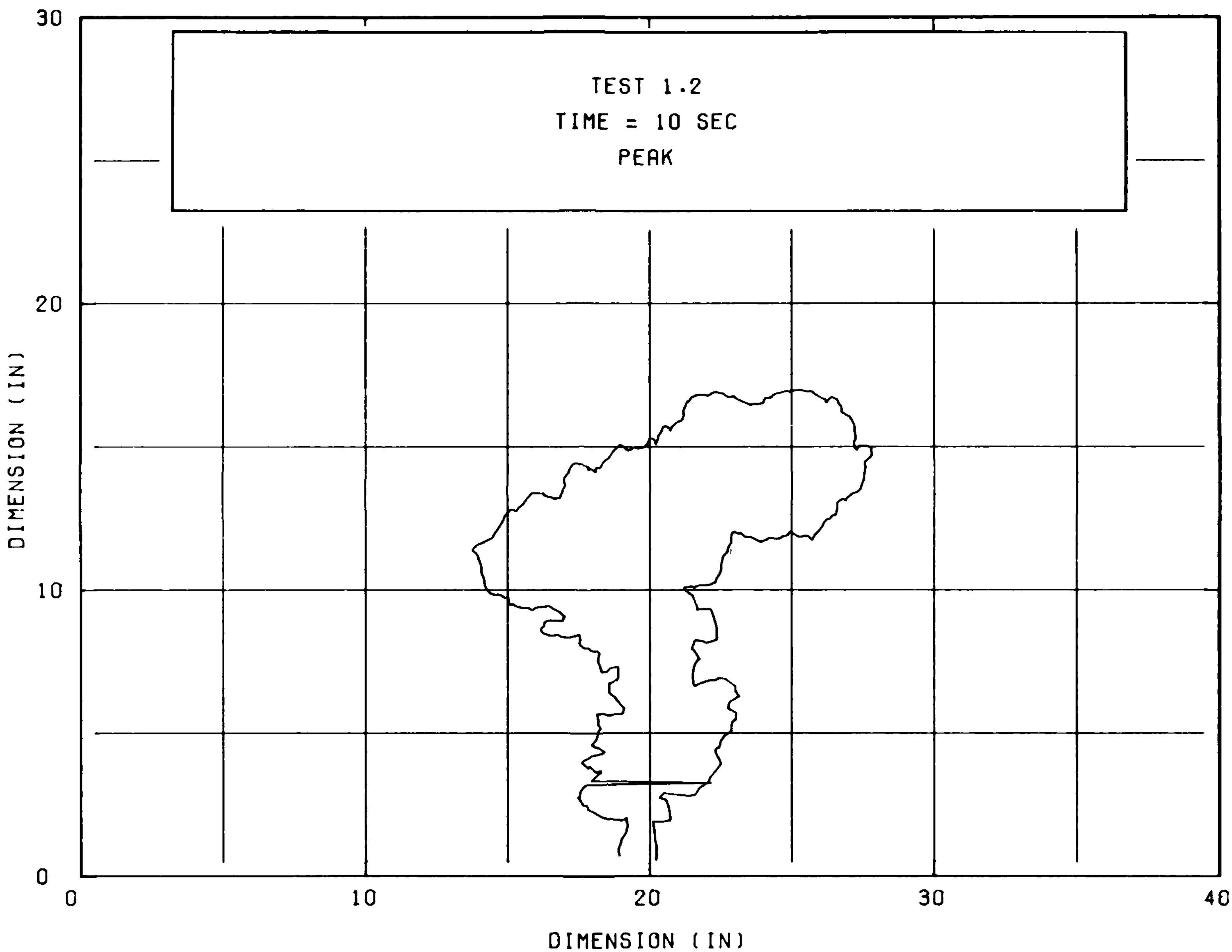

Figure 3-25. Cloud Outline: Test No. 1.2,10 Seconds.

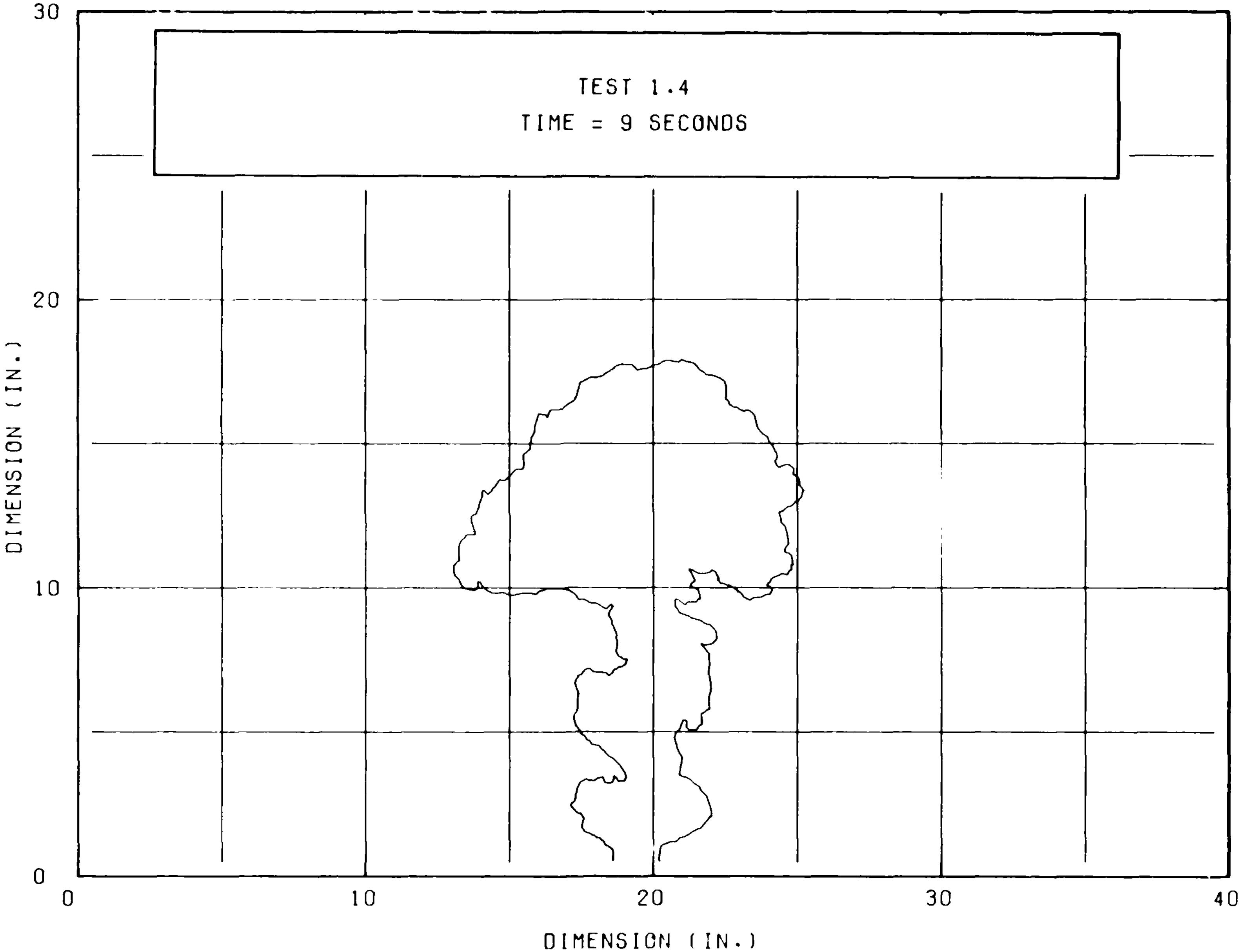

Figure 3-26. Cloud Outline: Test No. 1.4, 9 Seconds.

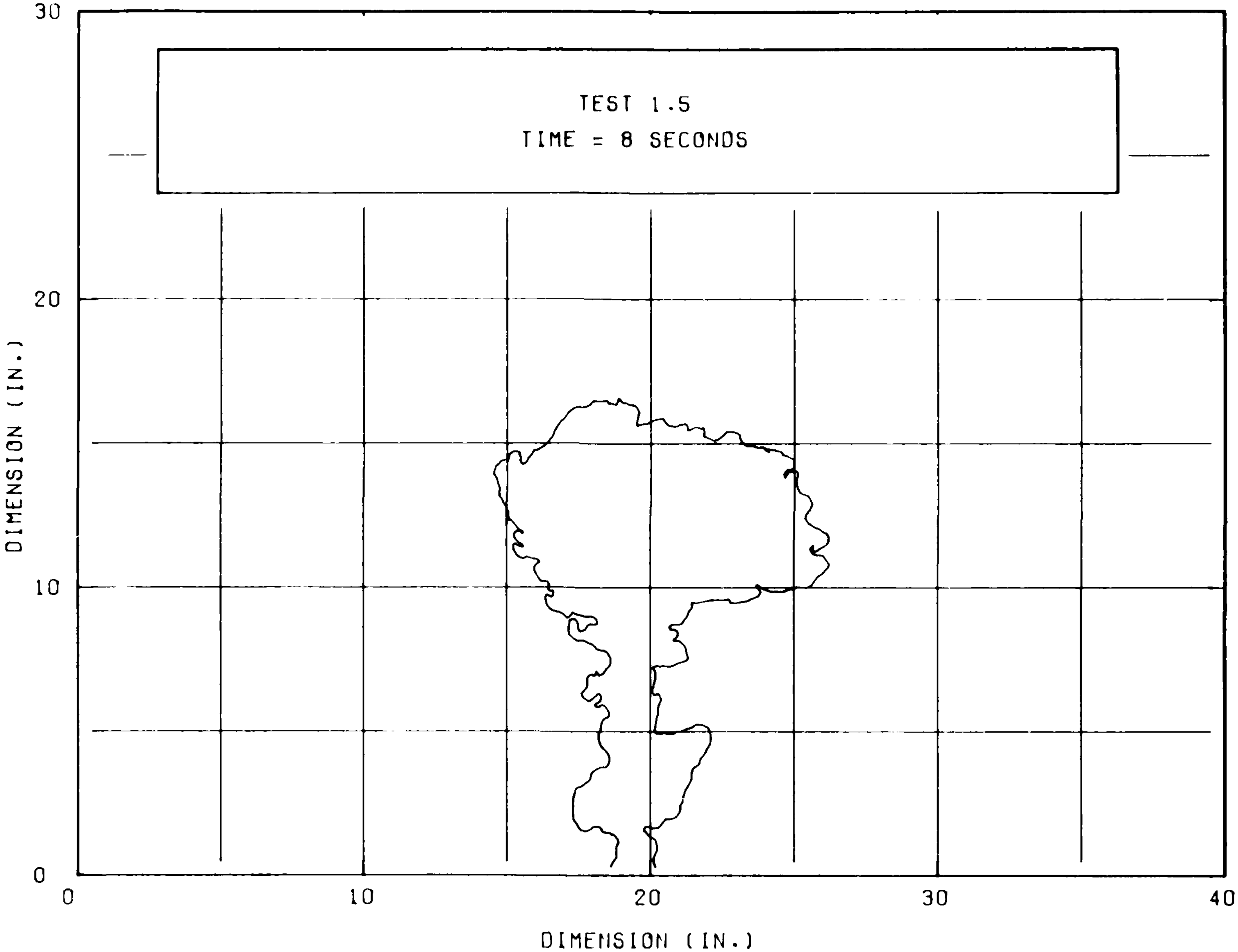

Figure 3-27. Cloud Outline: Test No. 1.5, 8 Seconds.

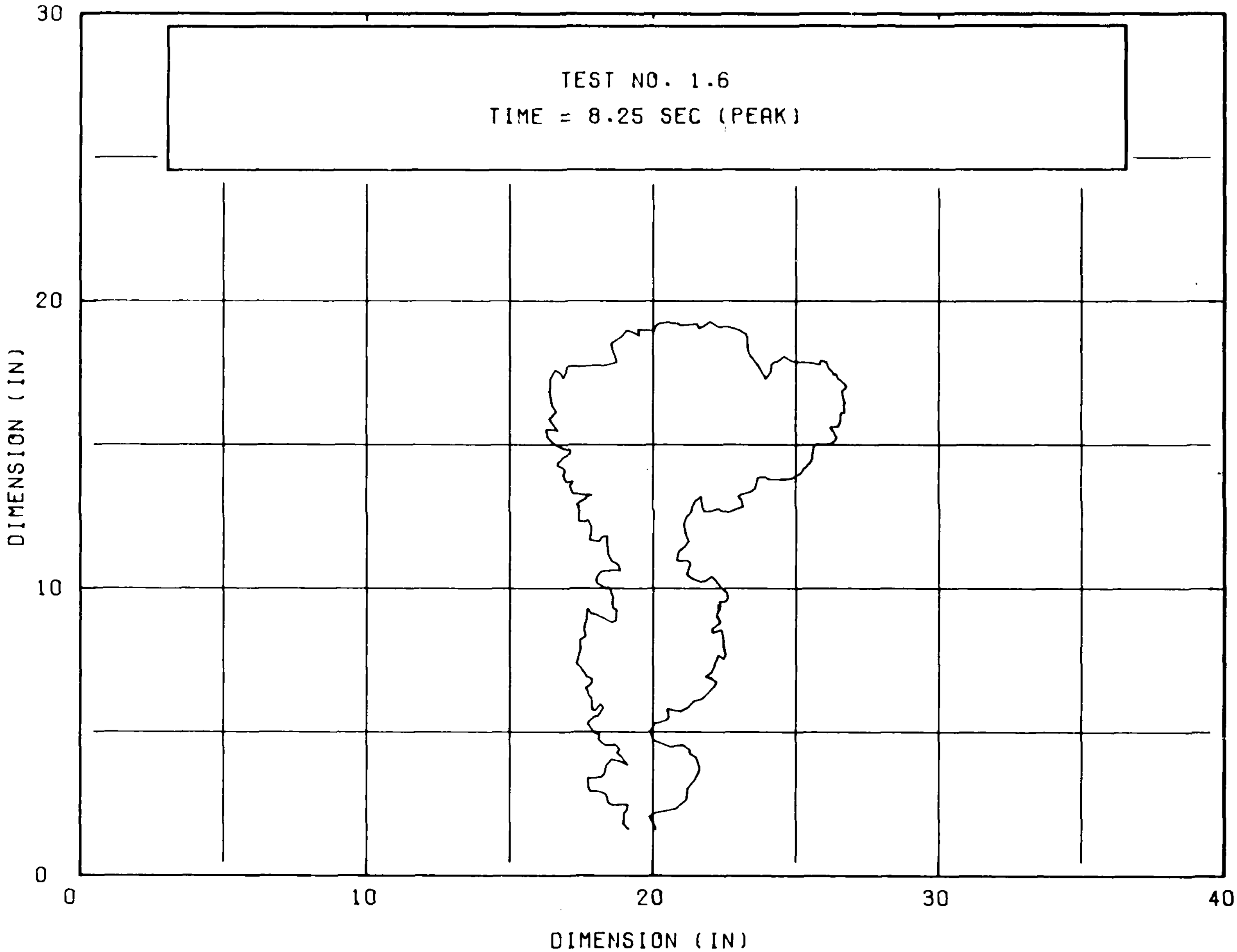

Figure 3-28. Cloud Outline: Test No. 1.6, 8.25 Seconds.

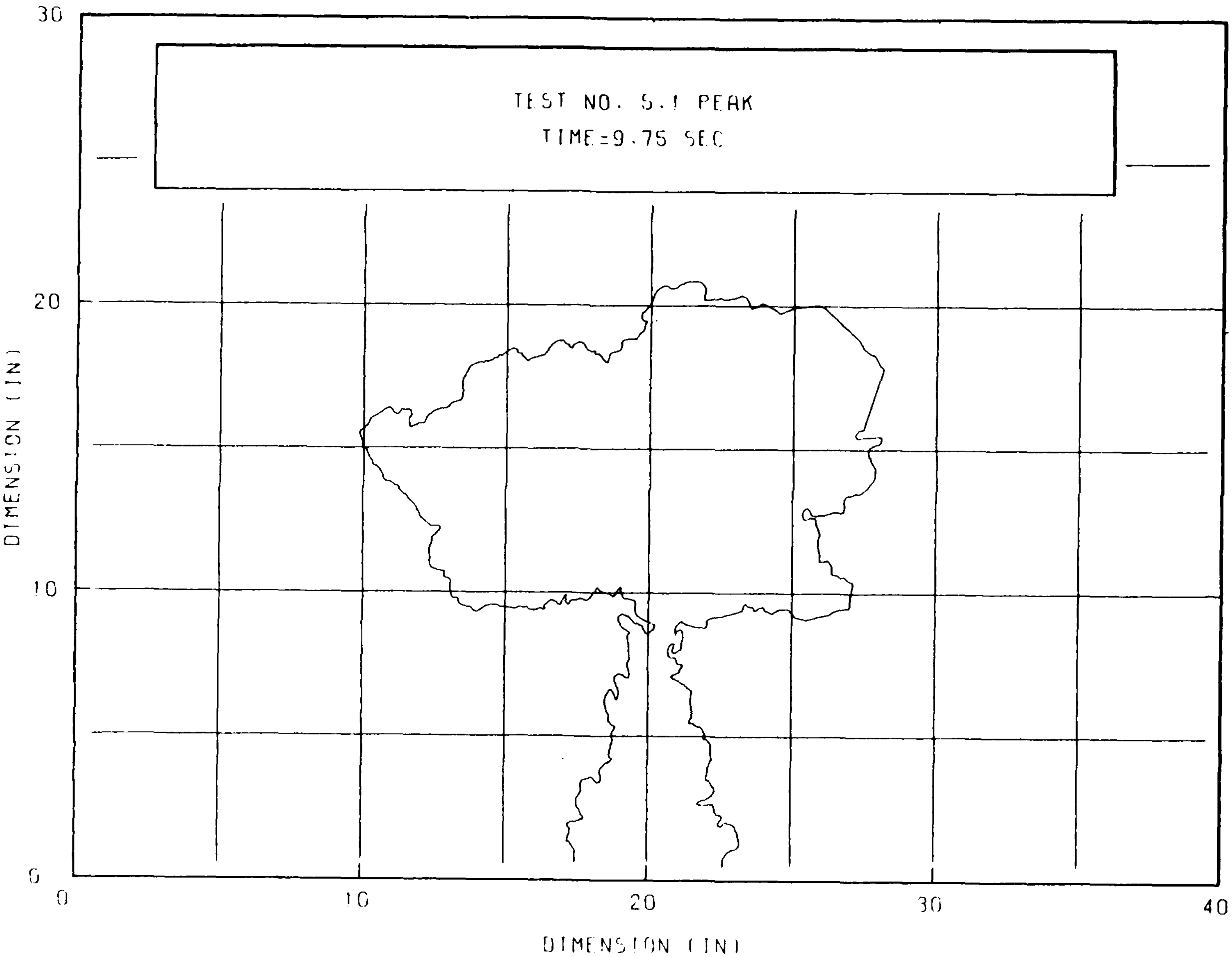

Figure 3-29. Cloud Outline: Test No. 5.1, 9.75 Seconds.

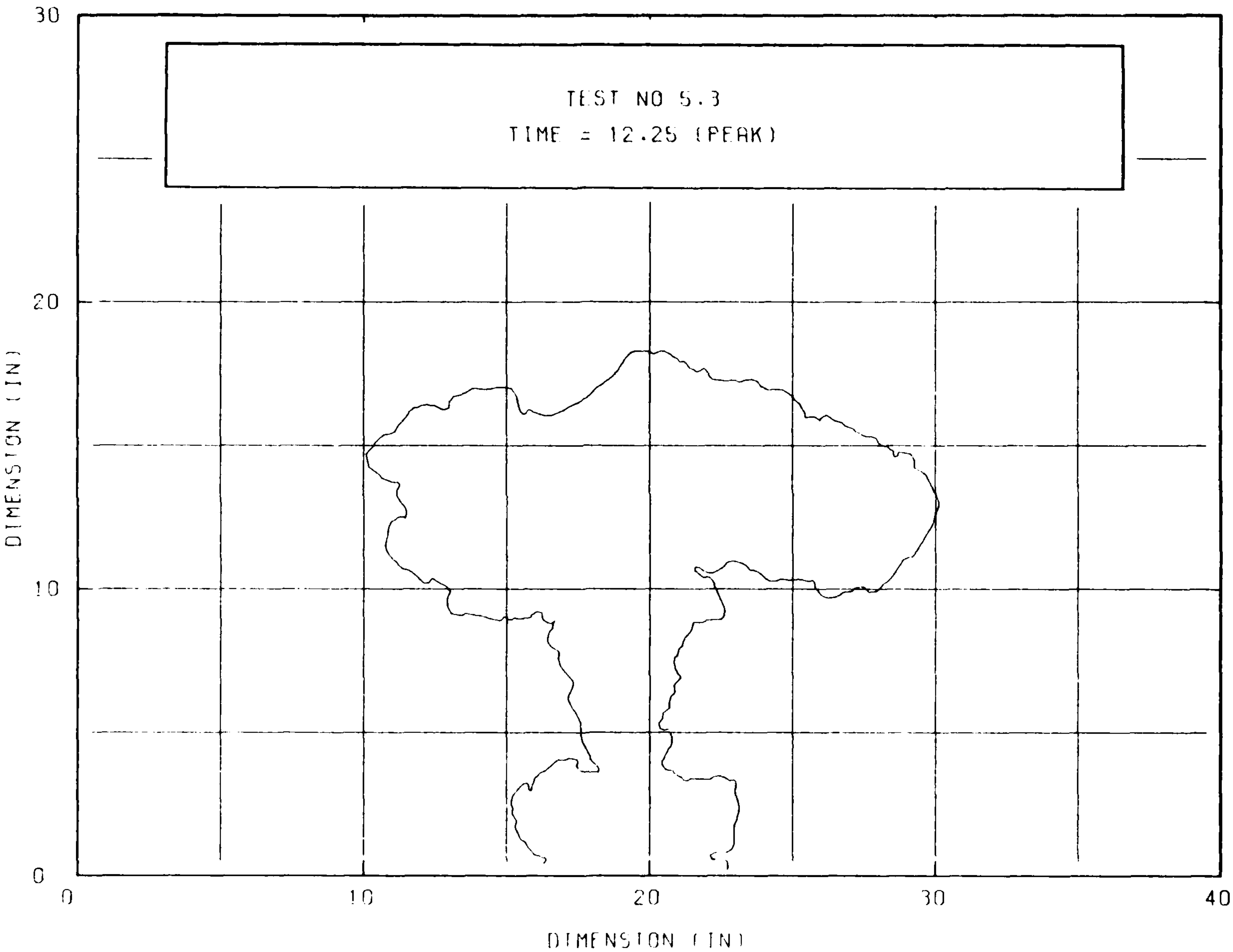

Figure 3-30. Cloud Outline: Test No. 5.3, 12.25 Seconds.

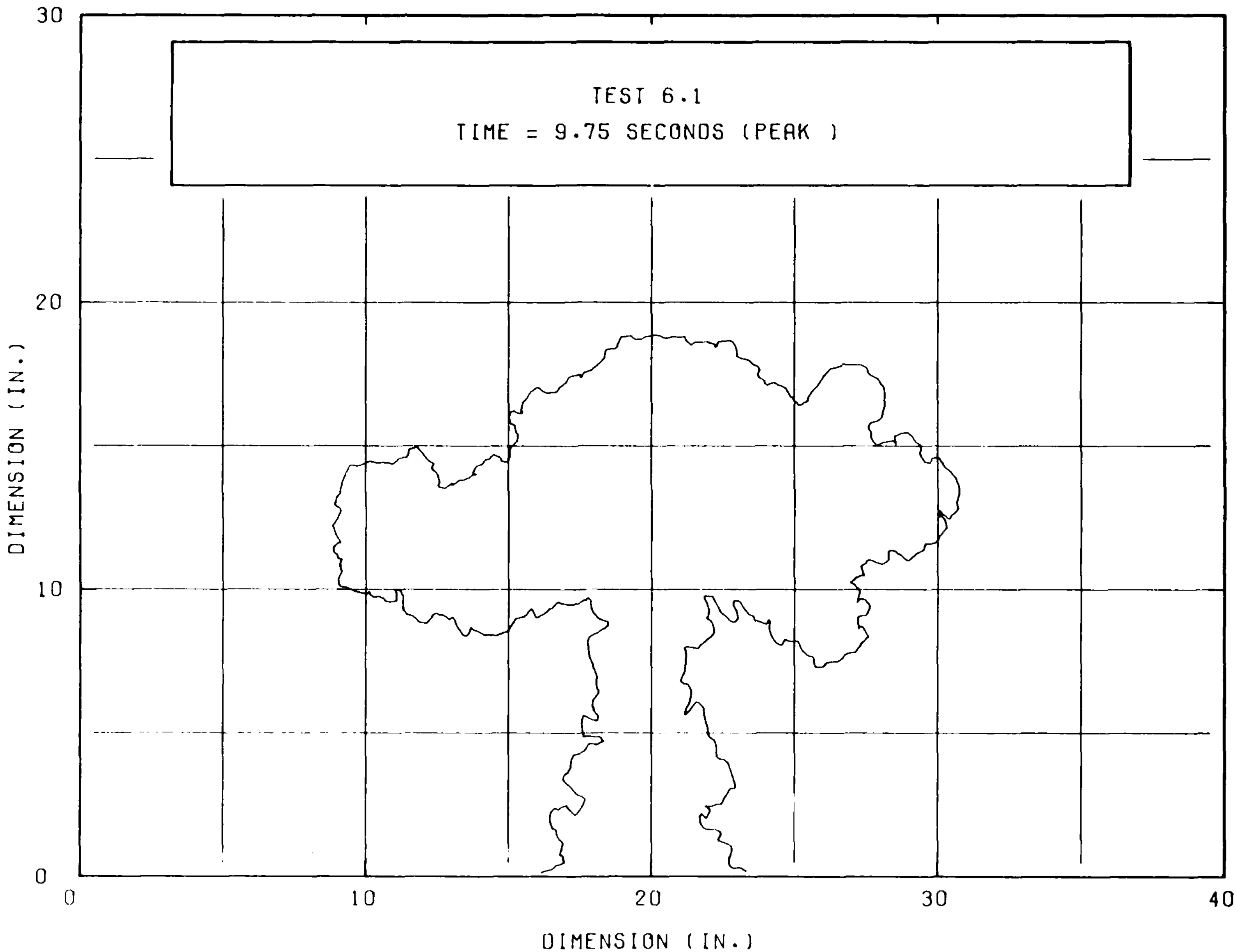

Figure 3-31. Cloud Outline: Test No. 6.1, 9.75 Seconds.

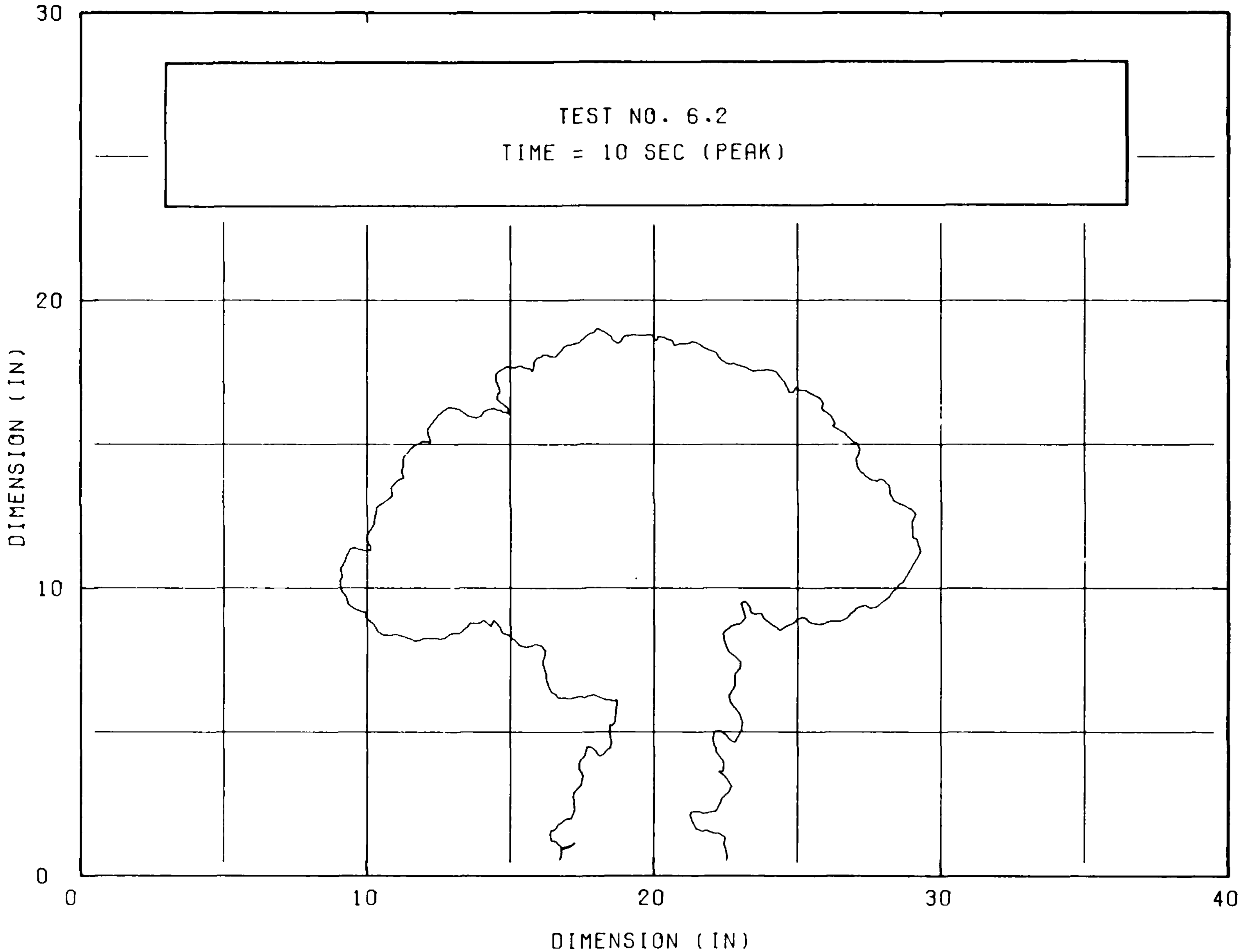

Figure 3-32. Cloud Outline: Test No. 6.2, 10 Seconds.

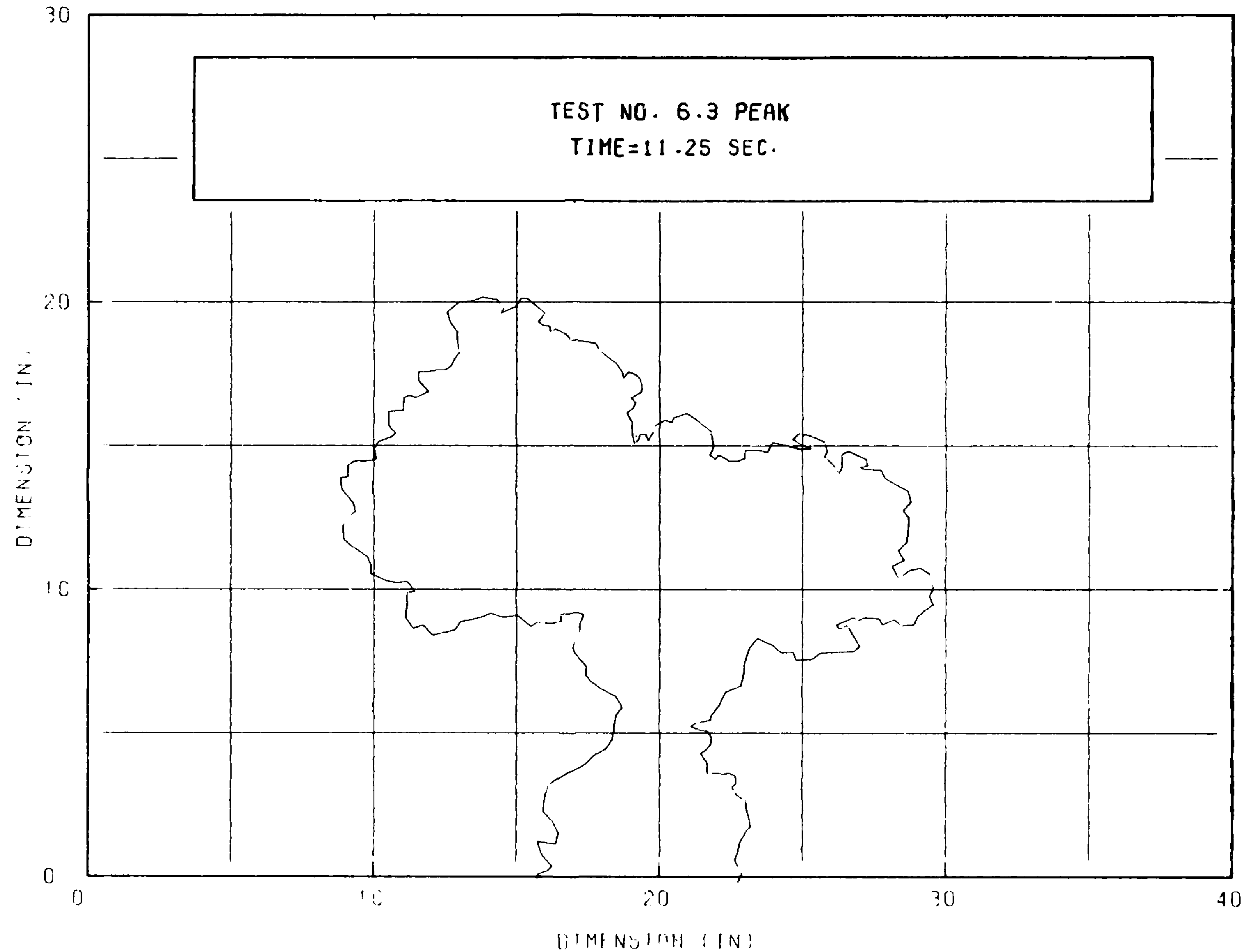

Figure 3-33. Cloud Outline: Test No. 6.3, 11.25 Seconds.

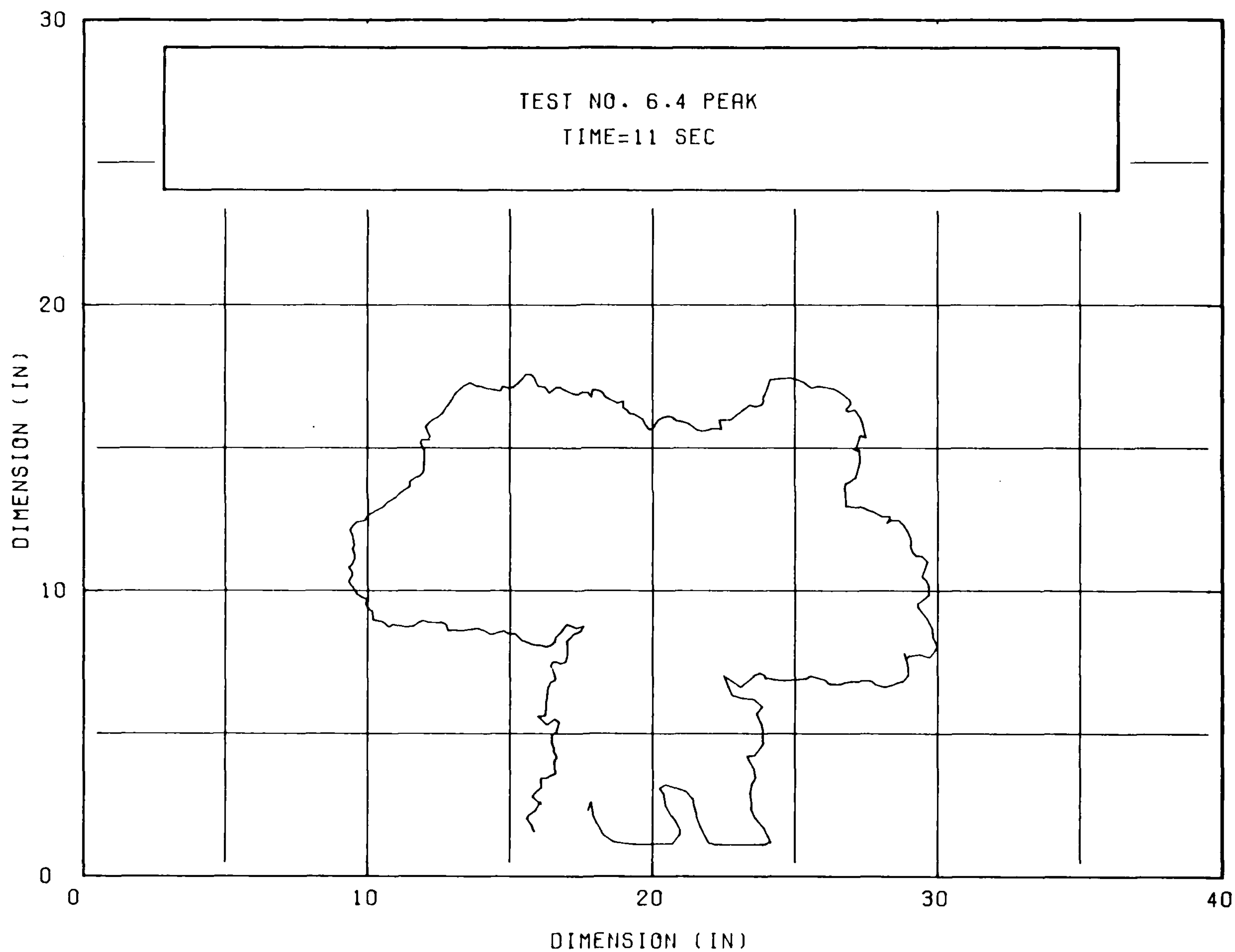

Figure 3-34. Cloud Outline: Test No. 6.4, 11 Seconds.

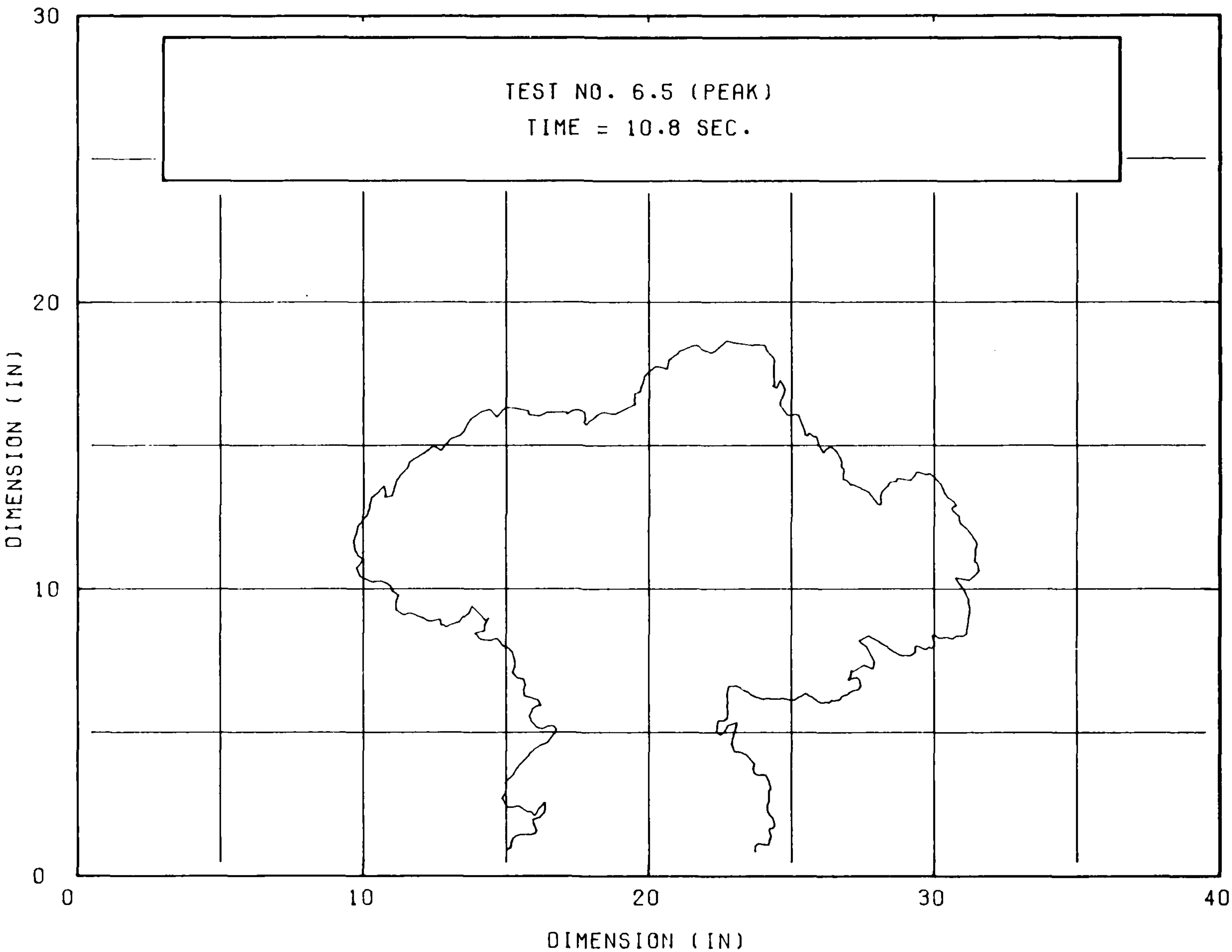

Figure 3-35. Cloud Outline: Test No. 6.5, 10.8 Seconds.

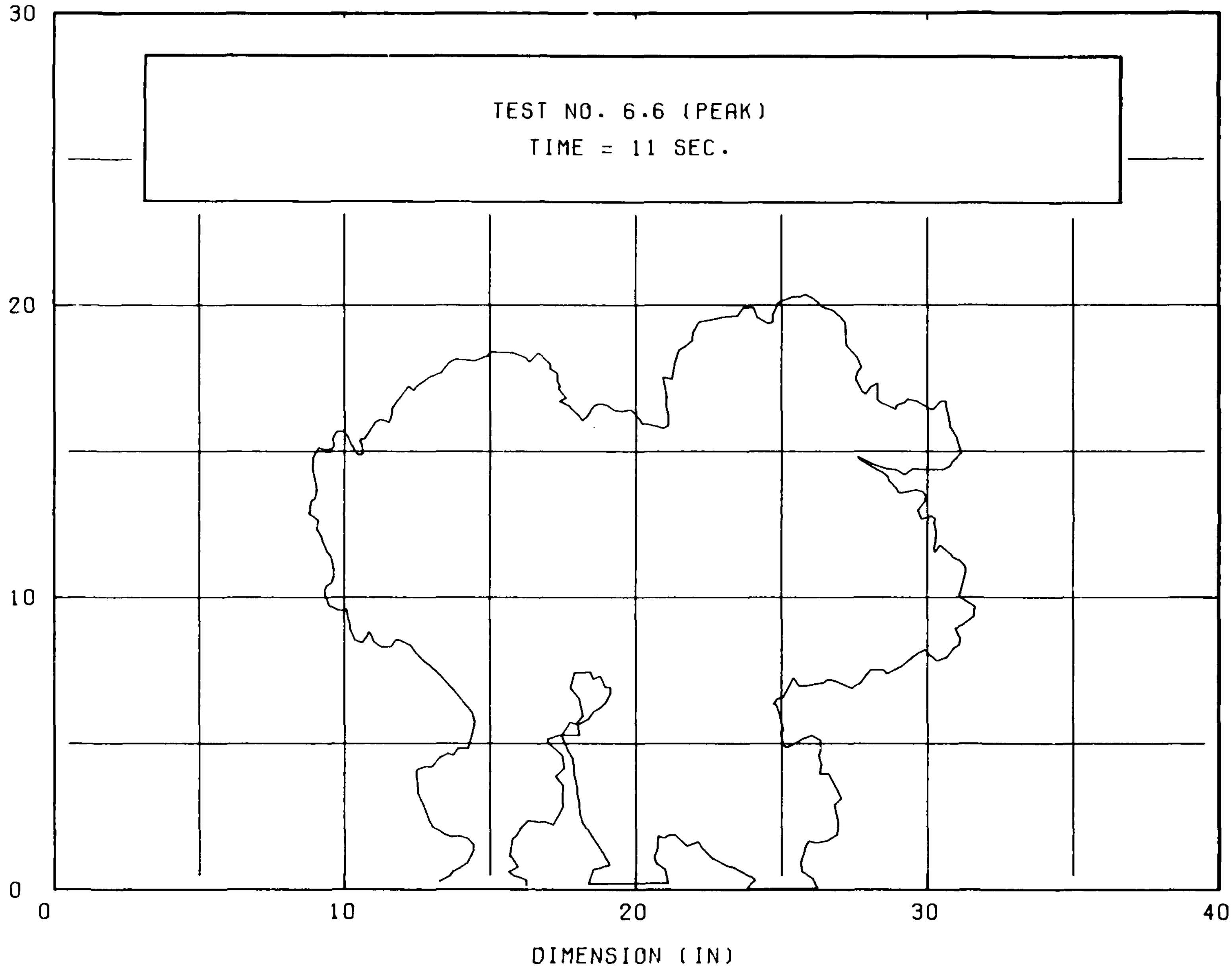

Figure 3-36. Cloud Outline: Test No. 6.6, 11 Seconds.

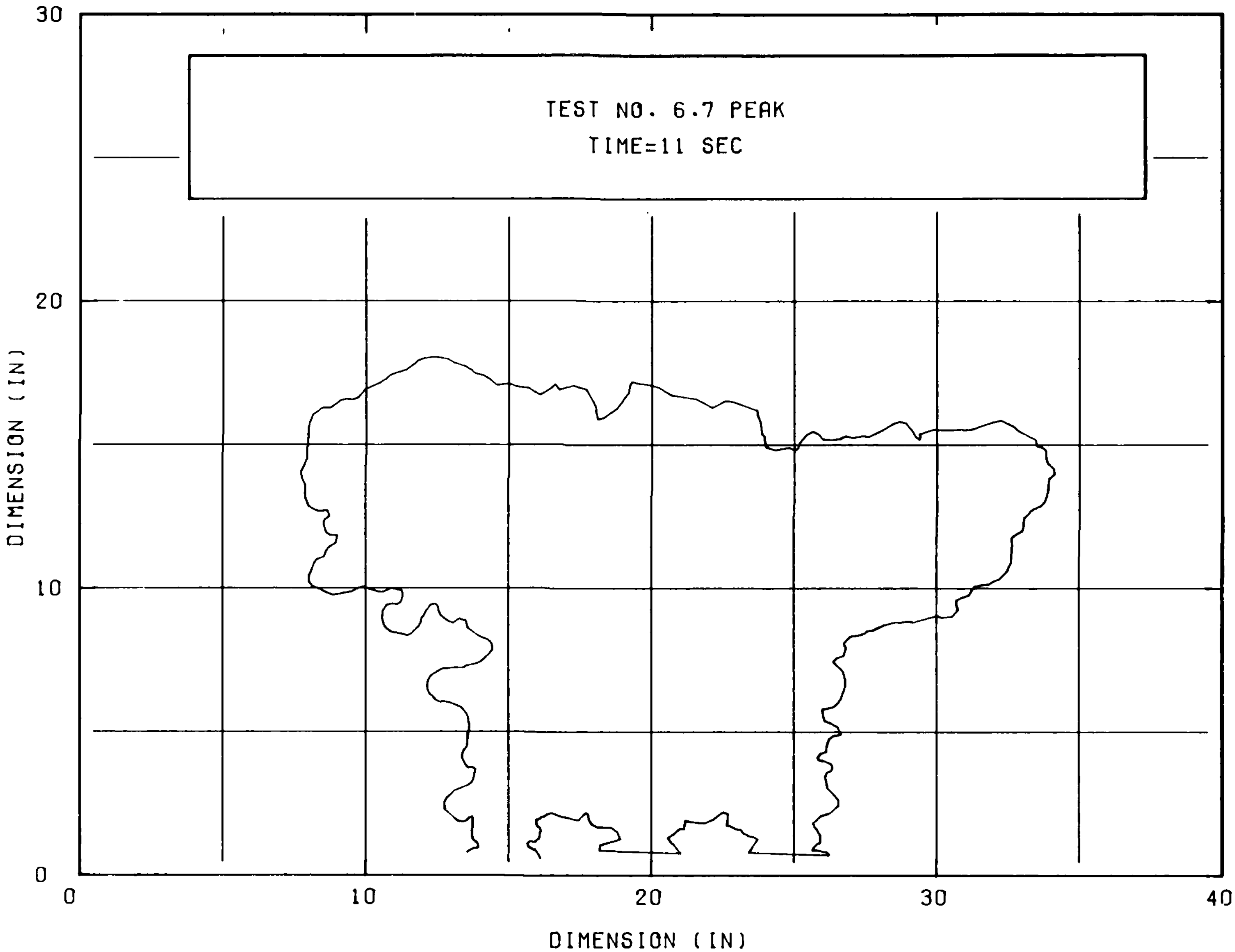

Figure 3-37. Cloud Outline: Test No. 6.7, 11 Seconds.

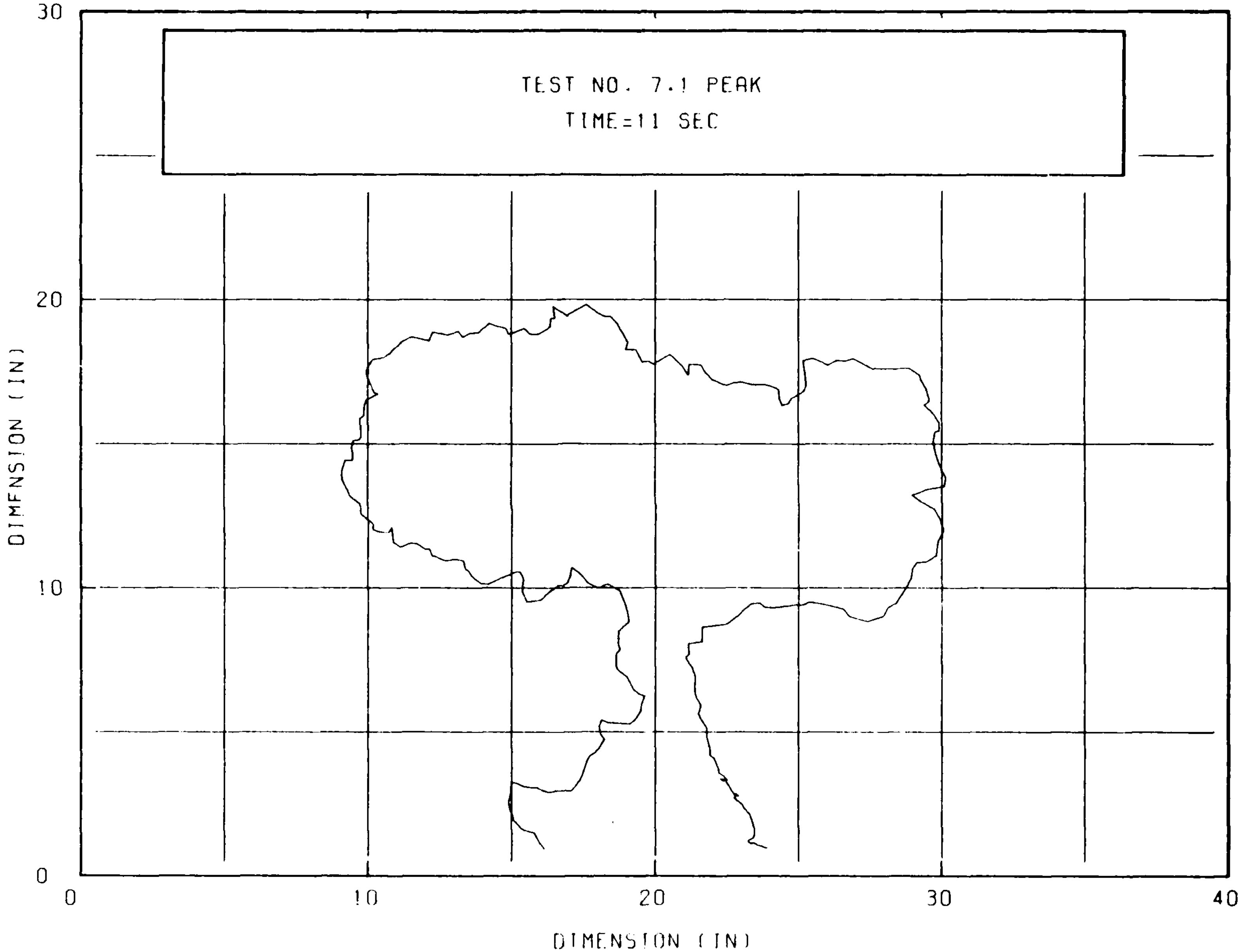

Figure 3-38. Cloud Outline: Test No. 7.1, 11 Seconds.

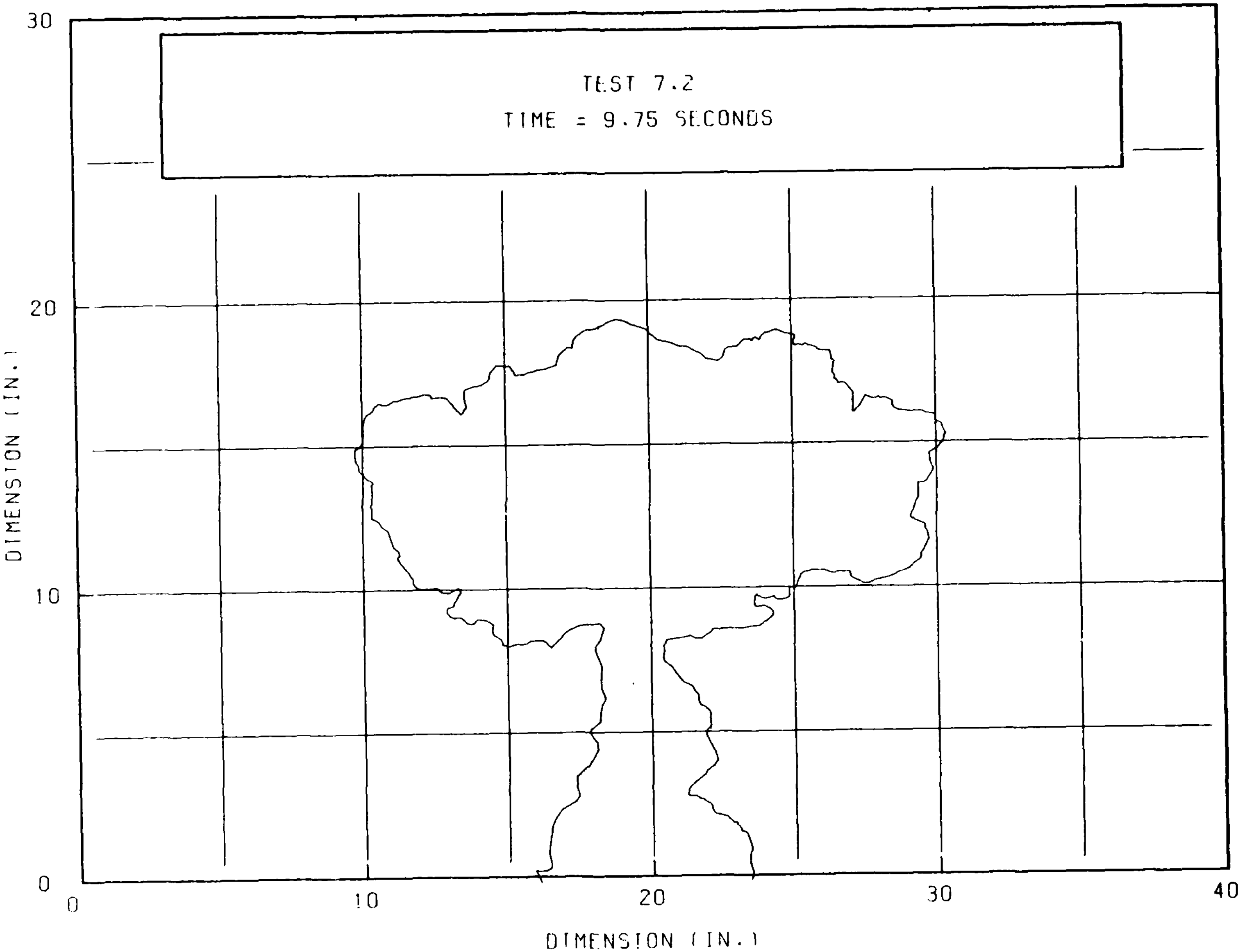

Figure 3-39. Cloud Outline: Test No. 7.2, 9.75 Seconds.

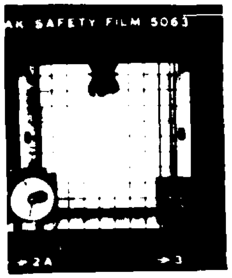

1.3 Seconds

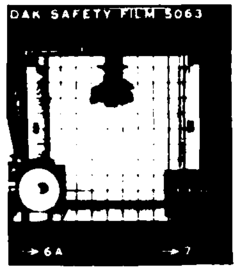

2.6 Seconds

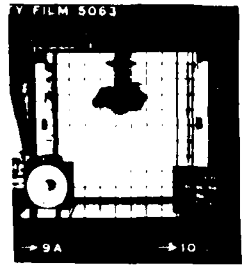

3.6 Seconds

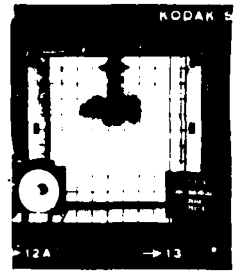

4.6 Seconds

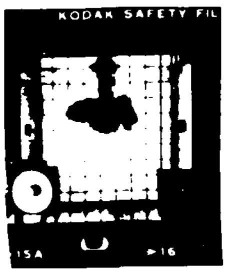

5.6 Seconds

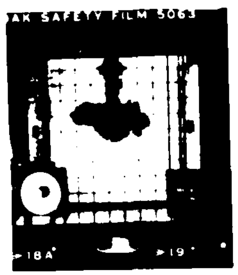

6.6 Seconds

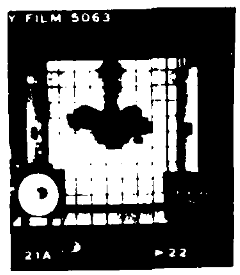

7.6 Seconds

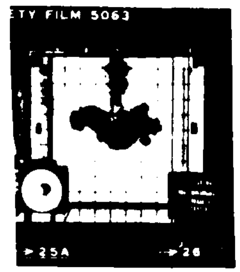

9.0 Seconds

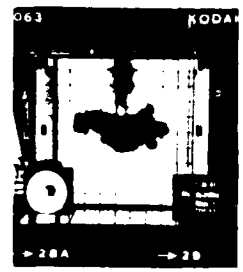

10 Seconds

Figure 3-40. Sample Test Photographs, Test 6.1.

4. ANALYSIS OF TEST RESULTS

4.1 SCALING

4.1.1 General

How well do these experiments simulate full-scale nuclear cloud rise? The simulation would be valid in all respects if it could be shown that the characteristic nondimensional parameters such as Reynolds number and Froude number remain the same in a nuclear cloud and in the experiments. However the length scale of the experiments is very much smaller than for a nuclear burst and the Reynolds number of the two flows differ by six orders of magnitude.

The experiments are nevertheless expected to be a good simulation. The height to which a cloud will rise and its diameter depend primarily on the efficiency of turbulent mass entrainment. Turbulent flows are insensitive to the Reynolds numbers as long as the flow is turbulent. The cloud rise in the experiments is clearly turbulent as is nuclear cloud rise and this is the primary requirement. According to Turner (Reference 2 p. 168), "Provided the Reynolds number Re = wb/ν is large enough, neither the molecular properties ν and κ of the fluid nor Re itself can enter directly into the determination of the overall properties of a turbulent plume". Plumes (steady sources) and thermals or clouds (instantaneous sources) rise and spread by the same mechanisms. Townsend (Reference 3, pg. 53) also states that turbulent flows are insensitive to the Reynolds number provided that it is high enough.

Another indication that the simulation is adequate is that theories of cloud rise (References 4 & 5 for example) are equally successful for nuclear clouds and for small-scale experiments in a water tank. These theories utilize the Taylor entrainment hypothesis (Reference 6) that the rate of entrainment is proportional to the mean vertical velocity of the cloud. Only global properties are predicted such as height, width, vertical velocity and buoyancy versus time.

4.1.2 Scaling Tests

A limited series of single-burst tests were conducted with the initial cloud density and the density gradient in the tank both doubled

from the nominal values used in this program. This changes the Froude number (intertial force/gravity force)$^{1/2}$ to more nearly simulate the initial nuclear cloud buoyancy when the fireball is still hot. It is possible that this is not important because the density of the nuclear cloud rapidly approaches a value near ambient and its late-time characteristics (height and radius) are primarily determined by the entrainment and rise that occur after near ambient density is attained.

These scaling tests were conducted to verify the cloud rise theory*, i.e. that the change in Froude number did not alter the success of the simulation. The experimental results are compared with theory in Figure 4-1. The agreement is very good and not better or worse than for the single cloud tests (1.1 to 1.3) with nominal densities. The latter comparison and the theory are discussed in Section 4.2. The principal effect of the changes was to accelerate the cloud rise. The maximum height is about the same but the peak occurs 2-3 seconds earlier than the tests with nominal densities.

4.2 SINGLE CLOUD TESTS

4.2.1 Single Cloud Theory

The classical analysis of turbulent gravitational convection in a nonuniform environment is due to Morton, Taylor and Turner (Reference 4). They found a closed form solution for cloud rise in a linearly stratified environment. Their solution is directly applicable to cloud rise in the atmosphere since the atmosphere is approximately linearly stratified up to the tropopause.

Morton, Taylor and Turner found a solution of the equations for conservation of mass, momentum and energy (buoyancy) for the cloud from an instantaneous point source of buoyancy using the following assumptions:

1) The fluids are incompressible and miscible except that small variations in density are allowed in the buoyancy terms.

2) The cloud is spherical and profiles of velocity and buoyancy through the cloud have the same form.

---

* The theory is discussed in Section 4.2

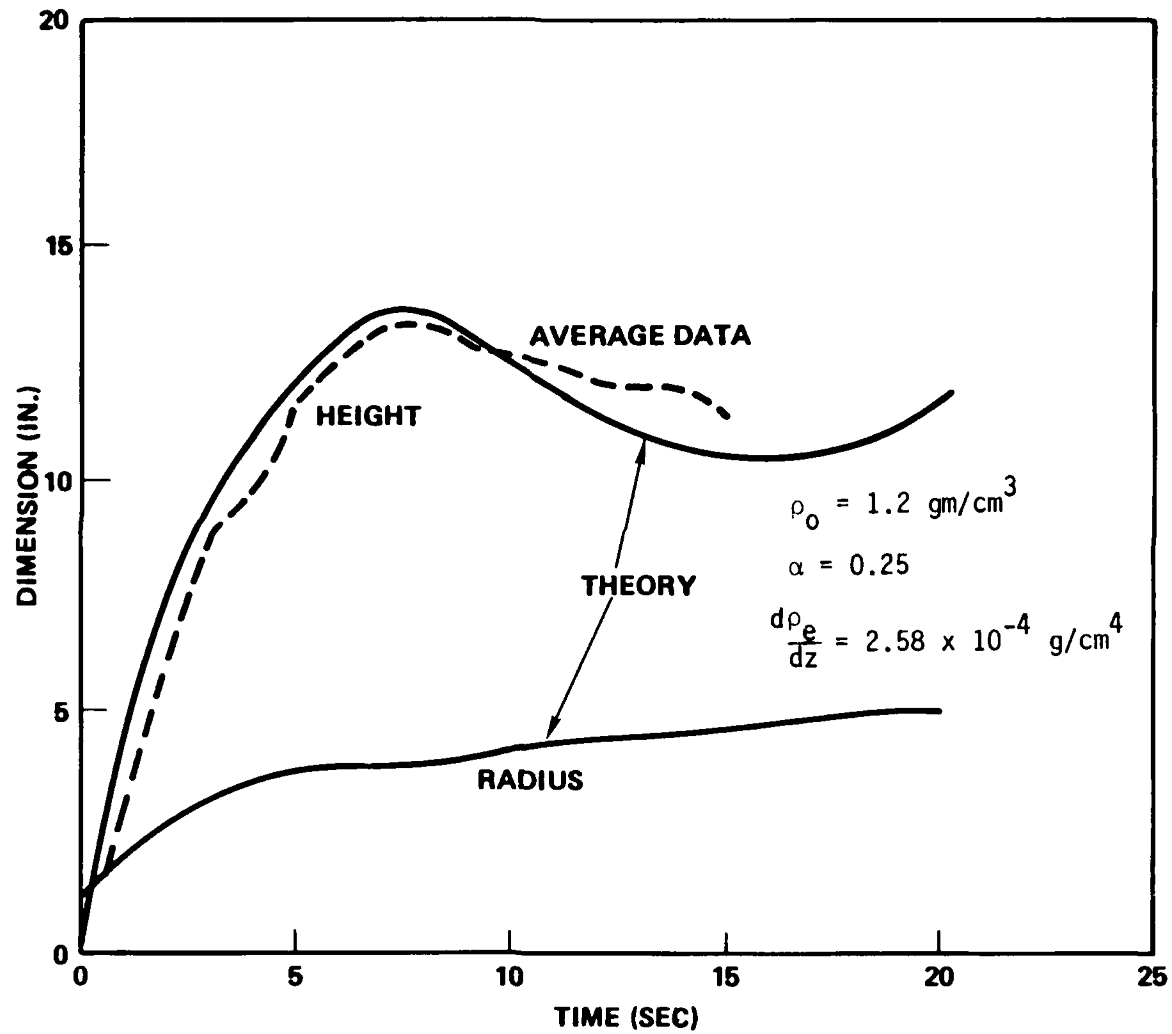

Figure 4-1. Comparison of Theoretical and Experimental Cloud Dimensions for Scaling Tests (1.4, 1.5 and 1.6).

3) The rate of entrainment of ambient fluid is proportional to the mean vertical velocity of the cloud.

Later investigators such as Maxworthy and Escudier (Reference 5) and Wang (Reference 7) have analyzed more general cases. These always require a digital computer to obtain a solution. Reference 5, in particular, treats the case of a cloud with a finite initial size and relaxes the assumption that variations in density must be small. This analysis also includes the influence of the virtual mass ignored by previous investigators. The analysis of Maxworthy and Escudier has been extended to the case of a linear density density gradient and programmed. It is utilized here for comparisons with single cloud results such as Figure 4-1 presented earlier.

4.2.2 Comparison of Test Results with Theory and with Earlier Tests

Figure 4-2 presents a comparison between average time-histories for the single cloud tests (1.1 & 1.2)* and the theoretical predictions for the test conditions. Very good agreement is obtained using an entrainment coefficient of 0.25. This is a typical entrainment coefficient derived from nuclear cloud rise data.

Maximum cloud heights obtained in an earlier test series (Reference 1) were significantly lower. A comparison like that in Figure 4-2 is shown in Figure 4-3 taken from Reference 1. The experimental results are again in agreement with predictions using the same code but a different entrainment coefficient (0.3) has been used. Not surprisingly, the maximum cloud height is fairly sensitive to the efficiency of mass entrainment. More time (and height) is required for the cloud density to reach the density of its surroundings if mixing with the surroundings is less efficient.

The tests reported here were done with the same apparatus as used in the earlier tests except that one change was made. The spring which rotates the cups and releases the initial bubbles (simulated fireballs) was replaced with a stronger spring. This change apparently led to a cleaner release and less efficient mixing-at least initially. The magnitude of the change was unexpected but data exist which support this explanation.

---

* The first three tests were done before a clock was acquired and there is substantial uncertainty in the starting time for test 1.3.

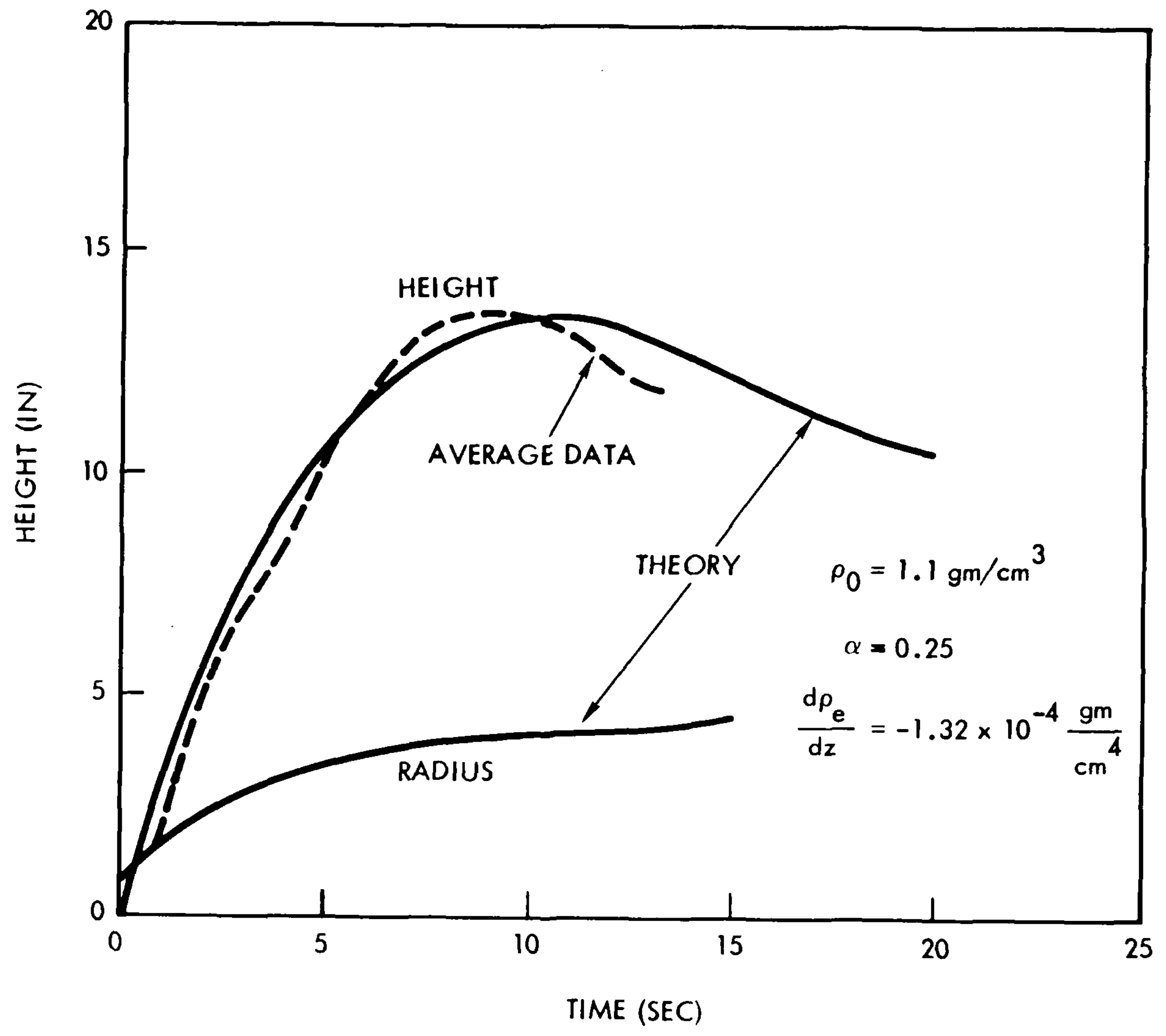

Figure 4-2. Comparison of Theoretical and Experimental Cloud Dimensions for Reference Single Burst Tests (1.1 & 1.2).

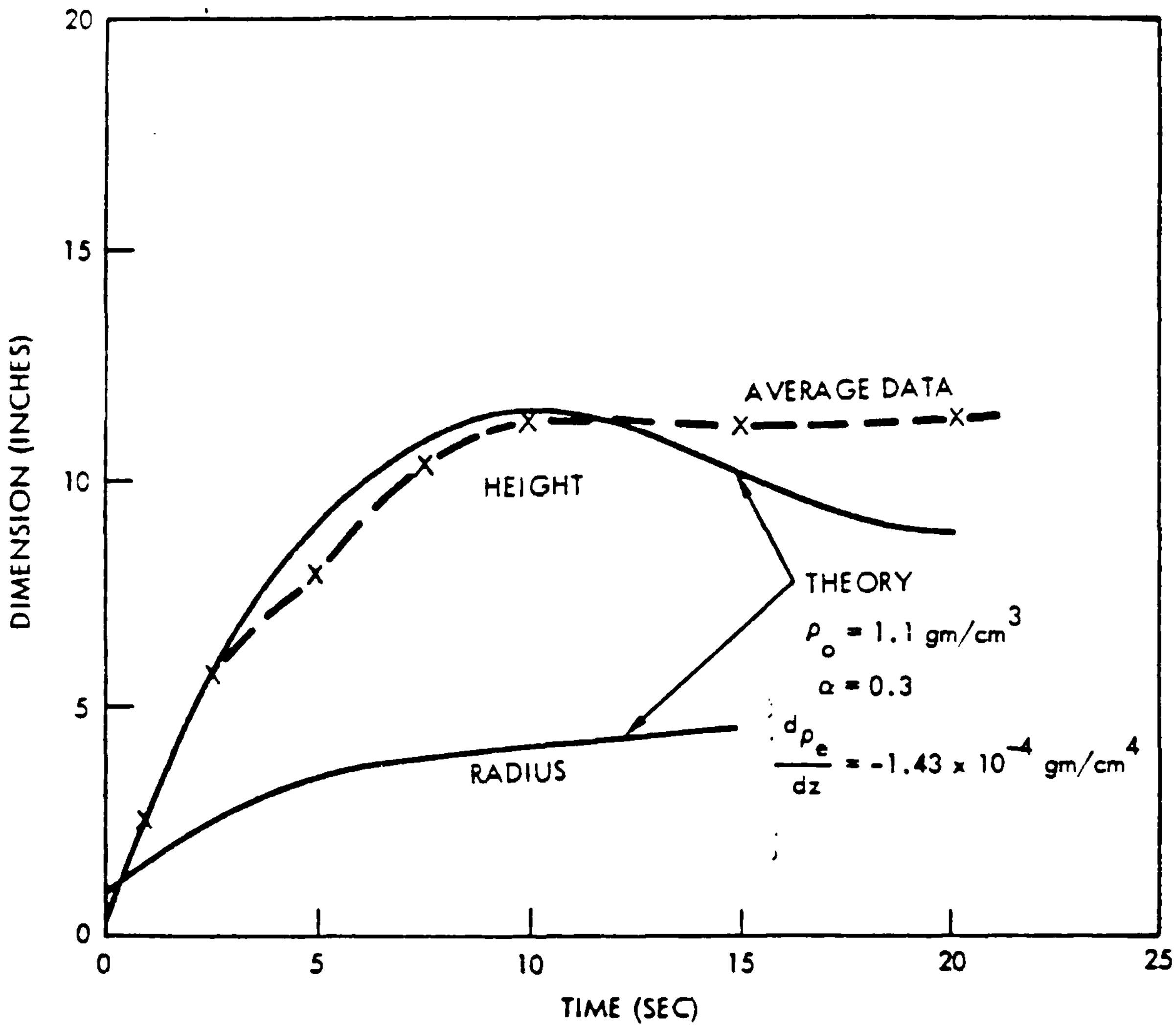

Figure 4-3. Comparison of Theoretical and Experimental Cloud Dimensions for Reference Single Bursts for Earlier Program (Reference 1).

Reference 8 reports experiments in which entrainment coefficients from 0.18 to 0.3 were obtained using different techniques to release the buoyant bubble.

4.3 MULTIBURST TESTS

4.3.1 Test Data Summary

The test results for all the tests are presented in some detail in Section 3. In this section, the cloud top height and horizontal radius at the stabilization time are tabulated for comparison with a multiburst cloud rise model. The theoretical stabilization time or time of the first peak is approximately 10 seconds in the experiments according to the code based on Reference 5. In an average sense, the experimental results agree but the stabilization time for a particular experiment may differ somewhat.

Table 4-1 presents cloud top height and horizontal radius at 10 seconds for each single burst test, each multiburst test and the averages for the tests at each test condition. The averages are used in the next section for comparison with model predictions.

Two tests, 1.3 and 5.2, were not used in determining averages. The first three tests were done before a clock was acquired and there is substantial uncertainty in the starting time for test 1.3. In test 5.2, one cup emptied only partially and the test was for four and some fraction bursts" rather than five.

4.3.2 Comparison with Test Results with Multiburst Model

A multiburst cloud rise model was recently developed by TRW for DNA (Reference 9). The model is based on the extension of Morton, Taylor and Turner's analysis (Reference 4) from a spherical cloud to a disc-like cloud appropriate to a large number of simultaneous bursts. This extension was published by one of us (Zimmerman) in Reference 10. The model in Reference 9 is identical with that given in Reference 10 except that a better fit to the data was obtained by eliminating the term for spacing between bursts. The limited data available is for small numbers of bursts or for spacings (as a number of fireball diameters) near unity and suggest little or no dependence on spacing. More data will be required to determine the dependence on spacing in a general case as opposed to a large number of bursts distributed in a circular disc.

The ratios of multiburst to single burst cloud dimensions from Reference 9 are given by

TABLE 4-1.

Cloud Top Height and Horizontal Radius at 10 Seconds
(Stabilization or Time of First Peak)

Test Number	Number Bursts	Spacing in.	H_{TOP} in.	Avg. H_{TOP} in.	D in.	Avg. D in.
1.1	1	2.4	17.84		11.79	
1.2	1	2.4	17.06		14.08	
1.3*	1	2.4	17.31		12.71	
1.1-1.3	1	2.4		17.45		12.94
5.1	5	2.4	20.76		17.67	
5.2*	5	2.4	17.47		20.69	
5.3	5	2.4	17.78		17.20	17.44
5.1,3	5	2.4		19.27		
6.1	6	2.4	19.06		22.29	
6.2	6	2.4	19.02		20.30	
6.3	6	2.4	20.02		20.00	20.86
6.1-6.3	6	2.4		19.37		
6.4	6	4.0	17.61		21.07	
6.5	6	4.0	18.65	18.13	21.44	21.26
6.4,5	6	4.0				
6.6	6	6.0	19.81		21.52	
6.7	6	6.0	17.73		25.61	23.57
6.6,7	6	6.0		18.77		
7.1	7	2.4	19.77		19.77	
7.2	7	2.4	19.33		20.80	
7.1,2	7	2.4		19.55		20.29

* Not used in averages. See text.

$$H_{MB}/H_S = \left(\frac{3}{2}\,\frac{\alpha_{SB}}{\alpha_{MB}}\right)^{3/4} N^{-1/8} \tag{1}$$

$$D_{MB}/D_S = \left(\frac{2}{3}\,\frac{\alpha_{MB}}{\alpha_{SB}}\right)^{1/4} N^{3/8} \tag{2}$$

where

D = cloud horizontal diameter

H = cloud height

N = number of bursts

α = entrainment constant (usually ~ .25 for individual clouds)

The quantity of α_{MB}/α_{SB} was chosen to give a good fit to the data and the values chosen are

$$\alpha_{MB}/\alpha_{SB} = \left.\begin{array}{ll} 0.6 & \text{air} \\ 1.0 & \text{water} \end{array}\right\} \tag{3}$$

These values were chosen solely to fit the data. The difference for the two media was unexpected but consistent with qualitative observations. This difference means that multiburst interactions lead to significantly higher clouds in air (compared with single clouds) but not in water. This has been observed. Further investigation of the entrainment process is necessary to determine the source of this difference.

The multiburst data from this program are compared with this model in Table 4-2. The comparison is seen to be quite good. This model is compared with other multiburst data in Reference 9 and the comparison is again found to be quite good.

4.4 APPLICATION TO NUCLEAR CLOUDS

The data from this program have been applied to verify a model which relates multiburst cloud dimensions to the dimensions from one burst. This model together with a single burst model can be used to predict multiburst cloud dimensions. Detailed comparisons were made at only time time (stabilization) but the ratios H_{MB}/H_S and D_{MB}/D_S are theoretically applicable

TABLE 4-2.

Model Predictions Compared with
Water Tank Experiments

TEST	NUMBER OF BURSTS	$\tilde{\Delta X}$*	H_{MB}/H_S		ERROR IN PREDICTION	D_{MB}/D_S		ERROR IN PREDICTION
			PREDICTED	EXPERIMENT		PREDICTED	EXPERIMENT	
5.1,3	5	1.2	1.11	1.10	.009	1.65	1.35	.222
6.1,2,3	6	1.2	1.08	1.11	.027	1.77	1.61	.099
6.4,5	6	2.0	1.08	1.04	.039	1.77	1.64	.079
6.6,7	6	3.0	1.08	1.08	0	1.77	1.82	.028
7.1,2	7	1.2	1.06	1.12	.054	1.88	1.57	.198
AVERAGE ERROR (%)					2.6%			12.5%

* Simulated distance between bursts ÷ Fireball diameter at pressure equilibrium.

at any time. Experiments with better instrumentation or better hydrocode calculations (probably three dimensional) are required to determine the details of the particle mass distribution within the cloud.

Several single burst models exist. Reference has been made to the models of Morton, Taylor and Turner (Reference 4) and Escudier and Maxworthy (Reference 5). Another model of interest (Reference 11) is used in the DOD Land Fallout Prediction System-DELFIC. This model takes account of the atmospheric humidity. The latter may have a substantial impact on the maximum cloud altitude.

The model of Morton, Taylor and Turner is most convenient (if more approximate) in that a closed form solution is available. From Reference 4

$$r = \left(\frac{3}{\pi}\right)^{1/4} \alpha^{1/4} F_0^{1/4} G^{-1/4} R \tag{4}$$

$$x = \frac{1}{4}\left(\frac{3}{\pi}\right)^{1/4} \alpha^{-3/4} F_0^{1/4} G^{-1/4} X \tag{5}$$

$$t = G^{-1/2} t_1 \tag{6}$$

$$R = \begin{cases} (1-\cos t_1)^{1/4} & 0 \le t_1 \le \pi \\ (3+\cos t_1)^{1/4} & \pi \le t_1 \le 2\pi \end{cases} \tag{7}$$

$$X = \begin{cases} 4(1-\cos t_1)^{1/4} & 0 \le t_1 \le \pi \\ = 8 \cdot 2^{1/4} - 4(3+\cos t_1)^{1/4} & \pi \le t_1 \le 2\pi \end{cases} \tag{8}$$

where F_0 is $(1/\rho_1)$x total buoyancy released from the source at t = 0, G is $-(g/\rho_1)$x the density gradient, α is the entrainment coefficient (about .25 for a nuclear burst), and ρ_1 is the ambient density at the source level. The nondimensional time (t_1) is π at stabilization. Refer to the Nomenclature for specific definitions.

Equations (4) through (8) together with Equations (1), (2) and (3) in Section 4.3 specify the cloud dimensions as a function of time for multi-burst clouds from simultaneous energy releases. The energy release may be a nuclear burst or a cup of liquid with negative buoyancy.

5. RECOMMENDED TEST FACILITY AND INSTRUMENTATION FOR EXTENDED CAPABILITY

5.1 INTRODUCTION

The objective for performing more multiple cloud tests would be to obtain data for more than the maximum of 7 clouds that was obtained on this contract, and to expand the data acquisition system so that a better picture of the dynamics of the problem can be obtained.

5.2 EXPERIMENTAL APPARATUS

5.2.1 Tank and Fill Apparatus

The tank used for the current contract is undersized: being one cubic meter in volume, it can only accomodate a maximum of 7 clouds; therefore a new and much larger test tank must be fabricated in order to simulate a significant part of an attack. One capable of handling up to about 70 bursts is considered adequate. The new tank can be constructed in such a way as to permit incremental changes in its volume. This has the advantage of running tests with possibly 30 clouds and then expanding the volume of the test tank to accomodate 70 clouds.

The tank required for a 70 cloud test has a volume of about 14 cubic meters (3 x 4 x 1.2 meters). The tank will be constructed with ½ inch tempered glass walls so that photographs of the developing clouds could be taken. One wall of the tank will have taps spaced 2-3 inches apart along the depth of the tank. The taps will be used to draw off small samples of water so that density measurements can be made with a refractometer.

Filling this new test tank with a stratified salt water solution will require a different technique then that used in the previous experiments. In the previous experiments, the volume of the tank was small. This made it relatively easy to fill the tank using the gravity feed method shown in Figure 5-1. The gravity feed method is not practical in filling the larger volume test tank because the water/salt water solution cannot be mixed well enough before it drains into the test tank.

A method using a metering pump and mixing pipe can be employed; Figure 5-2 shows the details of this setup. The water and salt water are

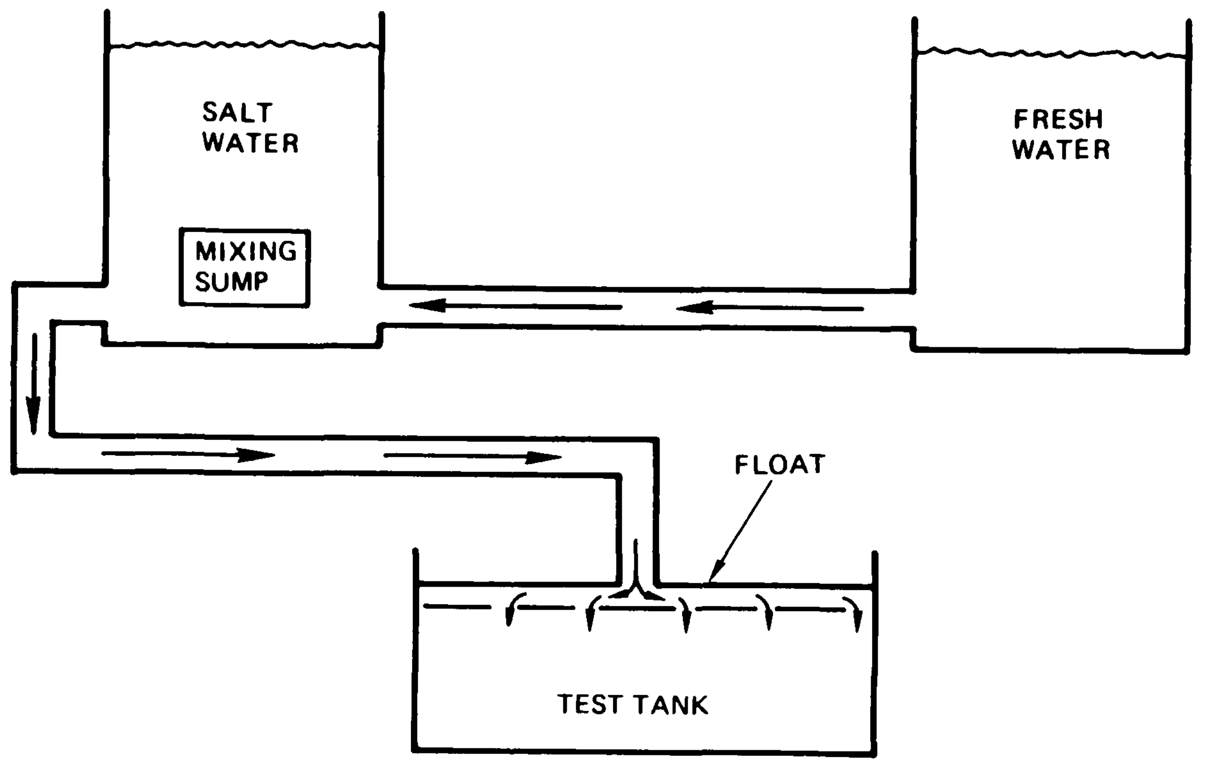

Figure 5-1. Gravity Feed Fill Method.

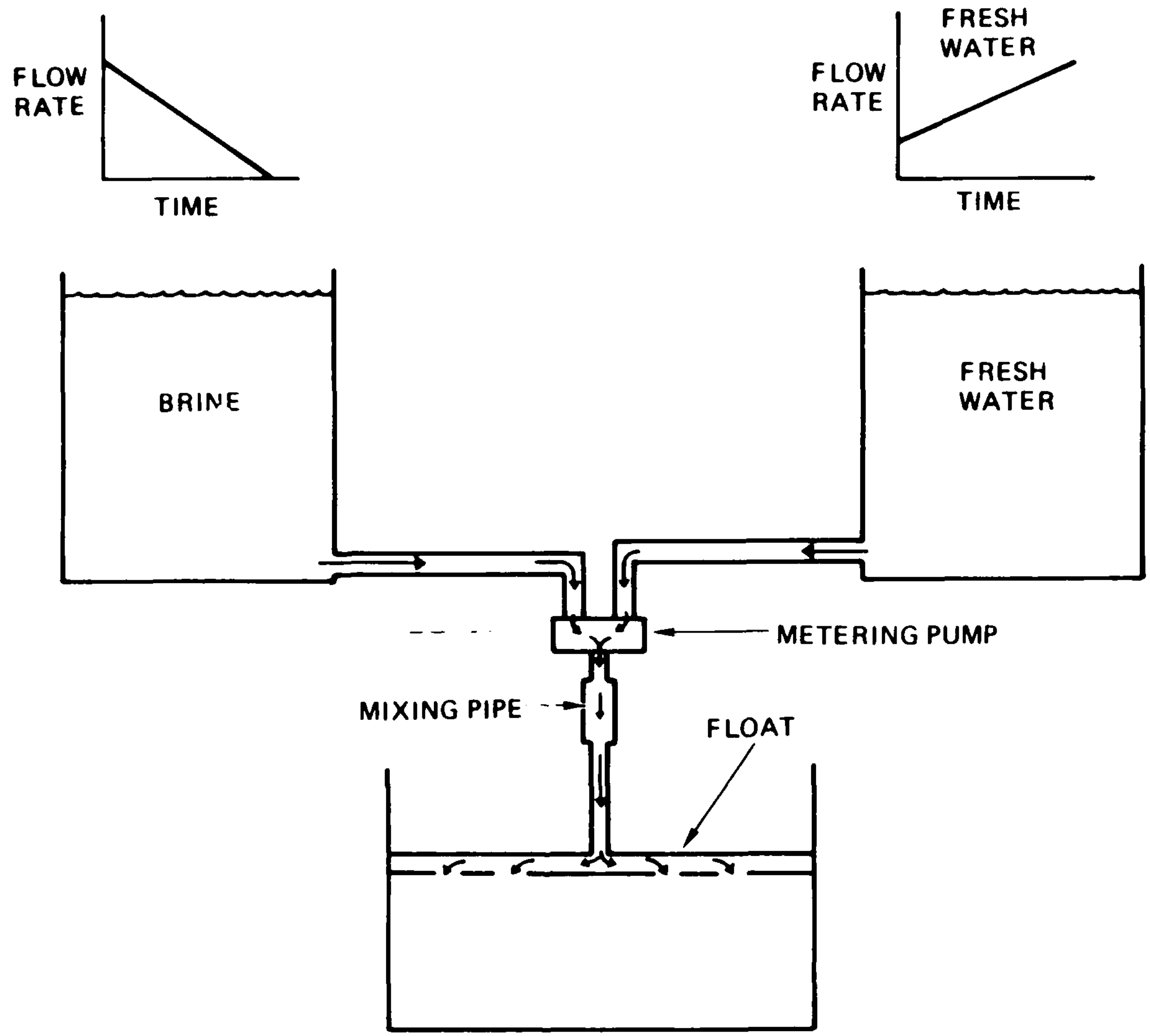

Figure 5-2. Metering Pump Fill Method.

pumped from the storage tanks by the combined flow metering pump and then enter a mixing pipe which drains into the test tank. The metering pump regulates the flow of salt water and fresh water in the proper proporations so that a linear density gradient can be obtained.

5.2.2 Cloud Release Mechanism

The cloud release mechanism must be designed so that it satisfies two basic requirements: 1) each cup or series of cups in the mechanism can be rotated independently and 2) that this rotation occurs at a precise time. These design requirements are needed so that walk attacks as well as spike attacks can be simulated.

Two designs are being considered. Both designs may be developed into prototypes and tested so that the best design can be chosen. Both designs are simple in concept; but a substantial amount of machinist labor is required to fabricate them.

The first design has each source (cup) released (rotated) individually. Each cup would be equipped with a solenoid release pin arrangement such that when a current is supplied to the solenoid it will pull out the locking pin thus causing the cup to rotate. Figure 5-3 shows some details of this design. This design has one disadvantage: the large number of solenoids will add complexity to the timing control system. The second design is a slight variation of the first. Instead of each cup being controlled individually, a series of cups will be controlled by one solenoid. Five or six cups will be rigidly connected together by a single shaft which is spring loaded and will rotate when the locking pin is pulled out by the solenoid. Figure 5-4 depicts some details of this design. This design has the advantage (over the first design) of a simpler timing control system. However this design does not allow for simulation of walk attacks that proceeed along a row because all cups in the row are released simultaneously. Another disadvantage is that the shaft that connects the cups will be submerged in the water and will add to the disturbance at the water surface that is already produced by the rotation of the cups.

5.3 INSTRUMENTATION

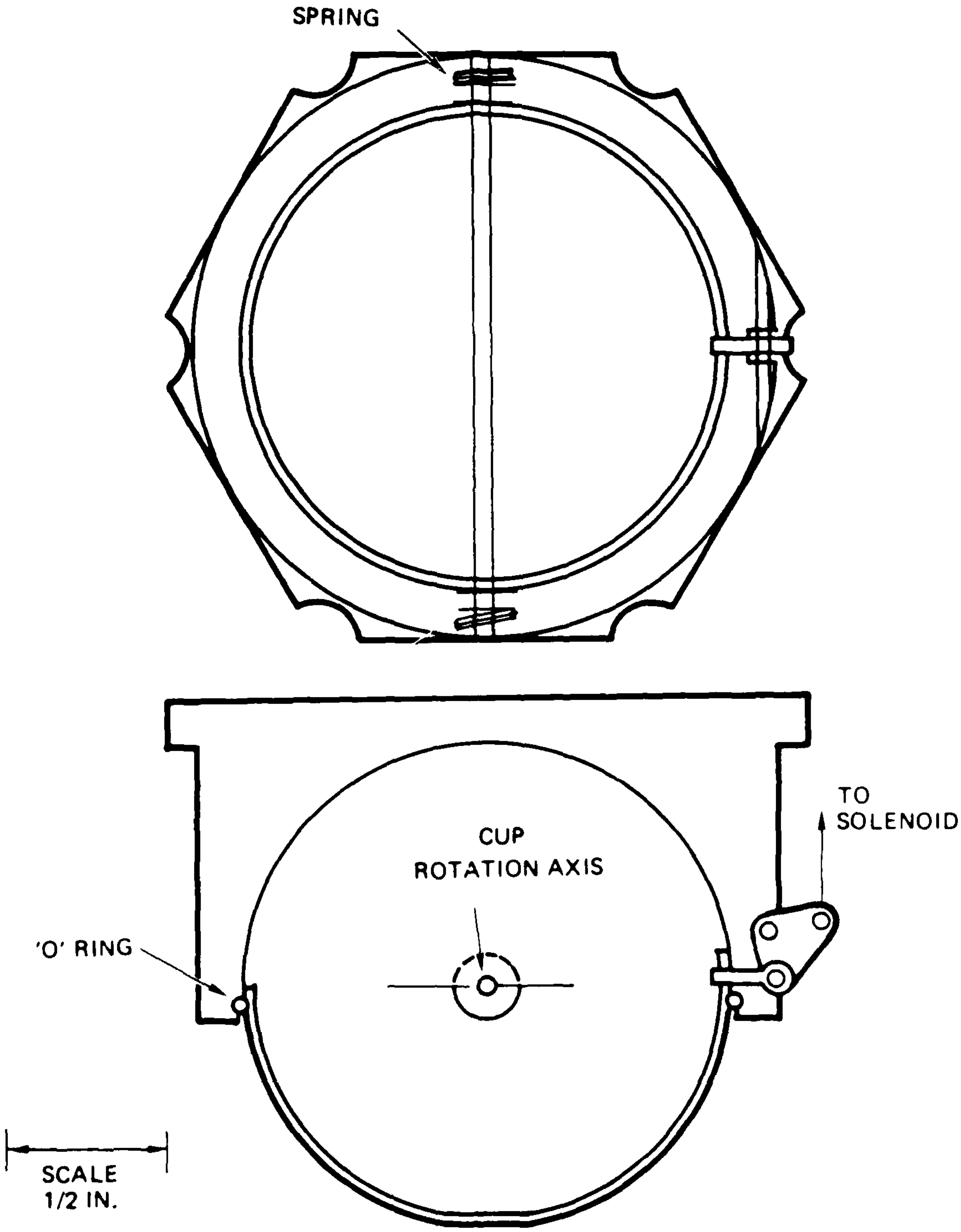

Figure 5-3. Release Mechanism Design #1.

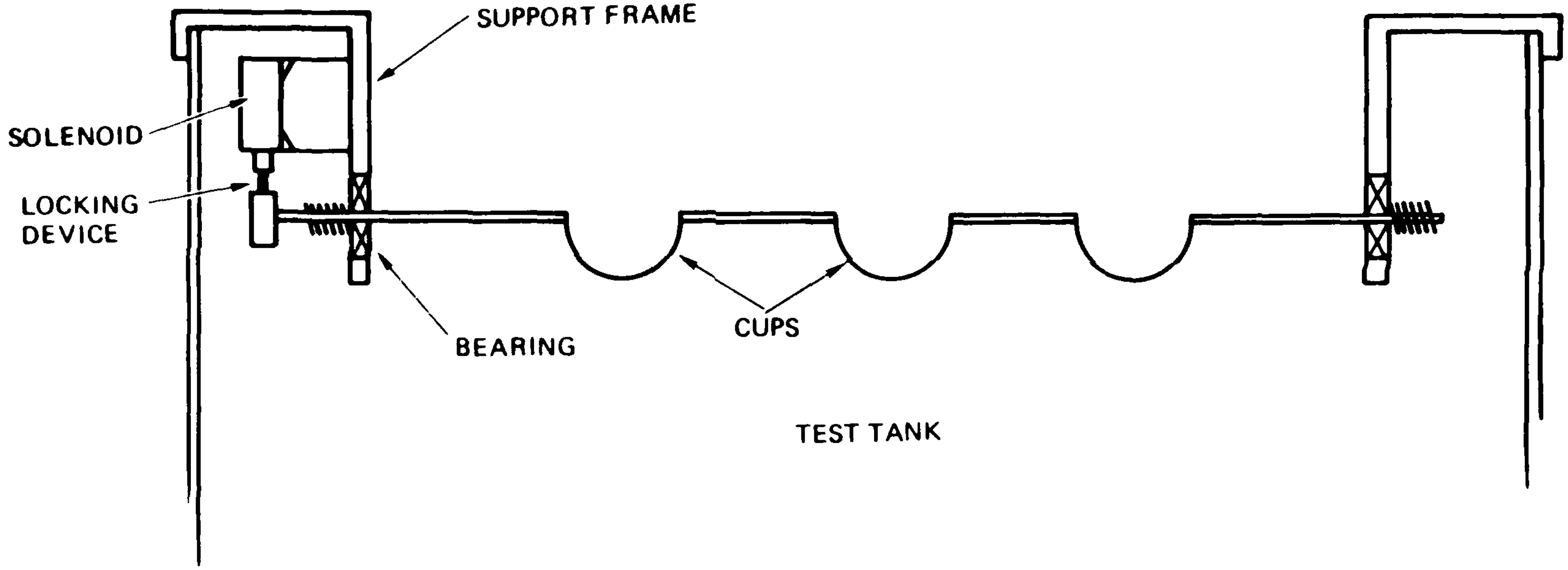

Figure 5-4. Release Mechanism Design #2.

5.3.1 General

Several techniques are available to obtain data on cloud densities, velocities, size, and mixing processes. The following describes the techniques and the instrumentation required by these techniques.

5.3.2 Laser Induced Fluorescence (LIF)

In addition to photographing cloud tests with 35 mm cameras, a technique called Laser Induced Fluorescence can be used to obtain information on the mixing processes that occur during multiple cloud development (Reference 12). By seeding the high density fluid (cup fluid) with a fluorescent dye and illuminating a cross section of the developing cloud with a "sheet" of laser light, qualitative and quantative information on the entrainment processes can be obtained. The "sheet" of light can also reveal information on density and can give a density map of a cross section of the cloud. In addition to illuminating the cloud with a sheet of light, the laser light beam can be directed through the thickness of the cloud. A photodiode placed on the opposite side of the test tank will measure an integrated density through the thickness of the cloud.

Some of the major components required for the LIF technique presently exist in house: they include a 3 watt argon ion laser, 35 mm cameras, and a Fairchild ccd 3000 video camera which has a 448 x 380 element solid state sensor. The Fairchild camera is ideal for obtaining dye dilution (density) information of the clouds. However, image processing capability necessary to provide quantitative image analysis currently does not exist. A significant effort (writing software, interfacing with the computer) is needed to provide this capability. An alternative to using the video camera to collect data is to use a photodiode array (Reference 13, pg 63). The array would be aligned perpendicular to the laser light "sheet". This arrangment of the photodiodes with the laser light sheet produces a photocurrent in the diodes that is linearly proporational to the light intensity or density. The method for transforming the photocurrent data into density data will require some development work.

In order to use the LIF technique an effective fluorescent dye concentration must be determined. If the concentration is too high, part of the cloud where the laser light first enters will be very bright, but

as the laser light travels through the cloud it becomes attenuated. Conversely, if the dye concentration is too weak, there will be little attenuation along the light path but the cloud brightness will be too low to allow for proper exposure of film or video. Choosing the best dye concentration requires trading off brightness to uniformity. To find this optimum dye concentration a series of calibration test must be made. Figure 5-5 illustrates the calibration setup. The laser is placed at one end of the tank and directly opposite a photo detector is located. Perpendicular to both these is a camera. The photo detector determines the laser irradiance into and out of the tank. This information is used to determine the absorption coefficient. The camera photographs the fluorescence and the photographs are used to determine the "photographability". The process is repeated until an optimum dye concentration is found.

5.3.3 Video Data Acquisition

Video cameras can be used to obtain density data for the developing cloud. Two low-distortion silicon target vidicons (cameras) are used. Vertical and horizontal views are used to view a uniformly illuminated area of the test tank. The light that reaches the cameras is a function of density of the cloud; and the image is recorded on the video tape. The video tape is processed to produce time-evolved, integrated path density data.

The processor of this data would be the TRW Capistrano Test Site (CTS) facility. CTS has the required minicomputer, digital video processor, video image analyzer, and other devices to reduce the data. The data would be presented as isointensity (density) contour maps, isometric projections, profile plots for maximum horizontal and vertical dimensions.

The major disadvantage of the video technique is that density information on a cross section can not be obtained, only information on the amount of mass through the thickness. Another disadvantage is that the acquisition and data reduction process is expensive.

5.3.4 Velocity Measurements

Velocity data of the flow field within the developing cloud would be a useful addition to the density data obtained by the LIF or video technique.

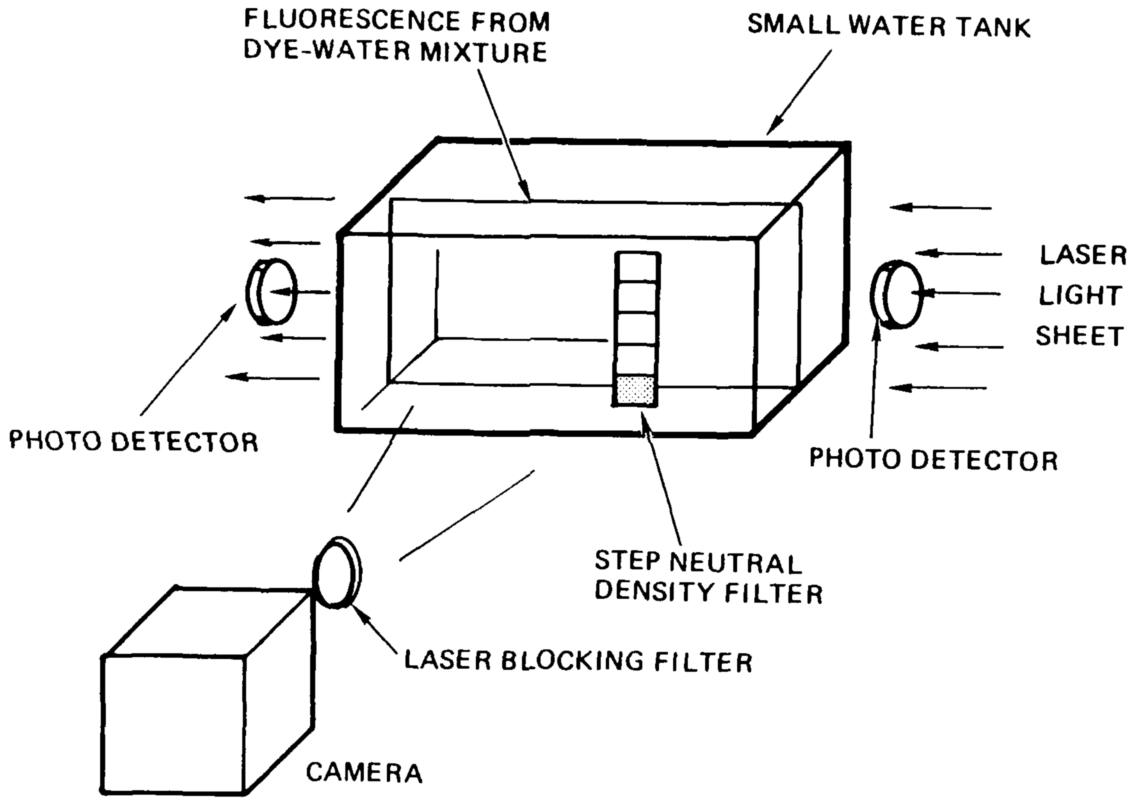

Figure 5-5. Laser Induced Fluorescence Calibration Setup.

Velocity data can be obtained using two techniques: hot wire anemometers and laser induced fluorescent particles. These two methods are proven and have been used extensively by TRW for other kinds of experiments. A hot wire anemometer is a fine wire which is heated and placed in a fluid flow. The rate of cooling of the heated wire by convection, measured indirectly by a ammeter depends on (among other things) the speed of the flow. A properly calibrated anemometer will give an accurate measurement of the speed of the flow. Hot wires will give data on the speed of the flow, but will not give data on flow direction; therefore a complete description of the velocity flow field with hot wires is not possible.

Laser induced fluroescing particles can be used to seed the high density cup fluid. The particles should have neutral buoyancy relative to the average density in the test tank. This should keep the particles suspended for the duration of the test. However, some testing will be required to find the optimum density of the particles used.

The developing cloud containing the particles will have a "sheet" of laser light cutting through a particular cross section. The laser light will make visiblethe fluorescing particles moving in the flow field, and give an indication of the direction and an approximate speed of the flow.

When these two methods are used together a complete picture of the velocity flow field can be obtained. However, the number of hot wires used during an experiment is limited because they interfere with the flow; therefore,data for only a few regions of the flow can be obtained.

6. CONCLUSIONS AND RECOMMENDATIONS

CONCLUSIONS

1) The final height of a buoyant cloud is sensitive to the way in which the initial buoyancy is released.

2) For multiburst events in water (up to 7 simultaneous bursts) the differences between multiburst and single burst cloud heights are small.

3) Cloud dimensions agree quite well with a model based on multiburst events in both air and water. The multiburst effect in air is observed to be substantially larger.

RECOMMENDATIONS

1) Experiments should be conducted in a larger tank to allow a significant fraction of an attack to be simulated.

2) Walk attacks should also be simulated. The cloud release mechanism can be designed to sequentially release individual clouds or rows of clouds.

3) The difference between multiburst cloud rise in air and water should be investigated.

7. REFERENCES

1. Zimmerman, A. W., "Dust Environment Uncertainty Effects on MX Launch Vulnerabilities," TRW Electronics and Defense, 14 February 1983, Unpublished.

2. Turner, J. S., Buoyancy Effects on Fluids, Cambridge University Press, Cambridge, 1973.

3. Townsend, A. A., The Structure of Turbulent Shear Flow, 2nd Edition, Cambridge University Press, Cambridge, 1976.

4. Morton, B. R., Taylor, G. I., and Turner, J. S., "Turbulent Gravitational Convection from Maintained and Instantaneous Sources," Proc. Roy. Soc. A., Vol. 234, January 1956.

5. Escudier, M. P., and Maxworthy, T., "On the Motion of Turbulent Thermals", J. Fluid Mech., Vol. 61, 1973.

6. Taylor, G. I., "Dynamics of a Mass of Hot Gas Rising in Air," U. S. Atomic Energy Commission, MDDC-919, 1945.

7. Wang, C. P., "Motion of a Turbulent Buoyant Thermal in a Calm Stably Stratified Atmosphere," Physics of Fluids, Vol. 16, June 1973.

8. Gorev, V. A., Gusev, P. A., and Troshin, Ya, K., "Effect of Formation Conditions on the Motion of a Cloud Rising Upward Under the Action of the Force of Buoyancy," Fluid Dynamics, June 1977, pp. 770-772; translation from Izv. Akad, Nauk SSSR, Mekh. Zhidk, Vol. 11, Sept-Oct, 1976.

9. Zimmerman, A. W., "Engineering Research Support to DNA ICBM Basing Programs, Vol. V: Multiburst Cloud Model for Laterally Separated Simultaneous Bursts," TRW Electronics and Defense, 30 November 1984 Unpublished.

10. Zimmerman, A. W., "Multiburst Cloud Rise," AIAA J., Vol. 16, June 1978.

11. Norment, H. G., and Woolf, S., "Department of Defense Land Fallout Prediction System, Vol. III-Cloud Rise (Revised)," Defense Atomic Support Agency (now Defense Nuclear Agency), DASA-1800-111 (Revised), Sept. 1970.

12. Personal Communication with R. N. Wagner, TRW.

13. Koochesfahani, Manoochehr Mohseni, "Experiments on Turbulent Mixing and and Chemical Reactions in a Liquid Mixing Layer,"Phd Thesis, California Institute of Technology, Pasadena California, November 1983.

DISTRIBUTION LIST

DEPARTMENT OF DEFENSE

DEF RSCH & ENGRG
ATTN: STRAT & SPACE SYS (OS)
ATTN: STRAT & THTR NUC FOR/F VAJDA

DEFENSE INTELLIGENCE AGENCY
ATTN: RTS-2A (TECH LIB)
ATTN: RTS-2B

DEFENSE NUCLEAR AGENCY
ATTN: DFSP G ULLRICH
ATTN: SPAS C GALLOWAY
ATTN: SPAS D MUNNINGHOFF
ATTN: SPAS R ROHR
4 CYS ATTN: TITL

DEFENSE TECHNICAL INFORMATION CENTER
12 CYS ATTN: DD

FIELD COMMAND DEFENSE NUCLEAR AGENCY
ATTN: FCTXE
ATTN: FTTD
ATTN: FTTD W SUMMA

JOINT STRAT TGT PLANNING STAFF
ATTN: JKCS
ATTN: JPEP
ATTN: JPTM

DEPARTMENT OF THE ARMY

HARRY DIAMOND LABORATORIES
ATTN: SCHLD-NW-P
ATTN: SLCIS-IM-TL (81100) (TECH LIB)

U S ARMY BALLISTIC RESEARCH LAB
ATTN: SLCBR-SS-T (TECH LIB)

U S ARMY CORPS OF ENGINEERS
ATTN: DAEN-ECE-T

U S ARMY ENGINEER CTR & FT BELVOIR
ATTN: TECHNICAL LIBRARY

U S ARMY ENGINEER DIV HUNTSVILLE
ATTN: HNDED-SY

U S ARMY ENGR WATERWAYS EXPER STATION
ATTN: E JACKSON, WESSS-O
ATTN: J JACKSON, WESSD
ATTN: J ZELASKO, WESSD-R

U S ARMY NUCLEAR & CHEMICAL AGENCY
ATTN: LIBRARY
ATTN: MONA-NU MR LONG

U S ARMY STRATEGIC DEFENSE COMMAND
ATTN: DASD-H-L
ATTN: DASD-H-SAV R K DUDNEY

DEPARTMENT OF THE NAVY

NAVAL RESEARCH LABORATORY
ATTN: CODE 2627 (TECH LIB)
ATTN: CODE 4040 D BOOK
ATTN: CODE 4040 J BORIS

NAVAL SURFACE WEAPONS CENTER
ATTN: CODE R44 H GLAZ
ATTN: CODE X211 (TECH LIB)

NAVAL SURFACE WEAPONS CENTER
ATTN: TECH LIBRARY & INFO SVCS BR

DEPARTMENT OF THE AIR FORCE

AIR FORCE CTR FOR STUDIES & ANALYSIS
ATTN: AFCSA/SAMI (R GRIFFIN)

AIR FORCE INSTITUTE OF TECHNOLOGY/EN
ATTN: LIBRARY/AFIT/LDEE

AIR FORCE WEAPONS LABORATORY, NTAAB
ATTN: NTED-A
ATTN: SUL

BALLISTIC MISSILE OFFICE/DAA
ATTN: ENSN
ATTN: MYEB D GAGE

STRATEGIC AIR COMMAND/NRI-STINFO
ATTN: NRI/STINFO
ATTN: XOBM

DEPARTMENT OF ENERGY

LOS ALAMOS NATIONAL LABORATORY
ATTN: C F KELLER
ATTN: M T SANDFORD
ATTN: R WHITAKER

SANDIA NATIONAL LABORATORIES
ATTN: DIV 7111 J W REED
ATTN: J R BANNISTER 7111
ATTN: ORG 7112 A CHABAI

OTHER GOVERNMENT

CENTRAL INTELLIGENCE AGENCY
ATTN: OSWR/NED

DEPARTMENT OF DEFENSE CONTRACTORS

AEROSPACE CORP
ATTN: H MIRELS
ATTN: LIBRARY ACQUISITION

APPLIED RESEARCH ASSOCIATES, INC
ATTN: N HIGGINS

APPLIED RESEARCH ASSOCIATES, INC
ATTN: D PIEPENBURG

BOEING CO
ATTN: G HALL
ATTN: G R BURWELL

CALIFORNIA RESEARCH & TECHNOLOGY, INC
ATTN: K KREYENHAGEN
ATTN: LIBRARY
ATTN: M ROSENBLATT

CALIFORNIA RESEARCH & TECHNOLOGY, INC
ATTN: F SAUER

CARPENTER RESEARCH CORP
ATTN: H J CARPENTER

DENVER COLORADO SEMINARY UNIVERSITY OF
ATTN: J WISOTSKI

H & H CONSULTANTS, INC
ATTN: J HALTIWANGER
ATTN: W HALL

H-TECH LABS, INC
ATTN: B HARTENBAUM

KAMAN SCIENCES CORP
ATTN: R RUETENIK

KAMAN TEMPO
ATTN: DASIAC

KAMAN TEMPO
ATTN: DASIAC

MCDONNELL DOUGLAS CORP
ATTN: H HERDMAN
ATTN: R HALPRIN

NEW MEXICO, UNIVERSITY OF
ATTN: J KOVARNA

PACIFIC-SIERRA RESEARCH CORP
ATTN: H BRODE, CHAIRMAN SAGE

PACIFIC-SIERRA RESEARCH CORP
ATTN: D GORMLEY

PACIFICA TECHNOLOGY
ATTN: R ALLEN
ATTN: TECH LIBRARY

PHYSICS INTERNATIONAL CO
ATTN: H W WAMPLER

R & D ASSOCIATES
ATTN: T MAZZOLA
ATTN: TECHNICAL INFORMATION CENTER

R & D ASSOCIATES
ATTN: A POLK
ATTN: B WEBSTER

R & D ASSOCIATES
ATTN: G GANONG

RAND CORP
ATTN: B BENNETT

S-CUBED
ATTN: B PYATT
ATTN: C DISMUKES
ATTN: J BARTHEL
ATTN: LIBRARY

S-CUBED
ATTN: C NEEDHAM

SCIENCE APPLICATIONS INTL CORP
ATTN: H WILSON
ATTN: R SCHLAUG
ATTN: TECHNICAL LIBRARY

SCIENCE APPLICATIONS INTL CORP
ATTN: D BACON
ATTN: J COCKAYNE
ATTN: W LAYSON

SCIENCE APPLICATIONS INTL CORP
ATTN: G BINNINGER

SRI INTERNATIONAL
ATTN: J COLTON

TELEDYNE BROWN ENGINEERING
ATTN: D ORMOND
ATTN: F LEOPARD

TRW ELECTRONICS & DEFENSE SECTOR
2 CYS ATTN: A ZIMMERMAN
ATTN: M SEIZEW
2 CYS ATTN: R COLBERT
ATTN: TECH INFO CTR, DOC ACQ

TRW ELECTRONICS & DEFENSE SECTOR
ATTN: N GUILES
ATTN: N LIPNER

WEIDLINGER ASSOC, CONSULTING ENGRG
ATTN: I SANDLER

END

10-87

DTIC